UNIVERSIDADE DE SANTIAGO DE COMPOSTELA

ESCOLA TÉCNICA SUPERIOR DE ENXEÑARÍA

Departamento de Enxeñaría Química

AIR DRYING OF *FUCUS VESICULOSUS* SEAWEED AND ITS EFFECT ON PHYTOCHEMICAL CHARACTERISTICS OF AQUEOUS EXTRACTS

Memoria presentada por:

Santiago Gabriel Sexto Cancela

Como Trabajo de Fin de Máster

correspondiente al

"Máster en Ingeniería Química y Bioprocesos"

Santiago de Compostela, febrero de 2015

RAMÓN FELIPE MOREIRA MARTÍNEZ, Profesor Titular, y **JORGE SINEIRO TORRES PÉREZ**, Profesor Contratado Doctor, del Departamento de Enxeñaría Química de la Universidade de Santiago de Compostela,

INFORMAN:

Que la memoria titulada "*Air drying of Fucus vesiculosus seaweed and its effect on phytochemical characteristics of aqueous extracts*", presentada por Santiago Gabriel Sexto Cancela para superar los créditos correspondientes al Proyecto de Fin de Máster correspondiente al Máster en Ingeniería Química y Bioprocesos, se realizó bajo nuestra supervisión en el Departamento de Enxeñaría Química de la Universidade de Santiago de Compostela y autorizan su presentación.

Para que así conste a los efectos oportunos, expiden el presente informe en Santiago de Compostela, febrero de 2015.

Los directores, El alumno

R.F. Moreira Martínez J. Sineiro Torres S. G. Sexto Cancela

Agradecimientos

Al Grupo GI-1618 de investigación de Tecnologías para el Desarrollo de Bioproductos Industriales por permitirme formar parte de su equipo y desarrollar este Trabajo de Fin de Máster.

A Ramón Moreira y Jorge Sineiro por la dirección y, sobre todo, la compañía y el apoyo aportados durante toda la duración del Trabajo de Fin de Máster.

A Francisco Chenlo por la compañía, las correcciones y el buen criterio proporcionados.

A Marivel Sánchez por su ayuda y paciencia en la introducción a las técnicas de laboratorio relacionadas con la extracción de compuestos bioactivos.

A Santiago Arufe, excelente compañero y mejor amigo.

Antón Taboada, gran amigo y compañero del Trabajo de fin de Máster.

Contents

1. Abstract

The purpose of this study was to determine the effect of air drying at four different temperatures (35, 50, 60 and 75ºC) on drying kinetics at different configurations (deep-bed and thin layer) and properties of dried *Fucus vesiculosus* seaweed and the phytochemical constituents of its aqueous extracts.

Water adsorption and desorption isotherms were also determined at four different temperatures (5, 25, 45 and 65ºC). Different models (GAB, BET, Caurie, Halsey and Oswin) were tested for water sorption isotherms modelling. Halsey model showed the best fit for all water sorption isotherms.

In the case of drying kinetics modelling for deep-bed configuration, bibliographic models were tested (Newton, Henderson-Pabis, Logarithmic, Two-Term, Weibull, Page and Modified Page). Page and modified Page models were selected as the most adequate under statistical analysis criteria. Thin layer dyring kinetics of *F. vesiculosus* showed a constant rate period and falling rate period at all drying temperatures tested. Critical moisture content increased with drying temperature. For post-critical period, Fick's second law equations were successfully applied and allowed the determination of effective coefficients of diffusion of water, which increased with drying temperature (from $95 \cdot 10^{-12}$ up to $260 \cdot 10^{-12}$ m^2/s). This water effective diffusivities were estimated considering the shrinkage of samples. The shrinkage analysis indicated that real shrinkage was larger than ideal shrinkage (evaluated by means of water loss). Effect of different load densities (from 1.25 up to 14.88 kg/m^2) was studied at 75ºC and a linear correlation between load density and drying time was achieved.

Dried seaweed at 75ºC exhibited the largest colour differences. Seaweed powders previously dried at 35, 60 and 75ºC exhibited an appreciable yellow-tone coloration, whereas system dried at 50ºC presented a greenish coloration.

F. vesiculosus extracts were obtained performing aqueous ultrasound assisted extractions. Two key extraction parameters (from 20 to 40 (g/g) liquid/solid ratio and contact time from 4 to 20 minutes) on the extraction yield of three bioactive compounds (polyphenols, carbohydrates and alginates) were studied for the system dried at 35ºC. The effect of drying temperature on antioxidant activity and the yield of bioactive compounds was studied by means of extractions performed at optimized L/S ratio of 30 (g/g) and contact

times of 4 minutes for all dried systems. Maximum phenolic content (1738 mg PHL/100 g_{dw}) and antioxidant activity (measured by means of DPPH• radical scavenging activity, 57%) were obtained for the system dried at 35ºC and declined significantly with drying temperature. Higher drying temperatures had a positive effect on alginate extraction yield (2069 mg GLU/100 g_{dw}). Total phenolic content of extracts from different particle size fractions of dried *F. vesiculosus* powder was determined. Maximum phenolic content was attained at intermediate fractions 80-200 µm (2272 GLU/100 g_{dw}).

2. Objectives

The **main objective** of this Master Thesis 'Air drying of *Fucus vesiculosus* seaweed: effect on phytochemical characteristics of aqueous extracts' is to study the effect of convective air drying temperatures on phytochemical constituents of the aqueous extracts of *F. vesiculosus* seaweed.

Specific objectives are summarised below:

- Bibliographic review of marine algae characterization, drying conditions and extraction of their bioactive compounds.
- Experience acquisition of experimental techniques and handling of different equipment to perform different operations such as drying, milling, sieving, colorimetry, ultrasound extractions and chemical analysis (antioxidant activity, carbohydrate content, polyphenols content and alginates content determination), among others.
- Determination of water sorption isotherms of *F. vesiculosus* at different temperatures and modelling of experimental data.
- Drying of *F. vesiculosus* at different temperatures. Obtention and modelling of experimental data.
- Evaluation of shrinkage and colour changes during drying.
- Granulometric and colorimetric characterization of *F. vesiculosus* powders previously dried at different temperatures.
- Obtaining *F. vesiculosus* extracts by means of ultrasound assisted extraction and evaluation of its feasibility as an alternative to obtain *F. vesiculosus* bioactive compounds.
- Phytochemical characterization of *F. vesiculosus* extracts previously dried at different temperatures.

3. Introduction

A large variety of reactive oxygen species (ROS); superoxide anion-radical ($O_2^{\cdot}$), hydroxyl radicals ($HO^{\cdot}$) and other non – radical oxygen derivatives (hydrogen peroxide) are generated by the metabolism in response to inflammatory reactions and as a result of exposure to environmental factors. These compounds circulate freely in all tissues and organs. There are several mechanisms by which these substances can cause damage to tissues, including damage to proteins and DNA, lipid peroxidation, oxidation of important enzymes, and stimulation of pro-inflammatory cytokine release by monocytes and macrophages. A substantial increase in the production of these species has been found in the presence of several diseases (Keyrouz et al. 2011). These include cardiovascular diseases, inflammatory conditions and neurodegenerative diseases such as Alzheimer's disease, mutations and cancer (Kuda et al. 2005b) Moreover, deterioration in some foods is caused by the oxidation of lipids and the formation of secondary lipid peroxidation products. Lipid oxidation by ROS also causes a decrease in nutritional value of lipid foods and appearance (Ngo et al. 2011)

Nowadays in the food and pharmaceutical industries the most used antioxidants are butylated hydroxyanisole (BHA), propyl gallate (PG), butylated hydroxytoluene (BHT) and tert-butylhydroquinone (TBHQ), which have been reported to have side effects such as liver damage and carcinogenesis (Shao et al. 2013).

In recent years, there has been an increased interest in natural antioxidants to replace synthetic additives in foods or nutraceuticals. Natural antioxidants not only have the capability to improve oxidative stability (preventing rancidity), but they can also provide a wide variety of additional health benefits. It is suggested that the addition of these compounds might enhance the body's defenses against ROS – related diseases. (Wang et al. 2012).

Although marine algae are exposed to light and oxygen, causing the formation of free radicals and other oxidizing agents, there is no presence of oxidative damage in the structural components of seaweeds and their stability to oxidation during storage. This suggests that their cells have protective antioxidative defense systems (Jiménez-Escrig et al. 2001). There are two types of substances present in marine algae that are strongly related to the antioxidant activity: certain polysaccharides (fucoidans) (Hahn et al. 2012) and polyphenols (phlorotannins) (Keyrouz et al. 2011).

Marine algae and brown algae represent a suitable supplement and additive for food due to their high nutritional value and the health benefits they can provide. This is why it is necessary to study how processing (collection, extraction, drying and storage) affects these properties.

South Asian countries were the first to introduce seaweeds for their utilization for medicinal and food purposes. Conventionally, Western World has used marine algae for the production of colloids. Around 18 million tonnes of marine algae and other aquatic plants are harvested annually with an estimated value of U.S $5,000 million. Even though, marine algae market is a multimillion dollar industry, it is mainly limited to the obtention of agar, carrageenan and alginates. Bioactive potential of these species is underexploited. Nowadays, many initiatives are being carried out in Europe to exploit these marine valuable resources. Marine algae are abundant in Europe and have the potential to become an excellent source of bioactive compounds such as dietary fiber, omega-3 fatty acids, carotenoids, vitamins, and minerals (Kadam et al 2013).

Some examples of the initiatives carried by the European Union for the exploitation of marine algae are listed below:

- Netalgae: follows the creation of a European network of organisations interested in the marine algae industry (http://www.netalgae.eu/es/netalgae-project.php, 16/01).
- Nutramara: aims the exploration of marine resources with potential for their utilization as sources of bioactive substances to be used as ingredients in foods (http://www.nutramara.ie/ 16/01).
- Marex: exploration of marine resources in search of bioactive compounds (http://www.marex.fi/ 16/01).

The main use of *F. vesiculosus* in Europe is related to weight loss applications. UK represents the biggest market where several products containing raw *F. vesiculosus* or extracts (mainly obtained with organic solvents) are commercialized. In Spain, the only known applications are linked to the use of raw *F. vesiculosus*, added to some foods as a supplement (i.e. Mar de Ardora, Galicia). Besides traditional uses, further research is needed regarding possible *F. vesiculosus* applications.

3.1. Brown algae

Edible marine macro algae or seaweeds are classified into three types: *Chlorophyceae* (green algae), *Phaeophyceae* (brown algae) and *Rhodophyceae* (red algae) according to their composition of pigments, being brown and red seaweeds the most used algae for human consumption. (Li et al. 2011).

Algae are of particular interest for human consumption for their high content in polysaccharides 33-50%, (g H_2O/ g dry solid, d.b.) and proteins (5-24% in brown algae; 10-47% in red and green algae), and their reduced content in lipids (1-2%) (Gómez-Ordóñez 2013).

3.1.1. Polysaccharides

The three types of algae are distinguished by their structural and reserve polysaccharide composition. Many of them cannot be obtained from terrestrial algae and are only produced by marine species, such as sulfated polysaccharides, hardly observed in land plants (Kim 2012). They are polymeric molecules linked by glycosidic bonds and have many known commercial applications as emulsifiers, thickeners or gelling agents. These polysaccharide can be mostly be considered fiber as they are not digested by the human enzymes in the stomach, although, some of them are partially degraded by enzymes produced by the colon bacteria. Table 3-1 shows the most important polysaccharides of each type of algae. Dietary fiber in brown algae can be divided in four groups: laminarans, alginates, fucans and cellulose (Gómez-Ordóñez 2013).

Table 3-1. Classification of the most important polysaccharides for human consumption present in algae (Gómez-Ordóñez 2013).

	Soluble fiber	**Insoluble fiber**
Brown algae (*Fucus, Laminaria, Undaria, Himanthalia*)	Laminarin Alginate Fucan	Cellulose
Red algae (*Chondrus, Porphyra, Mastocarpus*)	Agar Carrageenan Xylan	Cellulose
Green algae (*Ulva, Enteromorpha*)	Xylan Sulfated galactans	Cellulose

Additionally, polysaccharides can be classified into three types depending on their role: structural polysaccharide (cellulose), intercellular mucilage (alginate, fucoidan and laminaran) and storage polysaccharide (laminaran).

A brief description of the most important polysaccharides present in brown algae is shown below.

Laminarans are the main reserve polysaccharides of brown algae and they are found in higher quantities in laminarian (*Laminaria* and *Undaria*) and *Fucus* species. The content in laminarans varies depending on environment and season of the year, and it can reach values up to 36% d.w. Highest yields are achieved in autumn, between September and November, while it reaches reduced values in February and June. This variations must be taken into account when laminarans are the compound of interest in the algae. Laminarans are used as dietary fiber and among other properties, they show anticoagulant and antitumor activities (Gómez-Ordóñez 2013).

Alginates constitute the main structural polysaccharide in brown algae cell walls and they cannot be obtained from terrestrial algae. They can reach up to 40-47% d.w. of the seaweed, varying between seasons, reaching maximums in spring and minimums in autumn (Gómez-Ordóñez 2013). This polysaccharide has structural functions, it gives the algae both, mechanical strength and flexibility.

Alginates are a family of unbranched binary copolymers of (1-4)-linked-β-D-mannuronic acid (M) and α-L-glucuronic acid (G) residues (Figure 3-1). Proportions of these monomers may vary depending on the organisms that produces it and the tissue from which it is obtained, exhibiting each different physical properties. High glucuronic acid content is related with high rigidity of the tissue, while a lower content provides a more flexible structure. (Stephen et al. 2006).

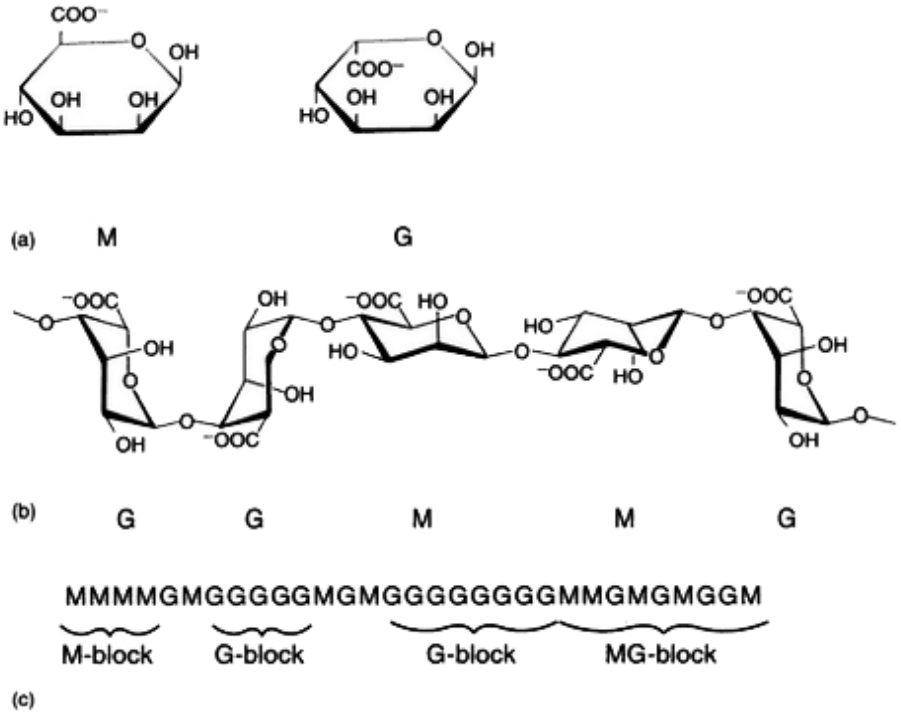

Figure 3-1. Haworth projection of alginate. a) Alginate monomers. M: β-D-mannuronate; G: α-L-glucuronate. b) Alginate in chair conformation. c) Symbolic representation of an alginate chain.

Alginates are widely used in food industries as thickeners and gelling agents. They also show antihypertensive and anti-inflammatory activities, as well as the capacity to reduce cholesterol levels in blood (Gómez-Ordóñez 2013).

Fucodains are sulfated water-soluble (highly hygroscopic) polysaccharides found in the cell wall or extracellular matrix of brown algae, of which they can contribute up to 40% d.w. It is not possible to fully define a chemical structure for these substances as it changes depending on species, part of the algae or the extraction method (Gómez-Ordóñez 2013). In Figure 3-2, a possible structure of fucoidans from *F. vesiculosus* is shown.

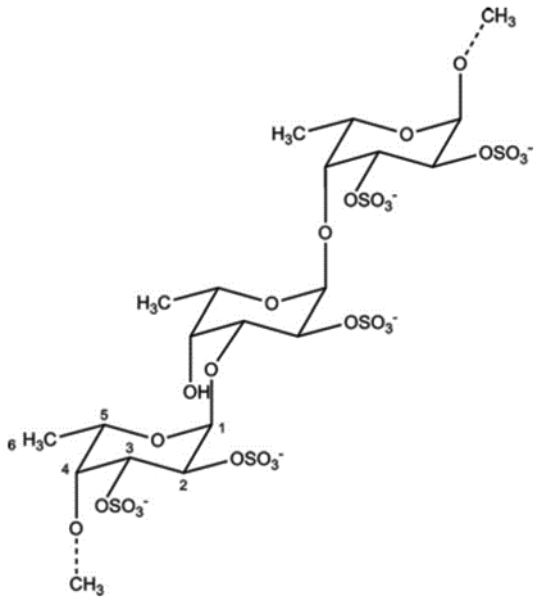

Figure 3-2. Proposed structure of fucoidans from *Fucus vesiculosus* (Hahn et al. 2012).

The bioactivity of the polysaccharide depends on its molecular weight, quantity, position and conformation of the sulfate groups of the polysaccharides. Different isolated fucoidans have been reported to show anticoagulant, antiviral, antitumor, antioxidant activities and anti-HIV activity (Gómez-Ordóñez 2013; Hahn et al. 2012; Thuy et al. 2015) and they are summarized in Figure 3-3:

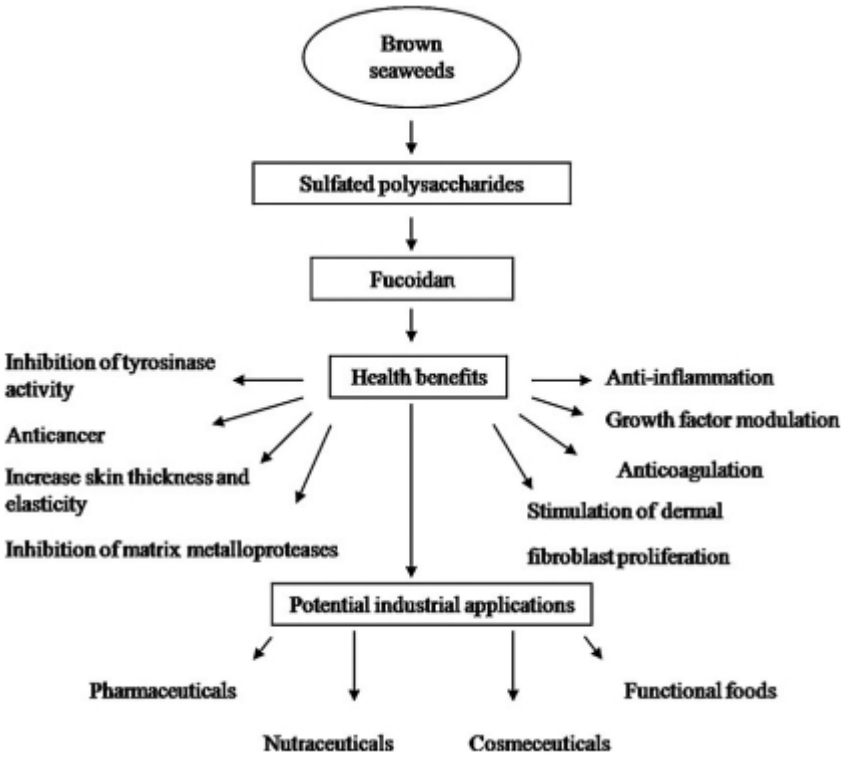

Figure 3-3. Biological properties and potential industrial uses of fucoidans (Wijesinghe & You-Jin 2012).

3.1.2. Proteins

Protein, peptide and amino acids content in brown algae is relatively low (5-24% d.w.) and it strongly varies depending on species and season (Gómez-Ordóñez 2013).

3.1.3. Lipids

Lipids are present in low quantities in seaweeds (<5% d.w.) and are responsible of their low calories content. As with protein and polysaccharide content, lipid content depends on the season of the year and other environmental factors. Both, brown and red algae are a valuable source of omega-3 and omega-6, which are recognized for their health benefits (Gómez-Ordóñez 2013).

3.1.4. Minerals

Seaweeds accumulate a high amount of **minerals** (8-40% d.w.) due to the wide variety of these compounds that can be found in marine environments. These minerals include sodium, calcium, magnesium, potassium, chloride, sulfates, phosphorous, fluoride, among others. Therefore, brown algae are a suitable as dietary supplement in foods. The mineral composition of seaweeds can vary depending on species and location. On the other hand, marine algae are good indicators of heavy metals bioaccumulation due to their capacity to hold these substances (Gómez-Ordóñez 2013).

F. vesiculosus is rich in light elements such as Mg, K, Ca and Na, and in halogens (Br, I, Cl). Regarding toxic elements, *Fucus* reported to present high concentrations of As (over 300 ppm in the Baltic Sea) and low contents on Hg, Sb and Se. In addition, mineral content in this algae does not depend on time of the year but on salt concentration of the seawater (Truus et al. 2001).

3.1.5. Polyphenols

Red and green algae contain little traces of **polyphenols** (<1% d.w.). Brown algae have higher fractions, with species like *Ascophyllum* and *Fucus* reaching up to 14% d.w. (Ordóñez 2013). Phenolics play a primary role as structural components of cell walls and may have secondary roles in signalling, defence or in responses to environmental stress. Polyphenols are compounds with an aromatic ring bearing one or more hydroxyl substituents and include simple phenols, coumarins, flavonoids, stilbenes, lignans, hydrolysable and condensed tannins, and phlorotannins (Figure 3-4). **Phlorotannins** have been reported to

show anti-inflammatory properties, therapeutic potential in arthritis treatment and antioxidant activities (Balboa et al. 2013).

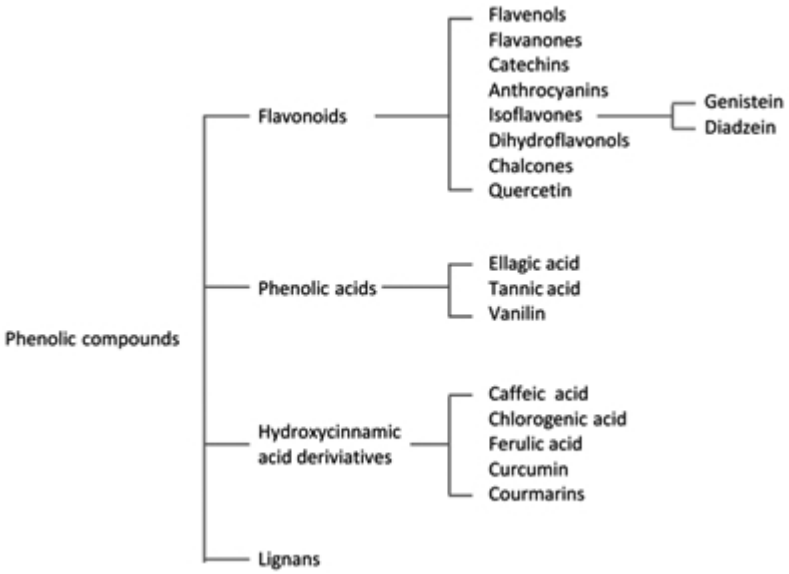

Figure 3-4. Classification of some phenolic compounds from natural sources (Kyung-tae 2012).

Phlorotannins are formed by the polymerization of phloroglucinol (1,3,5-trihydroxybenzene) monomer units and biosynthesized through the acetate-malonate pathway (polyketide pathway). They are highly hydrophilic components with a wide range of molecular sizes ranging between 126 Da and 650 kDa. Marine brown algae accumulate a variety of phloroglucinol-based polyphenols, as phlorotannins of low, intermediate and high molecular weight containing both, phenyl and phenoxy units. Depending on linkage, phlorotannins can be classified into four subclasses such as fuhalols and phlorethols (phlorotannins with an ether linkage), fucols (with a phenyl linkage), fucophloroethols (with an ether and phenyl linkage), and eckols (with a dibenzodioxin linkage). Figure 3-5 shows the structure of some phlorotannins found in marine brown algae:

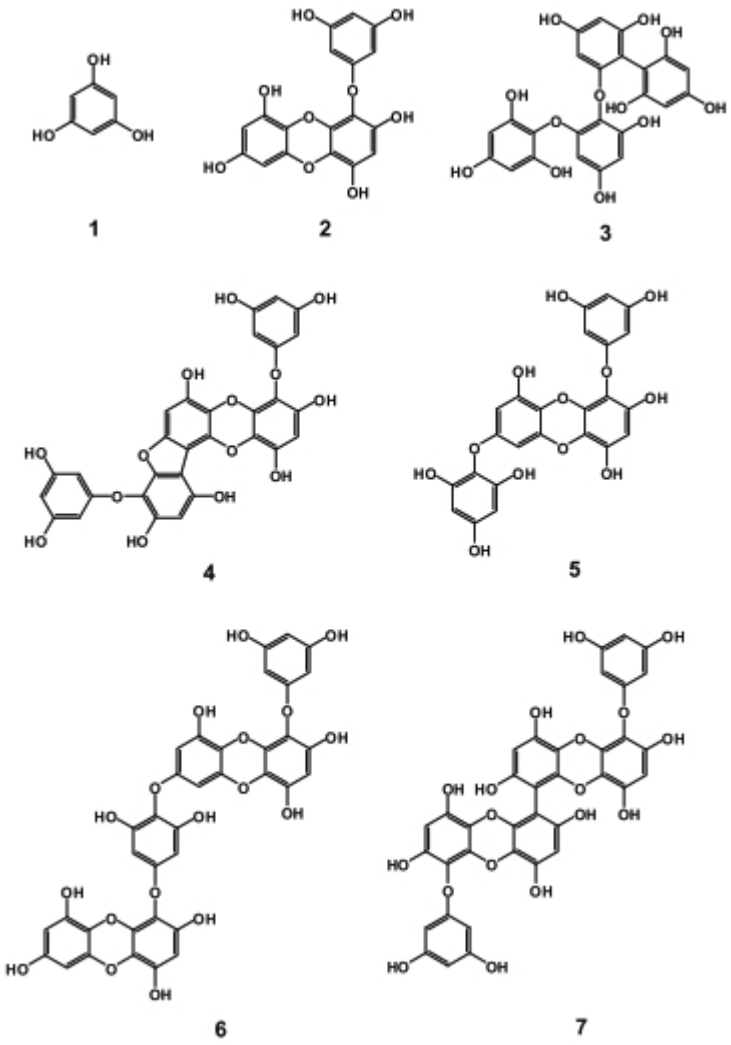

Figure 3-5. Structure of phlorotannins from marine brown algae. (1) phloroglucinol, (2) eckol, (3) fucodiphloroethol, (4) 7-phloroeckol, (6) dieckol and (7) 6,6'-bieckol (Li et al. 2011).

Several species of brown algae, such as *Ecklonia cava*, *Ecklonia kurome*, *Fucus vesiculosus*, *Hizika fusiformis*, and *Sargassum ringgoldianum*, have been found to possess a high content of phlorotannins, which is correlated with the antioxidant activity (Wang et al. 2012).

3.1.6. Carotenoids

Carotenoids are a family of pigmented compounds which are synthesized by plants, algae, fungi and microorganisms, but not by animals. They are the most important pigments in nature that are responsible for various colors of different photosynthetic organisms. Carotenoids are related to the prevention of many human diseases including cardiovascular diseases, cancer and other chronic diseases (Ngo et al. 2011).

Although chlorophyll is also present in seaweeds, in the case of brown algae, xanthophyll pigment or fucoxanthin (**Figure 3-6**) is the main responsible for its color (Li et al. 2011).

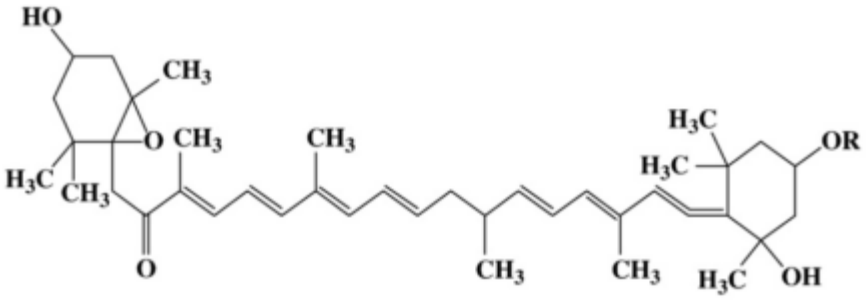

Figure 3-6. Structure of fucoxanthin, carotenoids found in Brown algae (Ngo et al. 2011).

3.1.7. *Fucus vesiculosus*

Fucus vesiculosus (Figure 3-7) is commonly known as *bladderwrack* (gaelic). It is a lower limit intertidal seaweed species and it adheres to and grows on stones (Kim 2012). It is a dominant species of macro alga in the northern Atlantic Ocean and, ecologically, it is the most important seaweed, providing shelter and food for associated flora and fauna. It shows a high genetic variability between geographic locations which provides *Fucus* a high capacity to cope with environmental stress (temperature changes, changes in salinity, exposure to sunlight). This feature could be important when analysing and comparing with bibliography the results of the present work (Tatarenkov et al. 2007; Lesser 2011).

Figure 3-7. *Fucus vesiculosus* underwater (Algae Base Database).

Fucus vesiculosus thallus has a strap-like geometry and forks towards the end. It has a thick midrib (holdfast) which attaches to subtract. Bladders or vesicles appear from the thallus, which helps the seaweed to stand erect underwater. In the tip of the thallus *Fucus* develops the receptacles, which host the conceptacles (fertile parts of the seaweed) (Hoek 1996).

The average composition of *Fucus vesiculosus* is shown in Figure 3-8. Polysaccharide content may vary and reach its maximum value after spring (growth season) to generate enough biomass to survive winter. Other authors determine that *F. vesiculosus* contains up to 65% of dry weight in polysaccharides (Rioux et al. 2007).

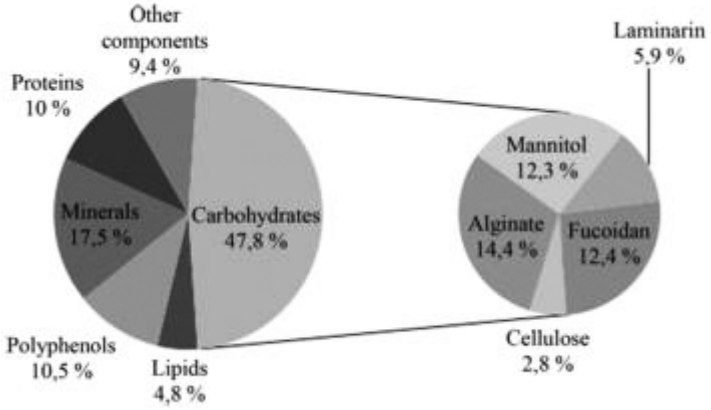

Figure 3-8. Average composition of *Fucus vesiculosus* in dry weight (Hahn et al. 2012).

3.2. Antioxidant activity

Compounds present in *F. vesiculosus* that have reported to show antioxidant activity and the mechanisms involved are detailed below.

Sulfated polysaccharides are present mostly as fucoidans in brown algae (*Phaeophyceae*), carrageenan in red algae (*Rhodophyceae*), and ulvan in green algae (*Chlorophyceae*). Fucoidans are responsible of the resistance to dryness of brown algae and contribute to the formation of a gel network (Kim 2012). There is a close connection between molecular weight of these molecules and their antioxidant activity. The lower the molecular weight, the higher the antioxidant activity. Low molecular weight molecules are able to easily diffuse through cell membranes to donate protons in a higher effective way. Besides, sulfated polysaccharides are important free-radical scavengers and antioxidants for the prevention of oxidative damage and sulfated groups provide anticoagulant activity (Ngo et al. 2011).

Phlorotannins are mostly extracted from marine brown algae and are responsible for antioxidant activities and have shown protective effects against hydrogen peroxide-induced cell damage. Phlorotannins act as free radical scavengers, reducing agents and metal chelators, inhibiting lipid oxidation.

Antioxidant activity reported by **carotenoids** is due to its highly unsaturated nature, which leads to their own oxidation instead of other molecules. The antioxidant properties of carotenoids are based on their singlet oxygen quenching properties or their ability to trap free radicals. Antioxidant activity depends on the number of conjugated double bonds of the molecule and carotenoid end groups or the nature of substituents in carotenoids containing cyclic end groups (Ngo et al. 2011).

3.3. Drying fundamentals

Drying is one of the studied processes worldwide as it accounts for about 10-25% of the total energy consumption in manufacturing processes. It represents an important step in the food processing industry. Almost every food product is dried at least once at one point of its preparation (Mujumdar 2006). The main reasons why food products are dried are detailed below (Brennan 1994):

- Extended storage life: dried food products are less vulnerable to spoilage caused by bacteria, molds and insects. Activity of several microorganisms is inhibited in systems in which moisture is below certain levels. Additionally, enzymatic and oxidative reactions might not take place under low moisture conditions.
- Quality enhancement: many favorable qualities and nutritional values of food may be enhanced by drying. Palatability and digestibility are improved. Drying changes color, flavor, appearance and texture of a food item. These features may affect the decision of the end user to buy or not a certain food (Figure 3-9).
- Ease of handling: packing, handling and transportation of a dried product is considerably easier and cheaper because of weight and volume loss.
- Further processing: food products are dried for improved milling, mixing or segregation. In addition, dry milling is far cheaper than wet milling.
- Sanitation: during drying, insects and other microorganisms are destroyed.

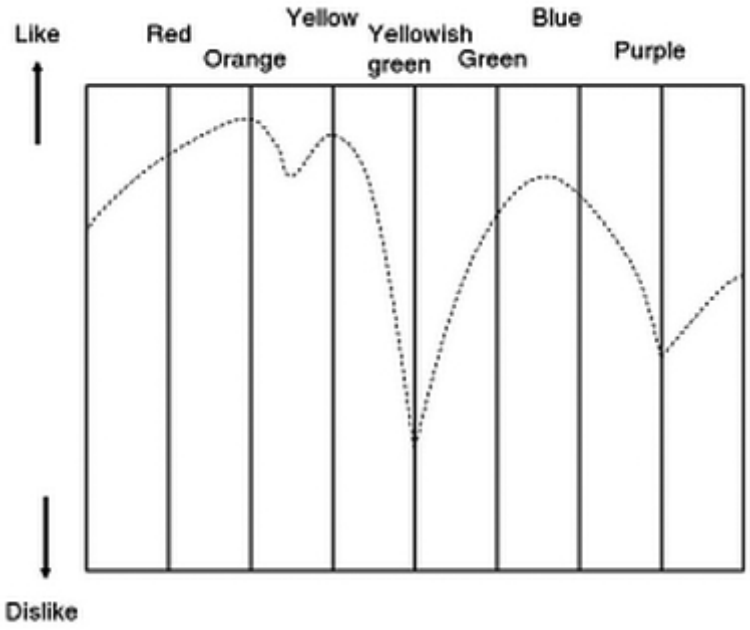

Figure 3-9. Illustration of the impact of the colour of a particular natural food product upon 'Like or dislike' (Birren diagram modified from that summarised by Li (1998)) (Chen & Mujumdar 2009).

Many foods and, more strictly seaweeds, are generally sundried, process that requires long periods of time. During recent years, an increase of production rates of marine algae requires the application of quicker industrial methods. The most frequently used industrial drying method in food industry is the convective air drying. This process is highly influenced by air temperature and material characteristics, as well as other parameters that must be controlled. For this reason, many researches in convective air drying of several seaweeds were carried out in the recent years: Vega-Gálvez et al. (2008) studied convective drying of *Macrocystis pyrifera*, Gupta et al. (2011) studied convective drying kinetics of *Himanthalia elongate*, Tello-Ireland et al. (2011) studied drying kinetics of *Gracilaria chilensis* and Fudholi et al. (2012b) studied drying kinetics of *Gracilaria cangii*.

Along with the benefits remarked before, drying, and particularly hot air drying, might have some undesirable secondary effects. Under hot air, food products undergo several reactions that alter their physical (rehydration, color loss), chemical (browning reaction, lipid oxidation) and nutritional (vitamin and protein loss, and microbial survival).

Seaweeds gained attention in the food industry for the antioxidant properties showed by some of their constituent components. In that matter, there are several researches carried out in the last ten years, which study the effect of varied convective drying conditions over antioxidant activity of many marine algae species (Tello-Ireland et al. 2011; Jiménez-Escrig et al. 2001; Kuda et al. 2005a; Kuda et al. 2005b; Le Lann et al. 2008).

Convective air drying of algae must be carried out finding a compromise solution to several factors: loss of bioactive properties, energy consumption, time and customer oriented properties.

3.3.1. Moisture in foods

Moisture is bonded to food, mainly, in two ways: to ionic groups, such as carboxyl groups and amino acids, and to hydrogen groups, such as hydroxyl and amides. In foods in which moisture is higher than 50% wet basis (kg water/100 kg food material), free water exists within the material pores and in intercellular spaces. The former is easier to remove than the latter and is evaporated in the first stages of drying.

Equilibrium moisture content (X_e) of a food material is reached when its internal vapor pressure is in equilibrium with the outside vapor pressure. The different states of equilibrium at any temperature are usually represented by a X_e versus equilibrium related humidity, or water activity. This plot, generally has a sigmoid (S) shape due to variations in the way that water bonds to the solid. Figure 3-10 shows the typical water sorption isotherm types for food systems. A totally dried solid introduced in a slightly humid environment will strongly retain water molecules in a single layer. As the ambient humidity grows, the solid will trap water molecules in the monolayer until it is full. Once this happens, water will start filling the capillary pores of the material. This process is affected by temperature and that is why equilibrium states are always represented referencing to a temperature, on the so called isotherms. Normally, food materials show a hysteresis phenomenon during adsorption and desorption processes, which is bound to irreversible physical and chemical changes.

The role of moisture in food drying and storage is expressed in terms of water activity (a_w). Water activity is defined in a similar manner as the relative humidity is defined in moist air, that is, the ratio of vapor pressure to the saturated vapor pressure at same temperature. It measures the chemical activity of moisture in food during drying and storage. Oxidation is avoided if water activity is lower than 0.4 and growth inhibition of most microorganisms is achieved at a_w lower than 0.7. At very low water activities, within the range 0.1-0.3, some enzymes may still be active, but their reaction rates are strongly diminished (Mujumdar 2006).

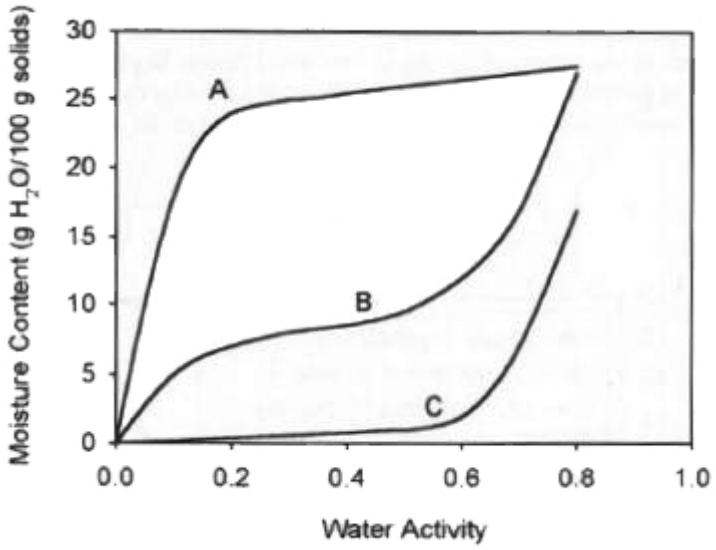

Figure 3-10. Typical isotherm shapes for food systems: type I isotherm (A), type II isotherm (B) and type III isotherm (C) (Bell & Labuza 2000).

Drying affects physical and chemical properties of food materials. Convective drying can cause changes in appearance. Most food materials shrinkage while drying due to water removal and structural modifications. Besides, colour alterations can occur as a result of chemical reactions, colorants leaching or degradation while drying. Thereby, it is mandatory to study physical and chemical alterations of food materials along with drying kinetics.

3.3.2. Drying kinetics

High moisture foods (>50% wet basis) show two different drying rate behaviours (Mujumdar 2006):

- Constant drying rate period: during constant drying rate, moisture at the surface is eliminated and hence, the only limitation is that offered by the rate at which water can evaporate. When surface moisture is evaporated, drying rate starts to decrease. Moisture content at which this occurs is called critical moisture content, and there might be several for each food system, depending on drying conditions.
- Falling rate drying period: after water from the surface is depleted, moisture from the interior of the food item is diffused to the surface for further elimination. The rate at which water diffuses through the material is delimited by a diffusion coefficient (m^2). Its value will depend on the type of the material, its geometry and external conditions.

A typical drying curve for food materials with both drying rate periods, and its relation with moisture content is shown in Figure 3-11.

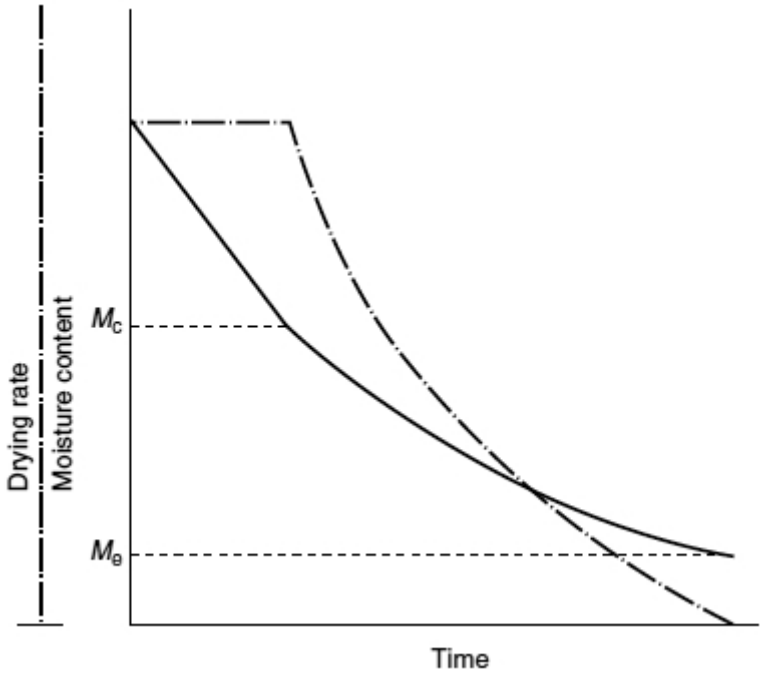

Figure 3-11. Drying curve for high moisture material (Mujumdar 2006).

3.4. Ultrasound assisted extraction

3.4.1. Introduction

The use of ultrasound technology is widely extended in the food industry. It has been implemented in several large-scale commercial applications such as emulsification, homogenization, extraction, crystallization, dewatering, low-temperature pasteurization, degassing, defoaming, activation and inactivation of enzymes, particle-size distribution and changing viscosity. In the recent years it has attracted the attention for its application for the extraction of natural products in a short time, which previously required, by conventional methods, many hours or days.

The conventional solvent extraction within the bodies of plants and seeds is based on the right choice of solvent and the use of heat and agitation. The use of ultrasounds improves solvent penetration and disrupts cell walls, releasing its content.

Ultrasound assisted extraction (UAE) usually reduces working times, increases yields and the quality of the extract. In recent years, there are several compounds that have been extracted by UAE, especially bioactive compounds in the food industry (Picó 2013).

3.4.2. Principles of ultrasound assisted extraction

Ultrasound comprises mechanical waves that need an elastic medium to spread. The difference between sound and ultrasound is the frequency of the wave: sound wave are at human hearing frequencies (16 Hz - 20 kHz) while ultrasound has frequencies above human hearing but below microwave frequencies (20 kHz – 10MHz). The main parameter taken into account for the classification of ultrasound applications is the amount of energy generated: sound power (W), sound intensity (W/m^2) or sound energy density (W/m^3). The applications of ultrasound are divided into two groups: high intensity and low intensity.

Low-intensity, high frequency (100 kHz – 1 MHz, low power ultrasound (<1 W/cm^2) is employed in non-destructive procedures, especially as an analytical technique to determine food physicochemical properties (firmness, sugar content, acidity). On the other hand, high-intensity, low frequency (16 – 100 kHz), high power ultrasound (10-100 W/cm^2) can affect food properties.

When applying ultrasound to a liquid medium, longitudinal waves are created leading to the formation of regions of compression and rarefaction waves. This way, cavitation takes place and gas bubbles are formed. These bubbles get larger during the rarefaction or expansion step, and collapse when the energy provided by the ultrasounds in the compression stage is not enough to keep the vapor phase in the bubble (Figure 3-12)(Picó 2013).

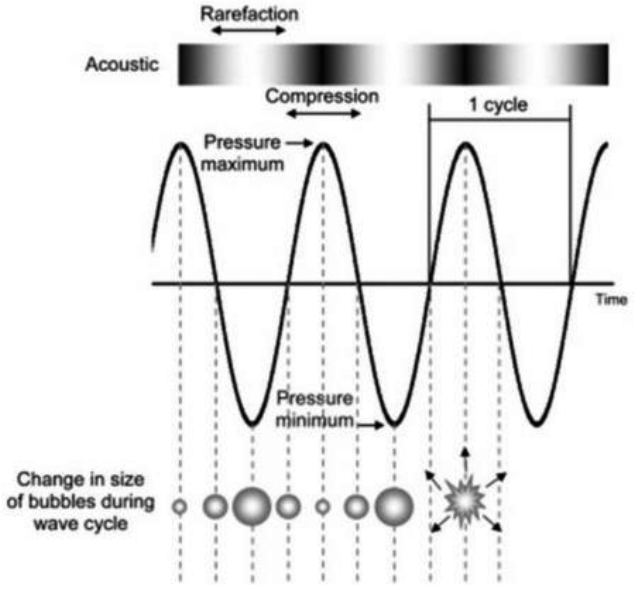

Figure 3-12. Cavitation formation during sonication (Soria & Villamiel 2010).

Afterwards, the vapour phase rapidly condensates and large amounts of energy are released. The condensed molecules collide creating shock waves. Cavitation can produce microstreaming, which improves heat and mass transfer. These microjets are useful in terms of improving solvent penetration and occasionally break cell walls, facilitating release of bioactives from the biological matrix. In Figure 3-13 it is shown how a bubble is formed (a) and soon thereafter it collapses (b) forming microjets which break down the cell wall (c) and release the cell content (d). (Picó 2013)

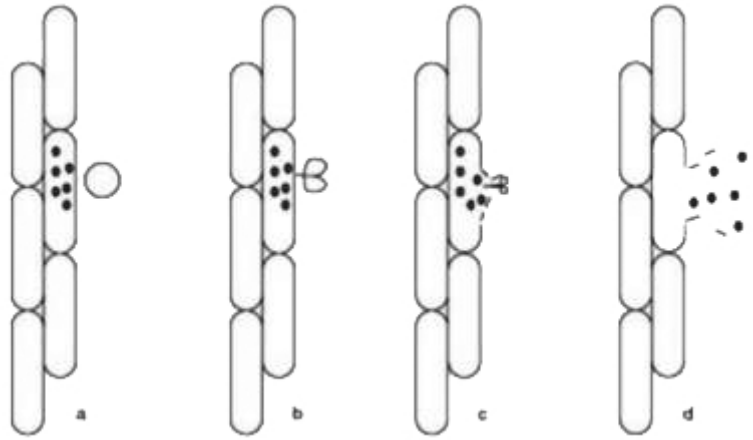

Figure 3-13. Ultrasound assisted extraction (Picó 2013).

Ultrasound extraction can be a simple, cost-effective and efficient replacement for traditional technologies employed to extract bioactive compounds from algae. It is a technology already in use for the extraction of lycopene from tomatoes (Lianfu & Zelong 2008), anthocyanins from raspberries (Chen et al. 2007), phenolic compounds from citrus peel (Ma et al. 2009) and coconut shell (Rodrigues et al. 2008). UAE facilitates the extraction of heat sensitive compounds with minimal damage. Equipment costs are lower than traditional equipment employed for novel extraction techniques and it can be used in combination with a wide variety of solvents, including water (for water soluble components). One of the drawbacks of the UAE is the weakening of sound waves in dispersed systems, making solid/liquid ratio a critical operation variable. Yet, UAE extraction technology has been employed in both, laboratory and large-scale industrial/commercialized applications (Kadam et al. 2013).

4. Experimental

4.1. Materials

4.1.1. Raw material

Fresh *Fucus vesiculosus* (84.41±2.88% of water, wet basis) were collected in the western coast of Galicia, Spain (geographical coordinates 42.782255 N, -8.929705 W) in October and November of 2014. Seaweed was washed with freshwater to remove sand, epiphytes (plant that grows on other plant but does not feed from it) and bugs, and stored (during a maximum of 1 week) at 5ºC until further treatment.

4.1.2. Reagents

Reagents employed in these work and their application is summarised in Table 4-1:

Table 4-1. Reagents employed during experimentation, application and safety data sheet.

Reagent	Application	Safety data sheet
Heptane	Shrinkage evaluation	Regulation (EC) 1907/2006
Sodium carbonate ($Na_2CO_3 \cdot H_2O$)	Polyphenols determination	Regulation (EC) 1907/2006
Folin-Ciocalteau	Polyphenols determination	Regulation (EC) 1907/2006
Sulfuric Acid (H_2SO_4, 98%)	Carbohydrates and alginates determination	Regulation (EC) 1907/2006
Phenol (C_6H_6O)	Carbohydrates determination	Regulation (EC) 1907/2006
Sodium tetraborate ($B_4Na_2O_7$)	Alginates determination	Regulation (EC) 1907/2006
Sulfamic acid (H_3NO_3S)	Alginates determination	Regulation (EC) 1907/2006
3-Hydroxybiphenyl	Alginates determination	Regulation (EC) 1907/2006

4.2. Experimental techniques and equipment

4.2.1. Physical and chemical characterization of seaweed

4.2.1.1. Water content

Moisture content was obtained gravimetrically. Dry basis was obtained by drying of samples in a vacuum oven (Heraeus 117 Vacutherm VT 6025) at 70ºC and 13kPa. Samples were weighed initially and periodically in a regular basis until constant weight was achieved (AOAC 1990).

Moisture content was determined by means of (4-1):

$$X = \frac{w_t - w_d}{w_d} \quad (4\text{-}1)$$

Where X (kg water / kg dried solid, d.b.) the moisture of the sample is in dry basis, w_t (g) is the weight of the sample and w_d (g) is the weight of the dried sample.

4.2.2. Water sorption isotherms

4.2.2.1. Gravimetric techniques for the determination of water sorption isotherms

The equilibrium moisture content of *F. vesiculosus* at different temperatures (T) (5, 25, 45 and 65ºC) was determined using a static gravimetric method (Wolf et al. 1985) was used. This method consisted in placing small samples in sealed jars, provided with a different salt solution to generate different humid atmospheres, until they reached equilibrium. The salts used and the water activity generated by their saturated solutions are shown in Table 4-2.

The amount of sample used for water desorption was 0.66±0.10 g and for water adsorption 0.47±0.04 g. Duplicate samples were placed into each jar. While fresh samples of seaweed were used for desorption isotherms, adsorption samples were previously dried in an oven at 40ºC until constant weight was achieved (approximately 3 days). A small quantity of thymol (substance with antiseptic properties) was added to jars with water activities higher than 0.5 to avoid bacterial growth. The jars containing the samples were placed in climatic chambers (5 – 25ºC) or in ovens (45 – 65ºC) until they reached equilibrium moisture, which happened within 6 months.

Table 4-2. Salts used in aqueous saturated solutions and the water activity generated.

Salt	Correlation to adjust temperature	Temperature (ºC)			
		5	25	45	65
LiCl	$\ln(a_w)=500.95/T-3.85$[1]	0.129	0.114	0.103	0.094
$MgCl_2$	$\ln(a_w)=303.35/T-2.13$[1]	0.354	0.329	0.308	0.292
$Mg(NO_3)_2$	$\ln(a_w)=356.6/T-1.82$[1]	0.584	0.536	0.497	0.465
NH_4NO_3		0.710[2]	0.650[2]	0.540[2]	0.500[2]
NaCl	$\ln(a_w)=228.92/T-1.04$[1]	0.805	0.762	0.726	0.696
KCl	$\ln(a_w)=367.58/T-1.39$[1]	0.890	0.843	0.791	0.739
$BaCl_2$		0.920[2]	0.910[2]	0.880[2]	0.860[2]

[1]: (Bell & Labuza, 2000).

[2]: (Moreira et al., 2005).

4.2.2.2. Modelling of water sorption isotherms

The resulting experimental data (equilibrium moisture (X_{eq}) and water activity, (a_W)) were fit using 5 mathematical models: BET, GAB, Caurie, Halsey and Oswin.

- Brunauer-Emmett-Teller (Brunauer et al., 1940): BET (Eq. 4-2) is the most used model to calculate monolayer values (X_m) due to its simplicity. The BET equation is valid for water surface adsorption and desorption, and, over a a_W of around 0.5, condensation becomes important and the model cannot be applied (Bell & Labuza, 2000).

$$X_{eq} = \frac{X_m C a_W}{(1 - a_W)(1 + (C - 1)a_W)} \quad \text{(Eq. 4-2)}$$

  Where X_m is the monolayer water content (d.b.) and C (-) is a constant related to the first layer heat of sorption (Polatoğlu et al., 2011).

- Guggenheim-Anderson-de Boer (van den Berg & Bruin 1981): GAB model (Eq. 4-3) is widely used as it accurately fits the water sorption isotherms of many food systems and was even recommended by the European Project Group COST 90 on physical properties of food as the fundamental equation for the characterization of water sorption by food materials. BET and GAB models are related as they derive from the same statistical model. Accordingly, GAB model also provides monolayer sorption values (m_0) and the energy constant (C), but is

provided with a third constant that adds a higher versatility, and can be applied within a higher range of water activities (0.05<aw<0.8-0.9) (Timmermann 2003).

$$X_{eq} = \frac{C_1 k m_0 a_W}{(1 - k a_W)(1 - k a_W + C_1 k a_W)} \quad \text{(Eq. 4-3)}$$

Where m_0 is the monolayer water content (d.b.), C (-) and k (-) are constants. The first one, as in BET model, related to the first layer heat of sorption, and the second related to the multilayer heat of sorption (Polatoğlu et al. 2011).

- Caurie: Caurie model (Eq. 4-4) was developed to cover deficiencies in BET model. One deficiency was already mentioned before and is related with the reduced range in which it is valid ($0.05<a_W<0.5$), and the other is linked with the complexity of the physical and chemical characteristics of stored food, especially due to its high content in polysaccharides. (Caurie 1970).

$$X_{eq} = e^{\left[a_W \ln(D) - 1/4.5 x_s\right]} \quad \text{(Eq. 4-4)}$$

Where X_s is the safe storage moisture content (d.b.) and D (-) is a constant.

- Halsey: Halsey model (Eq. 4-5) proved to be useful for systems with type I, II and III isotherms, and systems with high content in polysaccharides (Halsey 1948).

$$X_{eq} = \left(\frac{-A}{T \ln(a_W)}\right)^{1/B} \quad \text{(Eq. 4-5)}$$

Where T is the absolute temperature (K), and A (d.b.·K) and B (-) are constants.

- Oswin: Oswin equation (Eq. 4-6) is another wide used model that properly fits the isotherm behaviour of many food systems (Oswin 1946).

$$X_{eq} = E\left(\frac{a_W}{1 - a_W}\right)^F \quad \text{(Eq. 4-6)}$$

Where E (-) and F (-) are constants.

The goodness of the fit of each model was determined based on coefficient of determination (R^2) and root mean square error (E_{RMS}) (Eq. 4-7):

$$E_{RMS} = \left[\frac{1}{N}\right]\sum_{i=1}^{N}\left(X_{exp} - X_{cal}\right)^{1/2} \quad \text{(Eq. 4-7)}$$

The values of the parameters of five all models were obtained using Microsoft Excel 2013 (Solver add-on) by means of non-linear programming in which E_{RMS} is minimized.

4.2.3. Determination of drying kinetics

4.2.3.1. Determination of drying kinetics

Drying experiments were carried out in a hot air convective dryer (Angelantoni, Challenge 250, Italy) at different temperatures (35, 50, 60 and 75ºC) keeping relative humidity (30%) and air velocity (2 m/s) constant in all experiments. All experiments were performed until moisture content was close to equilibrium. For all cases, experiments were carried out in two different configurations: deep-bed configuration and thin layer disposition. In the first case, seaweed samples were selected on the basis of having similar sizes (length: 15 cm, width: 3 cm) and arranged in a metallic mesh (45x45x7 cm^3) to allow transversal flow with the same load density (14.88±0.08 kg/m^2). In the thin layer disposition experiments, the height of the bed was reduced so the seaweed added was only enough to cover like a monolayer the whole mesh surface (45x45x1 cm^3). In addition, experiments with different load densities (1.25, 2.48, 3.07 and 14.88 kg/m^2) were carried out at 75ºC. The whole seaweed with the exception of the holdfast, which was cut with a thin blade, was employed in the drying experiments. In order to use fresh algae, a new batch of seaweed was collected for each drying temperature studied. All experiments were carried out at least in duplicate.

Drying kinetics were determined by weight using a balance (Cobos D-6000-CS, ±0.1 g, España). Samples were withdrawn and weighed every few minutes in the first stages of drying and every hour towards the end until moisture content reached values close to 14% (d.b.).

Drying rate (r) was measured as follows (Eq. 4-8):

$$r = \frac{w_{t-1} - w_t}{t_1 - t_{-1}} \quad \text{(Eq. 4-8)}$$

Where r (g/min) is the drying rate, w (g) is the mass of seaweed in the interval of time (t, min) considered.

4.2.3.2. Drying kinetics modelling

Deep-bed and thin layer configurations were modelled separately. Thin layer was used to determine diffusional coefficients of water in seaweed, which can only be obtained if the water is mainly removed by diffusional drying. Drying curves were modelled by following the development of moisture ratio (MR, -) over time (t, min). MR was calculated as follows (Eq. 4-9):

$$MR = \frac{X_t - X_{eq}}{X_0 - X_{eq}} \quad \text{(Eq. 4-9)}$$

Where X_t is the moisture content (d.b.) at any time, X_0 is the initial moisture content (d.b.) and X_{eq} is the equilibrium moisture content of the sample (d.b.). Equilibrium moisture contents at each drying temperature are obtained from the water sorption isotherms.

The models selected for the adjustment of experimental data of *F. vesiculosus* in the case of deep-bed configuration are depicted below (Vega-Gálvez et al. 2008) (Fudholi et al., 2012a) (Tello-Ireland et al. 2011):

- Newton model (Eq. 4-10):

$$MR = e^{-kt} \quad \text{(Eq. 4-10)}$$

Where k is the drying rate constant (min).

- Logarithmic model (Eq. 4-11):

$$MR = ae^{-kt} + c \quad \text{(Eq. 4-11)}$$

Where k is the drying rate constant (min), and a (-) and c (-) are model constants.

- Henderson – Pabis model (Eq. 4-12):

$$MR = ae^{-kt} \quad \text{(Eq. 4-12)}$$

Where k is the drying rate constant (min) and a (-) is a model constant.

- Weibull model (Eq. 4-13):

$$MR = e^{\left(-\left[t/\beta\right]^{\alpha}\right)} \quad \text{(Eq. 4-13)}$$

Where α (-) and β (min) are the shape and scale parameters, respectively.

- Two – Term model (Eq. 4-14):

$$MR = ae^{(-k_0 t)} + be^{(-k_1 t)} \quad \text{(Eq. 4-14)}$$

Where k_0 (min^{-1}) and k_1 (min^{-1}) are drying rate constants, and a (-) and b (-) are model constants.

- Page (Eq. 4-15):

$$MR = e^{-kt^n} \quad \text{(Eq. 4-15)}$$

Where k (min^{-n}) is the drying rate constant and n (-) is a model parameter.

- Modified Page (Eq. 4-16):

$$MR = e^{-(kt)^n} \quad \text{(Eq. 4-16)}$$

Where k (min^{-1}) is the drying rate constant and n (-) is a model parameter.

Thin layer configuration drying experimental data were fit d by means of equations based on Fick's second law for different geometries, which goal is to determine the water effective diffusivity through the seaweed. The most relevant geometries are semi-infinite layer, sphere and semi-infinite cylinder. The latter is the one that better adjusted to the experimental data of the present work. The equations associated to the semi-infinite cylinder geometry and further elucidation are showed below.

The application of the Fick's second law derived equations is subject to two assumptions (Mujumdar 2006):

- Initially, the distribution of the moisture within the product is uniform.
- At t>0 surface reaches equilibrium moisture
- All resistances to water removal is inside the material. External resistances is negligible.
- There is no shrinkage of the material during drying.

To determine the effective diffusion coefficient, two equations must be applied, (Eq. 4-17) for short-time diffusion coefficient and (Eq. 4-18) for long-time diffusion coefficient (Crank 1975):

$$\frac{M_t}{M_\infty} = \frac{X - X_0}{X_e - X_0} = \frac{4}{\pi^{1/2}} \cdot \left(\frac{D_{eff} \cdot t}{r^2}\right)^{1/2} - \frac{D_{eff} \cdot t}{r^2} - \frac{1}{3 \cdot \pi^{\frac{1}{2}}} \cdot \left(\frac{D_{eff} \cdot t}{r^2}\right)^{\frac{1}{2}} + \cdots \quad \text{(Eq. 4-17)}$$

$$\frac{M_t}{M_\infty} = 1 - \sum_{n=1}^{\infty} \frac{4}{\alpha_n^2} \cdot e^{-D_{eff} \cdot \alpha_n^2 \cdot t / r^2} \quad \text{(Eq. 4-18)}$$

Where M_t (g) is the amount of water removed at time t (min), M_∞ (g) is the total amount of water removed when equilibrium is achieved, D_{eff} (m^2/s) is the water effective coefficient of diffusion, r (m) is the radius considered for the cylinder, α_n (-) are the roots of the first order Bessel function $J_0(x)$ for each term n (-) of the equation. In the present work, three terms of the (Eq. 4-18) were considered enough to fit the experimental data, so the expanded equation is as shown in (Eq. 4-19):

$$\frac{M_t}{M_\infty} = 1 - \left(\frac{4}{\alpha_1^2} \cdot e^{-D \cdot \alpha_1^2 \cdot t / r^2} + \frac{4}{\alpha_2^2} \cdot e^{-D \cdot \alpha_2^2 \cdot t / r^2} + \frac{4}{\alpha_3^2} \cdot e^{-D \cdot \alpha_3^2 \cdot t / r^2}\right) \quad \text{(Eq. 4-19)}$$

Where α_1, α_2 and α_3 are, respectively, 2.4048, 5.5201 and 8.6537.

The application of the short-time or the long-time diffusion equations is subject to the following conditions (Table 4-3):

Table 4-3. Conditions for the application of short or long-time Fick's second law diffusion equations (Fito et al. 2001).

Equation	Fick Number	Time	M_t/M_∞
Short-time	$D_{eff} \cdot t/r^2 < 0.5$-0.6	$<< r^2/D_{eff}$	0-0.6
Long-time	$D_{eff} \cdot t/r^2 > 0.5$	$>> r^2/D_{eff}$	0.4-1

Both equations, short and long-time diffusion equations (Eq. 4-17, (Eq. 4-19), were applied by iterating water coefficient of diffusion until conditions cited in Table 4-3 were fulfilled.

The goodness of the adjustment of each model was determined based on coefficient of determination (R^2) and root mean square error (E_{RMS}) (Eq. 4-7). The values of the parameters of diffusional models were obtained using Microsoft Excel 2013 (Solver add-on) by means of non-linear programming in which E_{RMS} is minimized.

4.2.3.3. Colorimetry

Surface colour of the samples was measured using a colorimeter (CR 400, Konika Minolta, Japan). Calibration of the colorimeter is done by measuring the colour parameters of a standardized white glossy ceramic tile. Colour was measured by means of CIELab coordinates (L*, a* and b*) (CIELab 2006). In addition, total colour difference (ΔE*) was calculated at each drying time with fresh seaweed as control value (Eq. 4-20):

$$\Delta E^* = \sqrt{(L^* - L_f^*)^2 + (a^* - a_f^*)^2 + (b^* - b_f^*)^2} \qquad \text{(Eq. 4-20)}$$

Where L* is whiteness (L*=0) or brightness (L*=100), a* is redness (a*>0) or greenness (a*<0) and b* is yellowness (b*>0) or blueness (b*<0) (Figure 4-1).

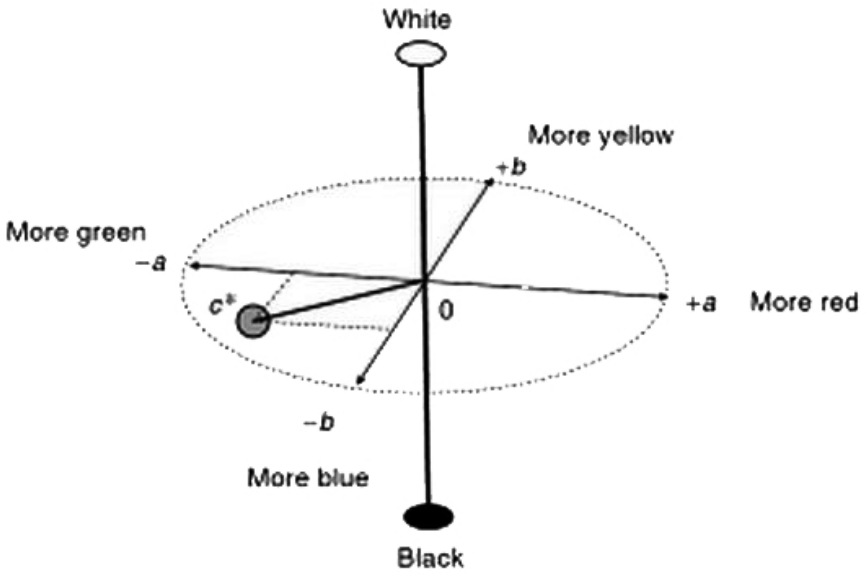

Figure 4-1. CIE-Lab colour expression system (Chen & Mujumdar 2009).

Colour measurement was made separately on the receptacles/conceptacles and on the lamina of the seaweed. Each measure was made nine times (three triplicates on three different surface points). To determine the qualitative effect of ΔE values,

Table **4-4** was employed:

Table 4-4. Colour difference evaluation (Li 1998).

Colour change	ΔE*
Trace level difference	0 – 0.5
Slight difference	0.5 – 1.5
Noticeable difference	1.5 – 3.0
Appreciable difference	3.0 – 6.0
Large difference	6.0 – 12.0
Very obvious difference	>12.0

4.2.3.4. Shrinkage

Most materials shrink as drying takes place. These volume changes were measured by applying Archimedes' principle of liquid displacement. Small seaweed samples (approximatively 0.5-1.5 g) were immersed in a probe filled with heptane at 25ºC at different drying times and the volume displaced was measured. From experimental shrinkage determination, a characteristic dimension (in this case, radius of semi-infinite cylinder) was calculated and then introduced into kinetic modelling. The variation of volume of the sample (V) is measured by means of variation in comparison to its initial volume (V_0). Its plotting vs volume reduction due to water removal, measures how distant from ideal behaviour (volume loss is only due to water removal) the system is.

Plotting of drying rate per unit of surface area (including effect of volume) against moisture was used to estimate the critical moisture content (X_c, d.b.) at different temperatures. Drying rate per unit of surface area was obtained applying (Eq. 4-21):

$$J_w = \frac{\frac{X_{t-1} - X_t}{t_1 - t_{-1}}}{a} \qquad \text{(Eq. 4-21)}$$

Where J_w (d.b..m^{-2}) is the specific drying rate a (m^2) is the area at the given interval.

4.2.4. Milling

After drying, *F. vesiculosus* was left aerating for 1-2 days. In order to facilitate milling dried seaweed was then triturated (seaweed size lower than ~0.5 cm) in a laboratory blender (Waring Blender HGBTWT, USA). Then, it was milled in an ultra-centrifugal mill

(ZM200 Retsch GmbH, Germany) using a 500 µm internal sieve. Afterwards, milled seaweed was storage at 4ºC in vacuum sealed bags until further utilization.

4.2.4.1. Physical and chemical characterization

4.2.4.1.1. Water content

The method used to determine the moisture content of the seaweed powder was the same as the one described in section 4.2.1.1 (Water content).

4.2.4.1.2. Granulometric characterization

Granulometric characterization of milled seaweed was carried out using sieves (Cisa Cedaceria Industrial, Spain) with different standardized meshes (500, 250, 125, 80, 63 and 40 µm). Size distribution curves were obtained, and the mass mean diameter D_w, (Eq. 4-22), the volume mean diameter D_v, (Eq. 4-23) and the surface mean diameter D_s, (Eq. 4-24) were calculated for each drying temperature.

$$D_w = \sum x_i D_{pi} \quad \text{(Eq. 4-22)}$$

$$D_v = \sum \left({}^{x_i}/_{D_{pi}} \right)^{-1/3} \quad \text{(Eq. 4-23)}$$

$$D_s = \frac{1}{\sum {}^{\Delta x_i}/_{D_{pi}}} \quad \text{(Eq. 4-24)}$$

Where D_{pi} (µm) is the mean diameter for each fraction and x_i (-) is the weight fraction.

Mass mean diameter is important for milling characterization. D_v provides information about pore surface area and may be used when equivalent volume is the main concern (buoyancy, fluidized beds). D_s is used when equivalent surface exposure area is important: reactions, adsorption or, for this matter, extractions.

4.2.4.1.3. Colorimetric characterization

Colorimetric characterization was carried out applying the method described in section 4.2.3.3. It was applied to all seaweeds, formerly dried at 35, 50, 60 and 75ºC. The colorimetric parameters were obtained for all fractions for each system.

In this case, the parameters used as control for the calculation of ΔE* of different fractions were the ones obtained for all the fractions mixed.

4.2.5. Extracts obtention and characterization

4.2.5.1. Ultrasound extraction

The dried samples of algae were treated with ultrasound in order to facilitate the extraction of the components of interest. The equipment employed was an ultrasound homogenizer, model UIP – 1000 hdT (Hielscher, Germany) (Figure 4-2). It can operate in batch or in continuous flow. In this study, all experiments were carried out in batch because of the low amount of seaweed powder employed, and for a greater ease of use and control of operation conditions. Extractions took place using a 200 mL beaker. The operation temperature was controlled employing a cold water bath to avoid temperatures higher than 40ºC that could affect antioxidant activity. All extractions were performed using water as solvent, except for one, carried out with acetone/water (70:30 v/v) to obtain an extract as a reference point. All systems were rehydrated during 15 minutes before the extraction.

Figure 4-2. Ultrasound transducer and generator model UIP – 1000 hdT (Hielscher).

The equipment operates with a frequency of 20 kHz and irradiation power up to 1000 W. The latter can be regulated in the panel in the ultrasound generator.

Extracts were centrifuged at 12400 rpm for 15 minutes using a Sigma 2 – 15 centrifuge (SciQuip, United Kingdom). The filtered supernatant (0.25µm) of the extracts were used for physical and chemical analysis.

4.2.5.2. Physical and chemical characterization of extracts

4.2.5.2.1. Antioxidant activity

Two main methods were used to measure antioxidant activity of the extracts: polyphenols content and DPPH scavenging activity.

4.2.5.2.1.1. Polyphenol content

The quantitative determination of polyphenols was put into practice applying the Single and Rossi method (Singleton & Rossi 1965). It is a colorimetric method based on the change in absorbance (765 nm) of the Folin-Ciocalteau reagent when reacting with the hydroxyl groups of the polyphenolic substances. The absorbance measure is introduced in the calibration line obtained for a known phenolic compound. In this study, the compound of choice is the phloroglucinol. Hence, polyphenols content of the extracts will be expressed as phloroglucinol equivalents.

4.2.5.2.1.2. DPPH scavenging activity

Antioxidant capacity of food systems is attributed to its capacity to inhibit the effect of different free radical substances. The DPPH assay proposed by Brand-Williams et al. (1995) measures the capacity of the system to react with a known free radical agent (2,2-diphenyl-1-picrylhydrazyl, DPPH). In its radical form, DPPH• absorbs at 515 nm, but upon reduction by an antioxidant (AH) or a radical species (R•) the absorption disappears. As the reaction takes time to fully develop, for the determination of the DPPH scavenging activity absorbance is measured every 5 minutes until it reaches the stationary state. Scavenging activity is measured by means of (Eq. 4-25):

$$\text{Scavenging activity (\%)} = \frac{(abs_{initial} - abs_{final})}{abs_{initial}} \qquad \text{(Eq. 4-25)}$$

Where $abs_{initial}$ (-) is absorbance at time 0 and abs_{final} (-) is the absorbance after one hour.

4.2.5.2.2. Carbohydrates

Carbohydrates content of the extracts was determined using the Dubois, et al. (1956) method. This method employs sulfuric acid and phenol as reagents. In the presence of strong acids and heat, carbohydrates undergo a series of reactions which lead to the formation of furan derivatives such as furanaldehyde and hydroxymethyl furaldehyde. These compounds condense with themselves or with phenolic substances leading to the formation of dark colored compounds (Figure 4-3).

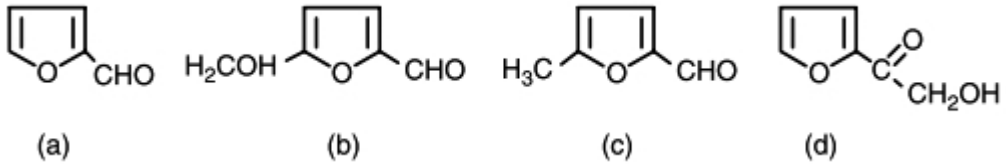

Figure 4-3. Furan derivatives from (a) pentoses and hexuronic acids, (b) hexoses, (c) 6-deoxyhesoses, and (d) keto-hexoses, respectively (Brummer & Cui 2005)

Furan derivatives from pentoses and hexoses exhibit peaks of light absorbance in the range of 480 – 490 nm (Figure 4-4) (Brummer & Cui, 2005) .

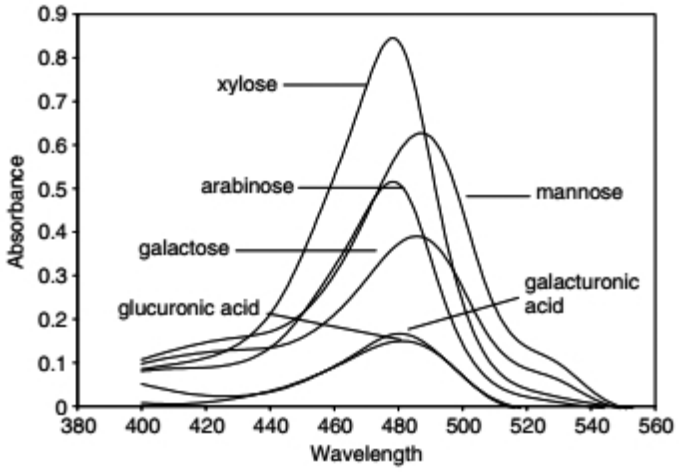

Figure 4-4. Phenol–sulphuric acid assay absorbance maxima for hexoses and pentoses (Brummer & Cui 2005)

For this work, the samples were evaluated measuring the absorbance read at 485 nm and glucose was used to draw the calibration curve. Hence, carbohydrates concentration is expressed as glucose equivalents.

4.2.5.2.3. Alginates

Alginate quantitative determination was carried out by means of Blumenkrantz & Asboe-Hansen (1973) method and a further modification by Filisetti-Cozzi & Carpita (1991). The assay consists on the measurement of absorbance at 520 nm of the samples in the presence of sodium tetraborate (increases the sensitivity of the reaction with uronic acids) in sulphuric acid and *m*-hydroxydiphenil as colour reagent. The modification proposed by Filisetti-Cozzi & Carpita introduces the use of sulfamate in order to reduce the interference of neutral sugars (development of brown pigments) in the measurement (Wrolstad et al. 2005). The compound of reference used for the construction of the calibration curve is the glucuronic acid. Therefore, all measurements are expressed as glucuronic acid equivalents (GLU).

4.2.5.2.4. Total solids content

Determination of total solids in the extracts was achieved by means of the 2540 B Standard Method (Symons & Morey 1941). This method consists on the determination of total solids in a sample by drying at 103 – 105ºC for 24 hours. Samples were weighed until constant weight is reached (in this case, a maximum of two consecutive measurements on two different days were done).

4.2.6. Statistical analysis

Differences among means were identified by one-factor analysis of variance (ANOVA), followed by the Scheffé test and considering significant P-values ≤ 0.05 (IBM SPSS Statistics 20.0.0).

5. Assayed systems

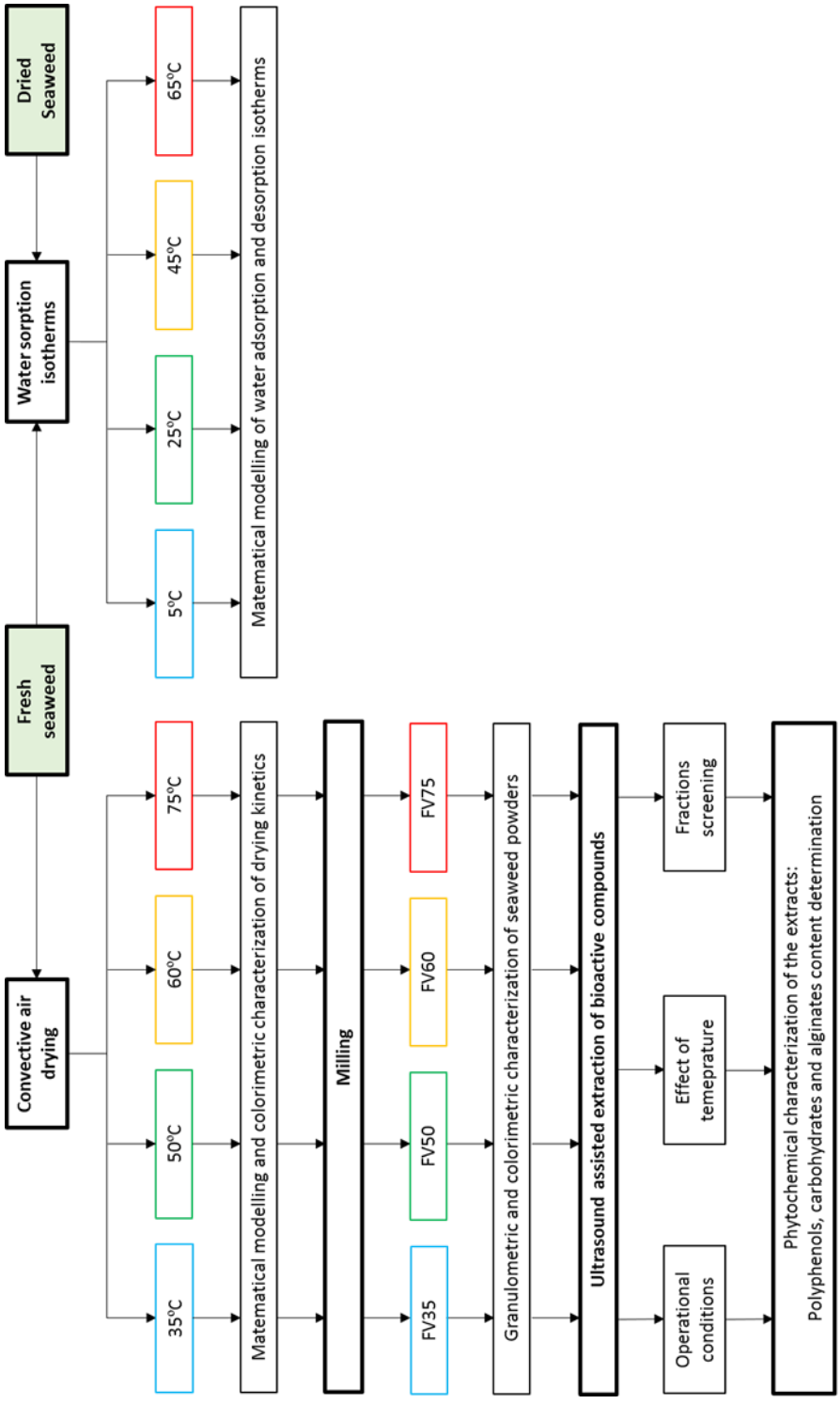

Figure 5-1. Work flow diagram and systems assayed.

6. Results and discussion

6.1. Determination of water sorption isotherms

Fucus vesiculosus experimental data of equilibrium moisture content at four different temperatures are shown in Figure 6-1. Equilibrium water content increases as temperature decreases from 65ºC to 5ºC. In addition, both adsorption and desorption isotherms, equilibrium moisture content increases with water activity. Water sorption isotherms show a type III tendency at lower temperatures (5 – 25 ºC) while, as temperature raises (45 – 65ºC), this trend leans towards a type II isotherm following Brunauer's classification (Brunauer et al. 1940).

At low water activity range (0.1 – 0.5), a difference between water adsorption and desorption isotherms is also noticeable. At low temperatures (5 – 25ºC), desorption isotherms present a higher water content than adsorption isotherms at the same water activity. This behaviour is known as hysteresis cycle. This behaviour does not seem noticeable as temperature is raised to 45ºC. When temperature is raised to 65ºC, adsorption isotherm appears to be over desorption isotherm and, thus, the hysteresis cycle is inverted.

In the upper range of water activities (0.7 – 0.9), adsorption and desorption isotherms exhibit a crosspoint in which the effect of temperature is inverted. At the same water activity, equilibrium moisture content is higher when temperature is increased.

These trends depicted before are linked with the solubility of polysaccharides at high temperatures and water activities (Bell & Labuza 2000). They are common tendencies among seaweeds such as alga *Gracilaria* (Lemus et al. 2008), *Gelidium sesquipedale* (Ait-Mohamed et al. 2005) and *Macrocystis Pyrifera* (Vega-Gálvez et al. 2008), which present a high polysaccharide content.

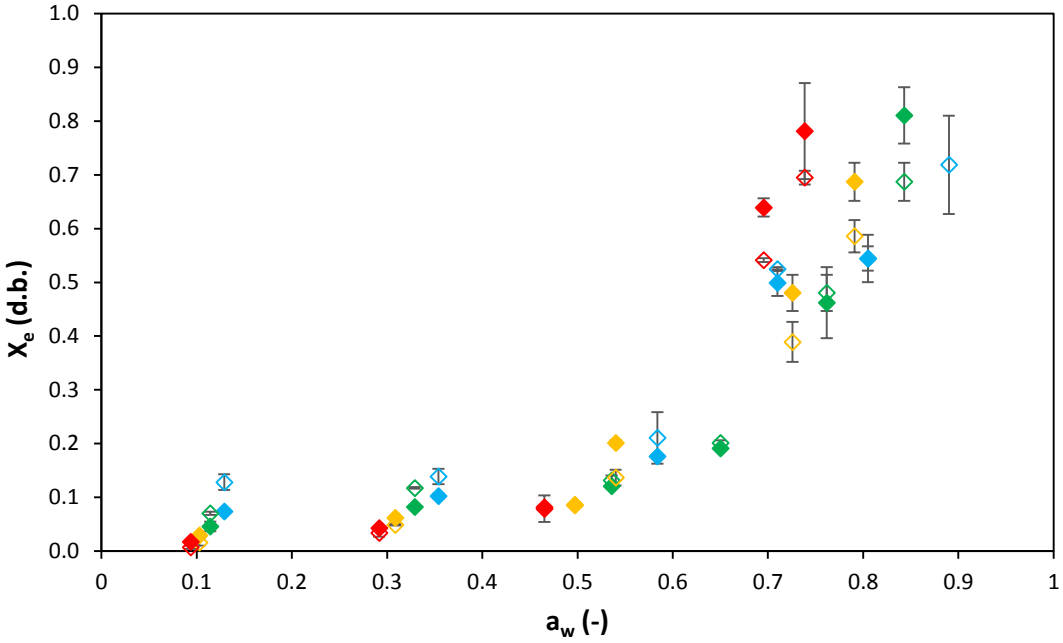

Figure 6-1. Experimental data. (5ºC (♦), 50ºC (♦), 45ºC (♦) and 65ºC (♦), empty symbols represent desorption data).

Table 6-1 shows the parameters obtained as a result of the adjustment of experimental data to the models introduced in chapter 4.2.2: GAB (Eq. 4-2), BET (Eq. 4-3), Caurie (Eq. 4-4), Halsey (Eq. 4-5) and Oswin (Eq. 4-6).

Table 6-1. Model parameters for adsorption and desorption isotherms at 5, 25, 45 and 65ºC. †

Model	Parameter	Desorption				Adsorption			
		5ºC	25ºC	45ºC	65ºC	5ºC	25ºC	45ºC	65ºC
GAB (Eq. 4-2)	m_0 (d.b.)	0.128±0.006	0.079±0.003	0.252±0.130	0.460±0.091	0.154±0.042	0.188±0.161	0.157±0.017	0.703±0.225
	C_1 (-)	7.308±1.424	8.807±5.117	0.319±0.115	0.147±0.044	2.131±1.230	1.406±1.618	0.112±0.017	0.113±0.018
	k (-)	0.910±0.035	1.026±0.028	0.997±0.049	1.061±0.002	0.950±0.034	1.021±0.077	0.911±0.014	1.042±0.055
	E_{RMS}	0.040	0.044	0.012	0.025	0.052	0.027	0.069	0.040
	R^2	0.95	0.99	0.93	0.996	0.98	0.990	0.98	0.992
BET ($0<a_w<0.5$) (Eq. 4-3)	X_m (d.b.)	0.092±0.023	0.066±0.005	0.057±0.007	0.064±0.002	0.073±0.003	0.060±0.001	0.064±0.040	0.062±0.002
	C (-)	116.00±1.41	93.50±2.12	2.87±0.88	1.75±1.06	40.98±2.86	12.02±1.38	8.75±4.51	2.59±0.18
	E_{RMS}	0.019	0.013	0.004	0.007	0.004	0.006	0.016	0.002
	R^2	0.95	0.94	0.996	0.98	0.997	0.993	0.991	0.997
Caurie (Eq. 4-4)	D (-)	120..0±95.2	559.7±584.4	421.1±102.4	1522.8±566.9	546.6±603.2	802.1±101.2	427.465±101.8	1808.9±1209.9
	X_s (d.b.)	0.049±0.001	0.041±0.009	0.042±0.002	0.039±0.002	0.043±0.011	0.038±0.001	0.045±0.002	0.039±0.003
	E_{RMS}	0.048	0.067	0.012	0.015	0.058	0.035	0.060	0.029
	R^2	0.96	0.98	0.997	0.999	0.98	0.999	0.97	0.990
Halsey (Eq. 4-5)	A (d.b.·K)	21.222±4.928	29.48±8.45	53.51±2.21	87.44±0.07	26.34±4.01	44.03±3.24	65.95±2.12	92.89±6.69
	1/B (-)	0.691±0.031	1.045±0.065	1.555±0.057	2.070±0.093	0.930±0.097	1.384±0.026	1.529±0.056	2.077±0.187
	E_{RMS}	0.043	0.048	0.014	0.026	0.042	0.026	0.077	0.040
	R^2	0.99	0.999	0.99	0.99	0.97	0.99	0.99	0.996
Oswin (Eq. 4-6)	E (-)	0.221±0.016	0.119±0.015	0.107±0.017	0.129±0.012	0.199±0.016	0.104±0.016	0.154±0.020	0.144±0.006
	F (-)	0.572±0.036	0.950±0.046	1.289±0.058	1.651±0.072	0.723±0.039	1.230±0.031	1.265±0.056	1.670±0.169
	E_{RMS}	0.411	0.457	0.408	0.409	0.631	0.409	0.415	0.410
	R^2	0.95	0.99	0.96	0.98	0.95	0.998	0.998	0.99

†: Data are presented as means of ± standard deviation.

Figure 6-2 shows the representation of sorption isotherms experimental data up to water activities of 0.5 and BET model adjustments for each temperature. BET model C values (Table 6-1) decrease as temperature is raised from 5 (40.99±2.86, adsorption; 116.00±1.41 desorption) to 65ºC (2.590±0.18, adsorption; 1.75±1.06 desorption). BET classification establishes that values of C over 1 describe type II isotherm systems. On the other hand, values far below 1 describe type III isotherms (Brunauer et al. 1940). This confirms the fact that, at higher temperatures, sorption isotherms change their behaviour from type II to type III isotherms. The hysteresis cycles and the changes they undergo with temperature are also observable on Figure 6-2.

The parameter X_m (monolayer water content) has physicochemical meaning as it represents the water molecules at the primary layer (Vega-Gálvez et al. 2008). It is also considered to be the optimum moisture content, at which food spoilages processes are minimized (Bell and Labuza 2000). X_m shows a considerable decrease between the 5ºC isotherms (0.073±0.003 d.b. for adsorption; 0.092±0.023 d.b., for desorption) and higher temperature isotherms (0.062±0.003 d.b., for both adsorption and desorption).

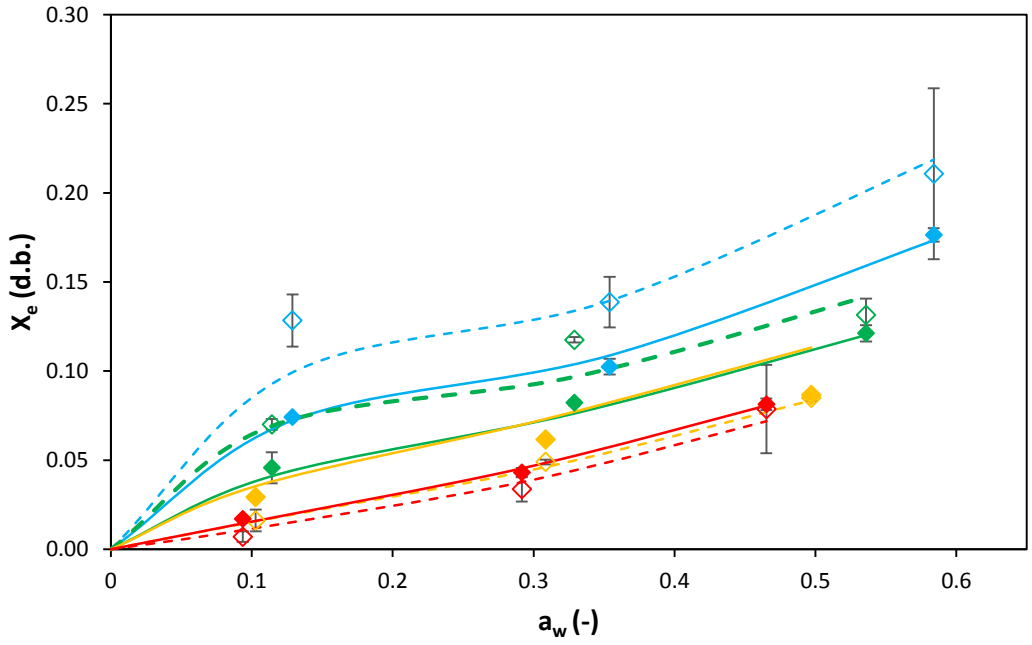

Figure 6-2. Experimental data (5ºC (♦), 50ºC (♦), 45ºC (♦) and 65ºC (♦), empty symbols represent desorption data) and BET (Eq. 4-3) model adjustment (5ºC (—), 50ºC (—), 45ºC (—) and 65ºC (—), dashed lines represent desorption isotherms) at low water activities.

Figure 6-3 and Figure 6-4 show the representation of the GAB, Caurie, Halsey and Oswin models:

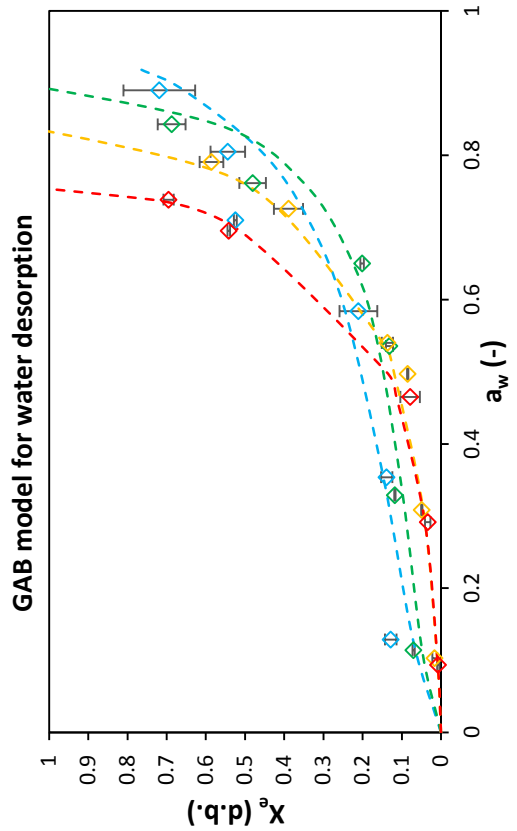

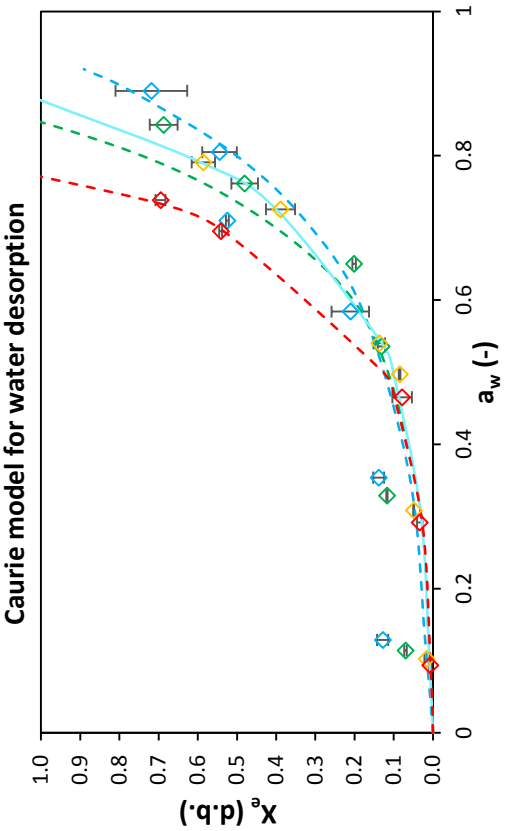

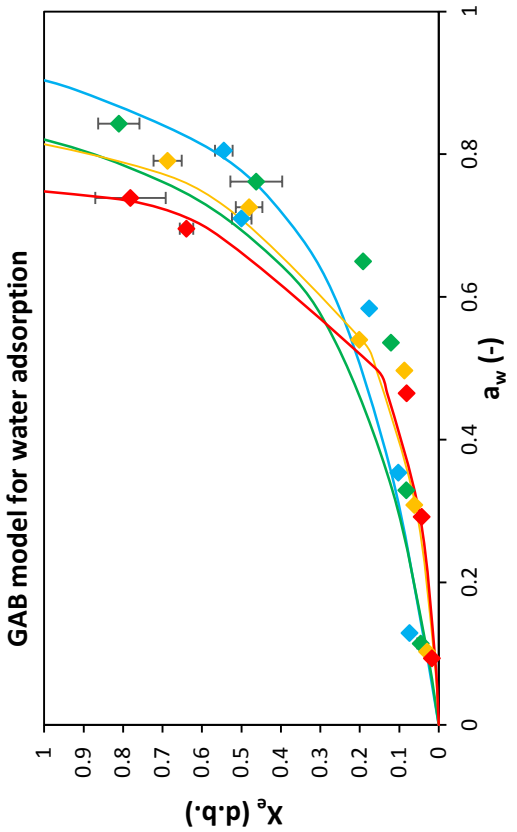

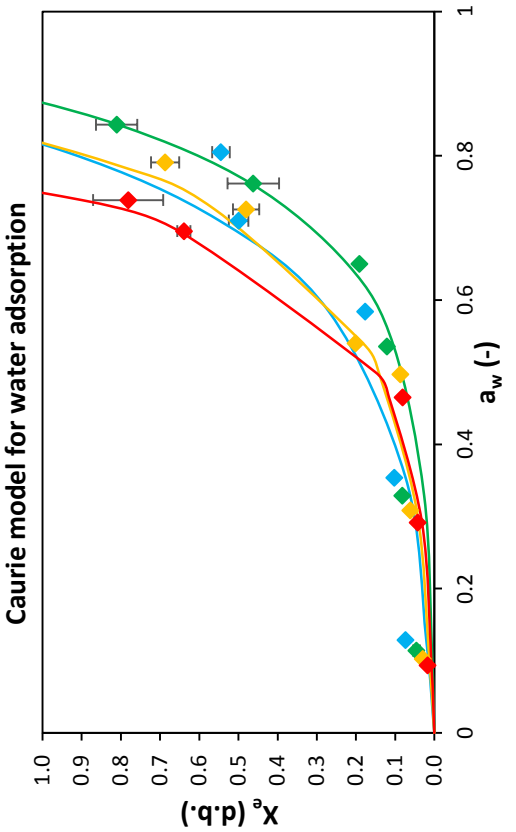

Figure 6-3. Experimental data of sorption isotherms along with GAB (Eq. 4-2) and Caurie (Eq. 4-4) models. 5°C (◆), 25°C (◆), 45°C (◆) and 65°C (◆). Adsorption adjustments are represented with straight lines: 5°C (—), 50°C (—), 45°C (—) and 65°C (—) (dashed lines represent desorption isotherms).

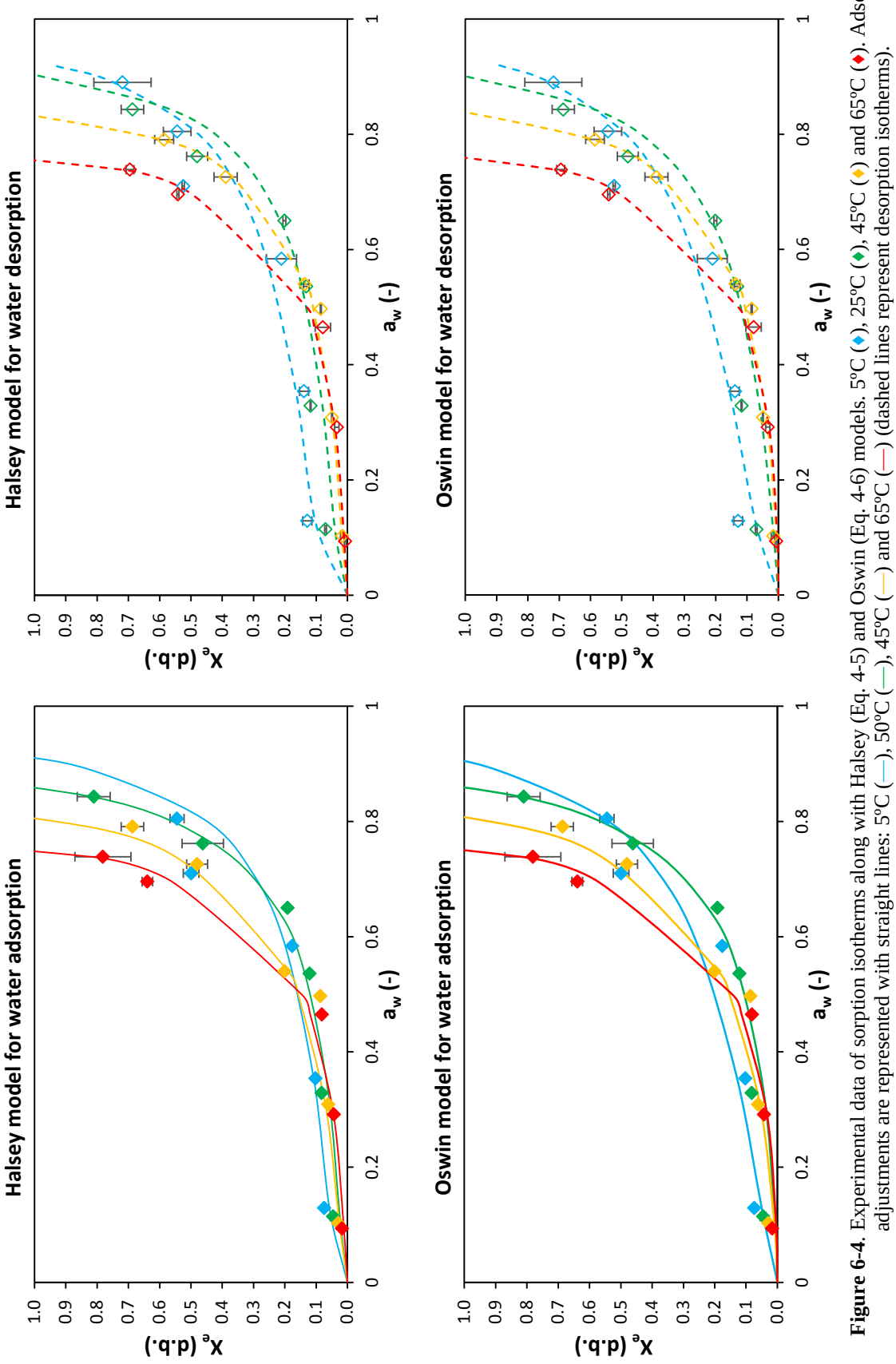

Figure 6-4. Experimental data of sorption isotherms along with Halsey (Eq. 4-5) and Oswin (Eq. 4-6) models. 5°C (◆), 25°C (◆), 45°C (◆) and 65°C (◆). Adsorption adjustments are represented with straight lines: 5°C (—), 50°C (—), 45°C (—) and 65°C (—) (dashed lines represent desorption isotherms).

Models plotting allow a clearer appreciation of the isotherms crosspoint at high water activities.

Oswin reported the lowest average R^2 values and the highest average E_{RMS} values, 0.985 and 0.444 respectively. In average, Halsey presented the best average R^2 (0.99) and E_{RMS} (0.040) coefficients. Caurie and GAB provide a good adjustment, but as it can be observed in Figure 6-3 and Figure 6-4 (and data provided by R^2 and E_{RMS} coefficients), said adjustment worsens at low temperatures. Halsey's model properly adjusts type II and III isotherms and, hence, shows the best adjustment for lower temperatures (5 – 25ºC, type II isotherm) and higher temperatures (45 – 65ºC, type III isotherm).

Halsey parameters have been found to follow linear (Eq. 6-1) and Arrhenius correlations (Eq. 6-2). The correlation of these parameters with temperature is shown in Figure 6-5.

$$A, {}^{1}/_{B} = a + b \cdot T \qquad \text{(Eq. 6-1)}$$

$$\ln\left(A, {}^{1}/_{B}\right) = \ln\left(A_0, {}^{1}/_{B_0}\right) - \frac{E_a}{R \cdot T} \qquad \text{(Eq. 6-2)}$$

Where a (-) and b (-) are equation parameters, T (K) is the temperature, E_a is the energy of activation (J/mol) and R (8.314 J/K·mol) is the universal constant of gases.

Constants of each correlation for both, adsorption and desorption Halsey model parameters, are shown in Table 6-2:

Table 6-2. Linear and Arrhenius correlations parameters.

	Adsorption			**Desorption**		
Linear (Eq. 6-1)	**a (d.b.·K)**	**b (d.b.)**	**R^2**	**a (d.b.·K)**	**b (d.b.)**	**R^2**
A (d.b.·K)	-284.091	1.108	0.991	-295.17	1.113	0.94
	a (-)	**b (K^{-1})**	**R^2**	**a (-)**	**b (K^{-1})**	**R^2**
1/B (-)	-4.04	0.018	0.96	-5.82	0.023	0.993
Arrhenius (Eq. 6-2)	**E_a (kJ/mol)**	**ln(A_0,1/B_0)**	**R^2**	**Ea (kJ/mol)**	**ln(A_0,1/B_0)**	**R^2**
A	16.38	10.38	0.998	18.88	11.10	0.98
1/B	9.82	4.21	0.96	14.42	5.88	0.998

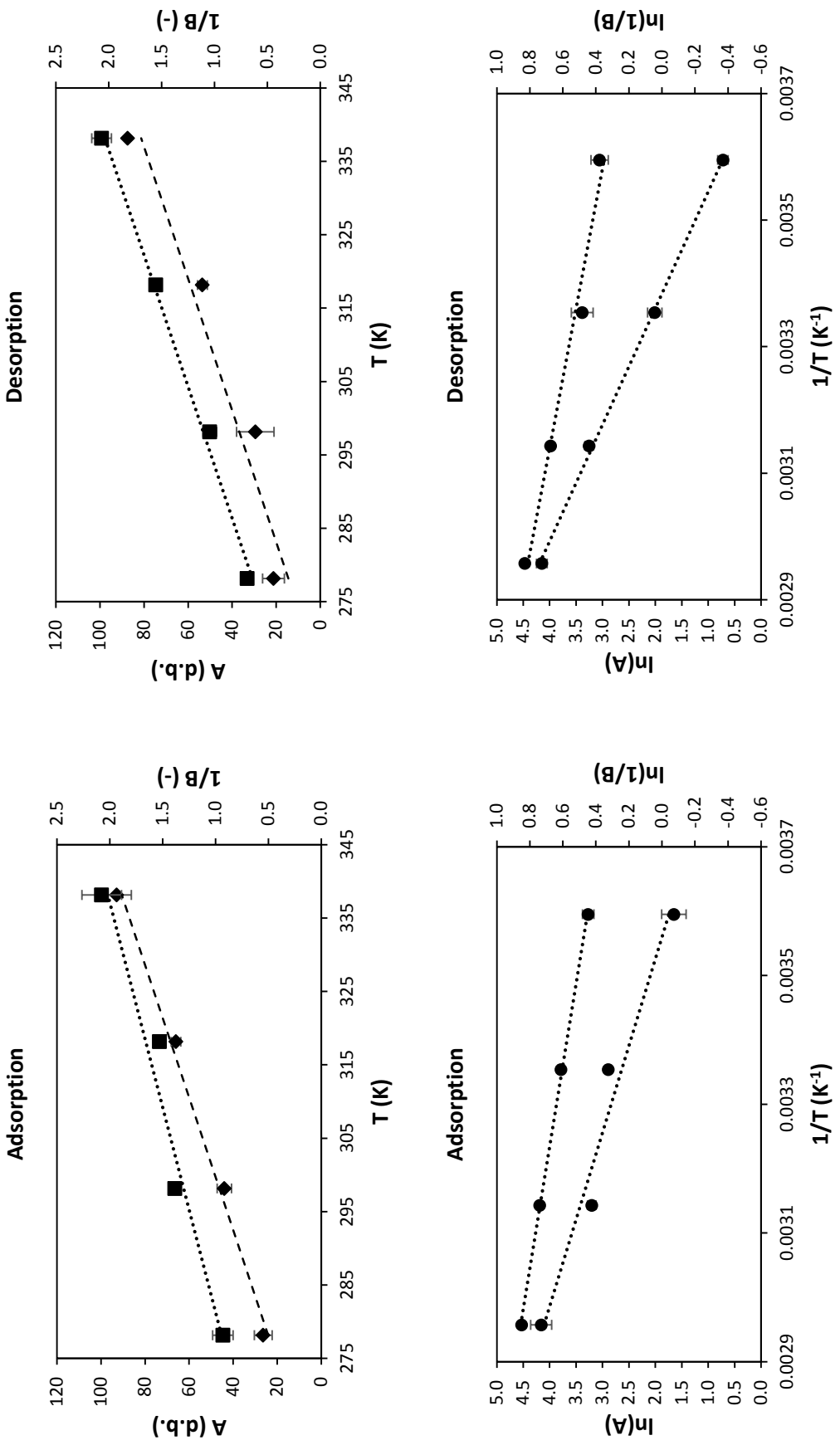

Figure 6-5. Linear and Arrhenius correlations of Halsey model parameters: A (◆, - - -) and 1/B (■, ····). Upper figures represent linear correlation (Eq. 6-1) for adsorption and desorption parameters at different temperatures. Lower figures represent Arrhenius correlation (Eq. 6-2) at different temperatures.

Both correlations can be introduced into Halsey model, resulting in models shown in equations (Eq. 6-3) and (Eq. 6-4):

$$X_{eq} = \left(\frac{-(a_A + b_A \cdot T)}{T\ln(a_W)}\right)^{(a_{(1/B)})+b_{(1/B)}\cdot T)} \quad \text{(Eq. 6-3)}$$

$$X_{eq} = \left(\frac{-A_0 \cdot e^{-E_{a,A}/R\cdot T}}{T\ln(a_W)}\right)^{1/B_0 \cdot e^{-E_{a,(1/B)}/R\cdot T}} \quad \text{(Eq. 6-4)}$$

Figure 6-6 shows the representation of both models fitting for water adsorption and desorption experimental data. Linear correlation presents a better adjustment (average R^2 of 0.990, average E_{RMS} of 0.075) than Arrhenius correlation (average R^2 of 0.980, average E_{RMS} of 0.100) for all temperatures.

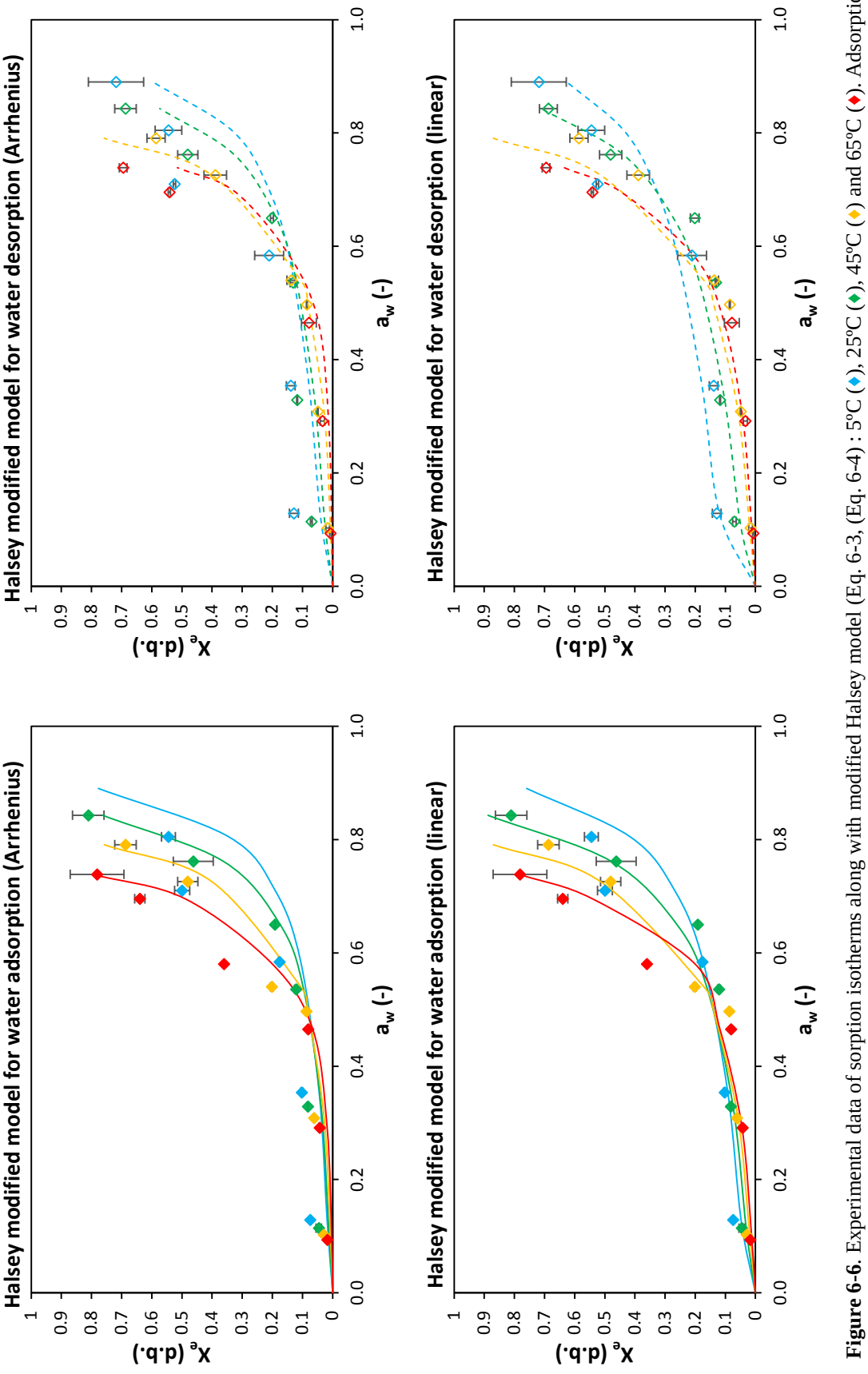

Figure 6-6. Experimental data of sorption isotherms along with modified Halsey model (Eq. 6-3, (Eq. 6-4) : 5°C (◆), 25°C (◆), 45°C (◆) and 65°C (◆). Adsorption adjustments are represented with straight lines: 5°C (—), 50°C (—), 45°C (—) and 65°C (—) (dashed lines represent desorption isotherms).

6.2. Determination of drying kinetics

As mentioned in chapter 4.2.3 (Determination of drying kinetics), experimental drying kinetics were determined using two configurations: deep-bed and thin layer configuration. Below, both configurations are treated separately.

6.2.1. Deep-bed configuration drying kinetics

Experimental drying of *F. vesiculosus* for bed configuration was carried out at four different temperatures (35, 50, 60 and 75ºC). Evolution of moisture was measured by means of moisture ratio and can be seen in Figure 6-7. All cases reached a final moisture ratio lower than 0.04 (close to equilibrium moisture). Drying temperature effect could be observed on total drying time, which was reduced as the former was increased. Drying at 35ºC exhibited the highest drying time to achieve a MR of 0.04 with 1517 min, followed by 50ºC with 1395 min, and 60ºC and 75ºC required the lowest drying time with 1200 min.

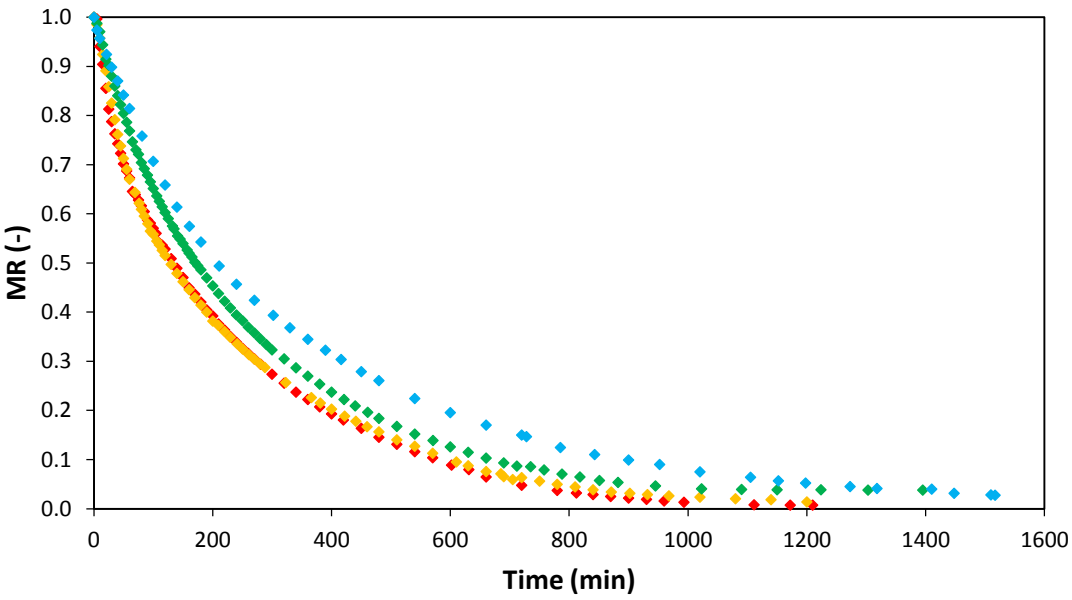

Figure 6-7. Experimental drying curves for *Fucus vesiculosus* (deep-bed configuration) at different drying temperatures: 35ºC (♦), 50ºC (♦), 60ºC (♦) and 75ºC (♦).

Drying rate can be measured, as shown in Figure 6-8, as means of variation of mass over time.

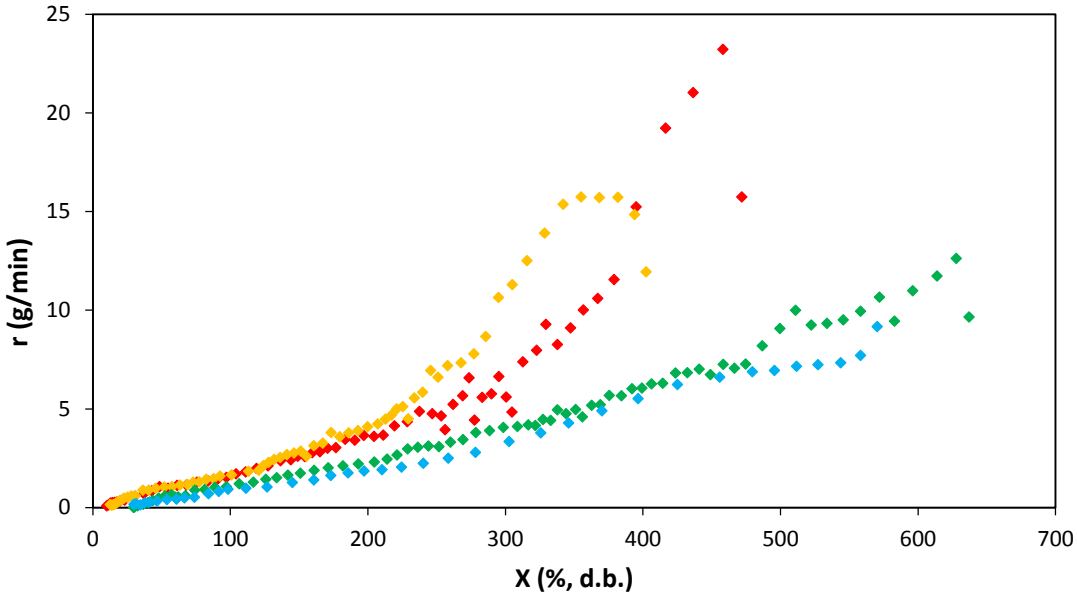

Figure 6-8. Drying rate curves for *Fucus vesiculosus* (deep-bed configuration) at different drying temperatures: 35ºC (♦), 50ºC (♦), 60ºC (♦) and 75ºC (♦).

Drying rate curves for 60 and 75ºC display a clear induction stage at high moisture. This phase corresponds to the unsteady state heating period. Afterwards, both systems show a similar trend to that displayed by the 35 and 50ºC cases for the whole experiment. This subsequent stage is characterized by a falling rate period, in which the rate of moisture migration to the surface is lower than the rate of evaporation and, thus, originating a dried surface and an increase in its temperature. This stage lasts until the equilibrium moisture is reached (Hui 2008).

Drying kinetics experimental data were fitted to the models mentioned in chapter 4.2.3.2 (Modelling of drying kinetics). Resulting parameters of the corresponding fittings are shown in Table 6-3. Two – term (Eq. 4-14), Page (Eq. 4-15) and modified Page (Eq. 4-16) presented the best adjustment (R^2 equal to 0.999 and E_{RMS} lower than 0.018). The former is a four parameter model and showed the best fit (E_{RMS}<0.007). Regarding Page and modified Page, these two only need two parameters to be adjusted, so they are simpler. Besides, Page model is the most used model to fit drying kinetics data.

Page model fit parameters are shown in Table 6-3. From the kinetic parameter *k* for each temperature, one can draw the same conclusion observed in Figure 6-7 but more clearly identified in Figure 6-8. There exists a gap between drying rate at 35-50 ºC and 60-75ºC.

Table 6-3. Drying models fitting parameters for each temperature (1) (Newton, Logarithmic, Henderson – Pabis models, Weibull and Two – term models). †

Model	**Newton (Eq. 4-10)**			**Logarithmic (Eq. 4-11)**					**Henderson – Pabis (Eq. 4-12)**			
T (ºC)	**k·10³(min⁻¹)**	**E_{RMS}**	**R^2**	**a (-)**	**k·10³(min⁻¹)**	**c·10³ (-)**	**E_{RMS}**	**R^2**	**a (-)**	**k·10³(min⁻¹)**	**E_{RMS}**	**R^2**
35	2.99±0.15	0.026	0.999	0.94±0.02	3.15±0.26	37.10±0.07	0.014	0.999	0.96±0.01	2.80±0.16	0.020	0.998
50	3.92±0.04	0.021	0.999	0.93±0.01	4.24±0.20	39.00±0.07	0.010	0.999	0.97±0.01	3.70±0.05	0.016	0.998
60	4.69±0.27	0.045	0.995	0.89±0.01	4.68±0.15	38.81±0.07	0.028	0.995	0.90±0.01	4.00±0.27	0.032	0.994
75	4.83±0.14	0.047	0.995	0.86±0.03	4.70±0.44	18.02±0.07	0.024	0.996	0.89±0.01	4.04±0.15	0.027	0.995

Model	**Weibull (Eq. 4-13)**				**Two – term (Eq. 4-14)**					
T (ºC)	**α (-)**	**β (min)**	**E_{RMS}**	**R^2**	**a (-)**	**k_0·10³(min⁻¹)**	**b (-)**	**k_1·10³(min⁻¹)**	**E_{RMS}**	**R^2**
35	0.86±0.01	335.2±6.1	0.009	0.999	0.31±0.02	7.50±2.33	0.69±0.02	2.13±0.18	0.005	0.999
50	0.89±0.01	262.8±12.1	0.007	0.999	0.22±0.04	12.43±1.92	0.79±0.04	3.07±0.15	0.004	0.999
60	0.78±0.01	209.7±12.1	0.016	0.999	0.30±0.01	25.52±1.90	0.75±0.01	3.18±0.22	0.007	0.999
75	0.77±0.02	233.2±18.1	0.013	0.999	0.25±0.05	45.43±4.89	0.81±0.1	3.53±0.19	0.004	0.999

Model	**Page (Eq. 4-15)**				**Modified Page (Eq. 4-16)**			
T (ºC)	**k·10³(min^{-n})**	**n (-)**	**E_{RMS}**	**R^2**	**k·10³(min⁻¹)**	**n (-)**	**E_{RMS}**	**R^2**
35	6.63±0.52^a	0.86±0.01^a	0.009	0.999	2.98±0.16^a	0.86±0.02^a	0.009	0.999
50	6.94±0.21^a	0.89±0.01^a	0.007	0.999	3.83±0.03^b	0.89±0.01^a	0.007	0.999
60	14.74±0.13^b	0.78±0.01^b	0.016	0.999	4.58±0.27^c	0.77±0.01^b	0.018	0.999
75	15.78±0.12^b	0.77±0.02^b	0.013	0.999	4.67±0.19^c	0.79±0.01^b	0.015	0.999

†: Data are presented as means of ± standard deviation. Data value of each parameter with different superscript letters in rows are significantly different, $P \leq 0.05$

This is noticeable on the kinetic parameter *k* for the Page model, which is significantly different for both pair of temperatures. This gap is substantially more evident at earlier stages of drying. At this period the sample undergoes an unsteady heating phase and resistance to drying is focused on external convection. On later stages, drying rate curves seem to match their trends because resistance to water removal is now strong on diffusion of water through the food material. This event is studied more thoroughly within the monolayer configuration drying chapter.

Page parameters for another macro algae species can be found in bibliography.

Vega-Gálvez et al. (2008) adjusted drying experimental data of *Macrocystis pyrifera* (intertidal brown algae) to the modified Page model for similar temperatures and obtained the following kinetic parameters (*k*): of $6.44 \cdot 10^{-3}$ min^{-n} at 50ºC, $9.71 \cdot 10^{-3}$ min^{-n} at 60ºC and $13.74 \cdot 10^{-3}$ min^{-n} at 70ºC. These parameters are substantially higher than those observed for *F. vesiculosus*.

Lemus et al. (2008) provides values of parameters for the convective drying of *Gracilaria chilensis* (intertidal red algae) for the modified Page model: $3.5 \cdot 10^{-3}$ min^{-1} at 40ºC, $7.3 \cdot 10^{-3}$ min^{-1} at 50ºC, $9.0 \cdot 10^{-3}$ min^{-1} at 60ºC and $13.7 \cdot 10^{-3}$ min^{-1} at 70ºC. These values are higher than those obtained for *F. vesiculosus* within the same range of temperatures.

Fudholi et al. (2012b) obtained the Page parameters values for the convective drying of *Eucheuma cottonii* (subtidal red seaweed): 0.99 min^{-n} (n = 0.83) at 40ºC, 1.00 min^{-n} (n = 0.90) at 50ºC and 0.94 min^{-n} (n = 1.03) at 60ºC. Values are considerably lower than those obtained for *F. vesiculosus*.

All parameters values are within the range of those consulted in bibliography. However, when comparing them with those obtained in this work, it must be taken into account that different configurations and conditions of drying were applied.

In Figure 6-9 and Figure 6-10, the drying experimental data is shown along with the models adjusted for each temperature.

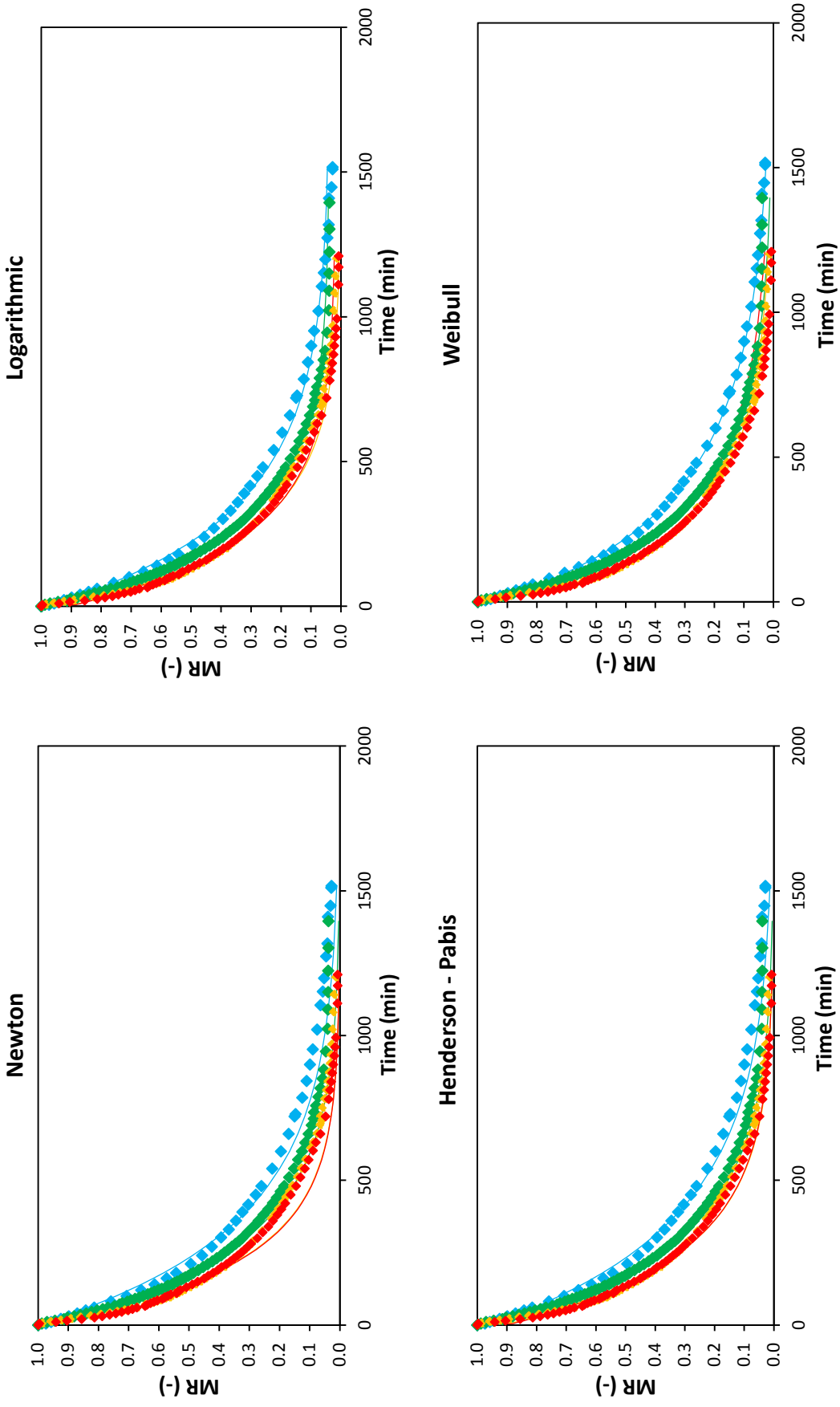

Figure 6-9. Experimental drying curves for *Fucus vesiculosus* (deep-bed configuration) at different drying temperatures: 35ºC (◆), 50ºC (◆), 60ºC (◆) and 75ºC (◆).The respective model fittings are represented by lines.

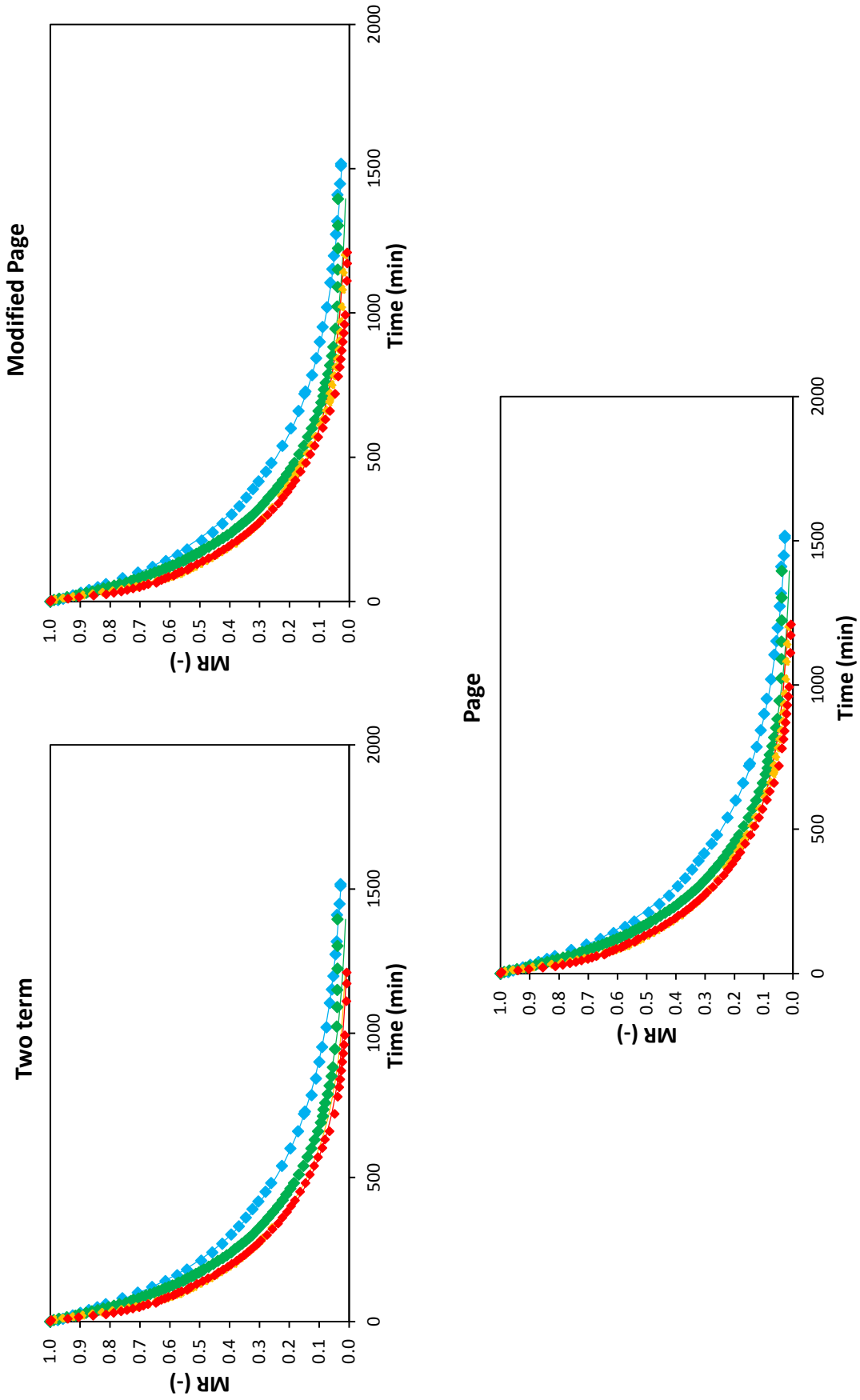

Figure 6-10. Experimental drying curves for *Fucus vesiculosus* (deep-bed configuration) at different drying temperatures: 35ºC (◆), 50ºC (◆), 60ºC (◆) and 75ºC (◆).The respective models fittings are represented by lines.

Figure 6-11 shows the adjustment of drying rate calculated with Page Model parameters and with experimental data. Models accurately predict the behaviour of drying rate with the exception of the initial stages of drying for high temperatures (60, 75ºC). At these phases, induction takes place. It is also observable that there are two different behaviours at low (35, 50ºC) and at high (60, 75ºC) temperatures. Induction is not appreciated at low drying temperatures. In addition, the slopes of both cases are clearly different.

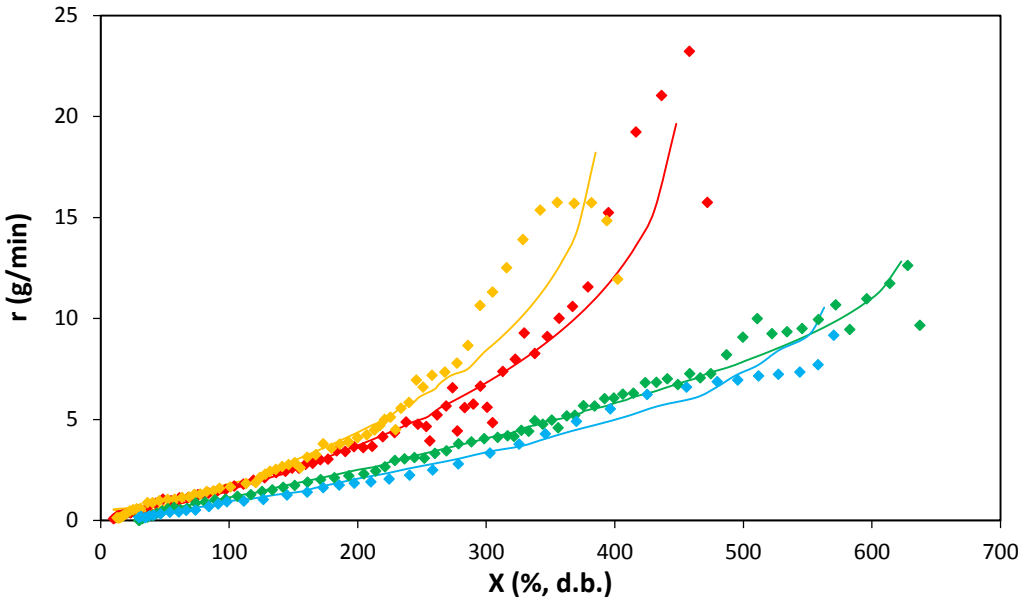

Figure 6-11. Drying rate curves for *Fucus vesiculosus* (deep configuration) at different drying temperatures: 35ºC (♦), 50ºC (♦), 60ºC (♦) and 75ºC (♦). The respective models adjustments are represented with a straight line.

6.2.2. Thin layer configuration drying kinetics

Besides seaweed arrangement, drying conditions were the same as those applied with bed configuration. That is, four drying temperatures were studied (35, 50, 60 and 75ºC) and drying experiments were finished once MR reached values below 0.04. Drying times were 130 (75ºC), 180 (60ºC), 305 (50ºC) and 355 (35ºC) minutes.

Below, in Figure 6-12, the drying curve for all temperatures is shown:

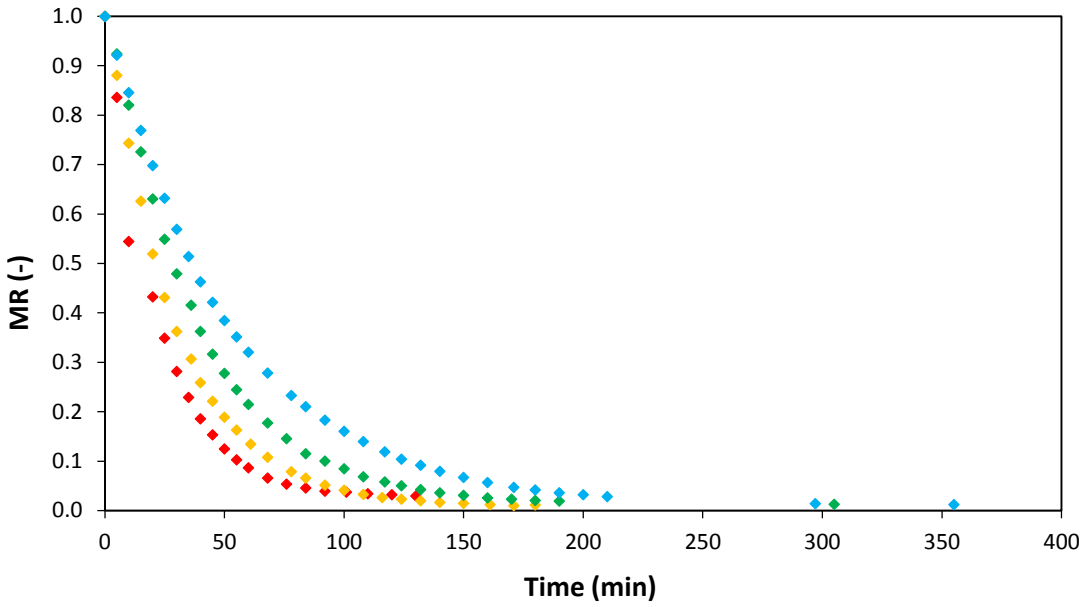

Figure 6-12. Experimental drying curves for *Fucus vesiculosus* (thin layer configuration) at different drying temperatures: 35ºC (♦), 50ºC (♦), 60ºC (♦) and 75ºC. (♦).

The impact of drying temperature can be easily assessed, as its increase enhances drying rate and, therefore, reduces drying time. Figure 6-13 shows the effect of temperature on drying rate. Apparently, no effect of temperature on drying rate for the thin layer configuration is observed.

This result may suggest that the main difference between configurations (deep-bed and thin layer) can be attributed to the difficulty of free water of seaweed inside the bed to migrate to the surface. Consequently, high mass transfer resistance in the deep-bed configuration are involved during drying.

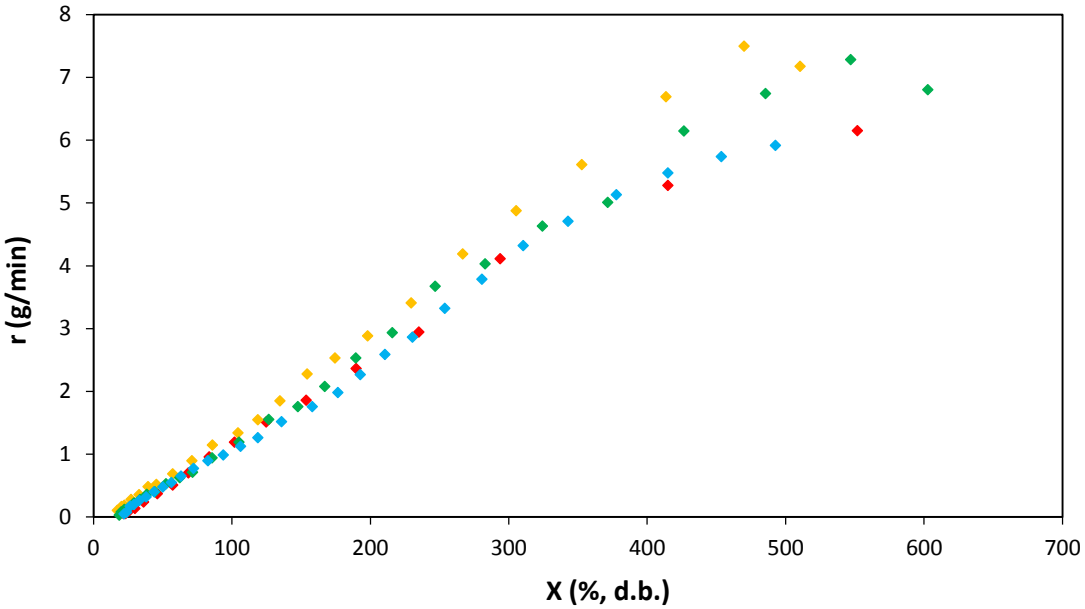

Figure 6-13. Drying rate curves for *Fucus vesiculosus* (thin layer configuration) at different drying temperatures: 35ºC (♦), 50ºC (♦), 60ºC (♦) and 75ºC (♦).

With the intention to validate or debunk this hypothesis, drying rate was measured as means of mass loss over time taking into consideration the effect of volume reduction. In order to do so, shrinkage was introduced to the drying rate curves. Beneath, shrinkage and its effect on drying is studied, along with the modelling of the drying curves for the thin layer configuration experiments.

6.2.2.1. Shrinkage

During drying, food materials can undergo shrinkage. This fact can be caused due to, firstly, the ideal shrinkage (reduction in volume equal to that equivalent to the loss of water) and, secondly, an additional volumetric reduction as a result of structural collapse during drying. This is noticeable in Figure 6-14, which displays the volumetric loss of the seaweed against the water loss in volume.

The diagonal line represents the ideal volume reduction, which is equal to the volume loss in water removed. All systems show a similar behaviour, as in all of them volume is more reduced than in the ideal case.

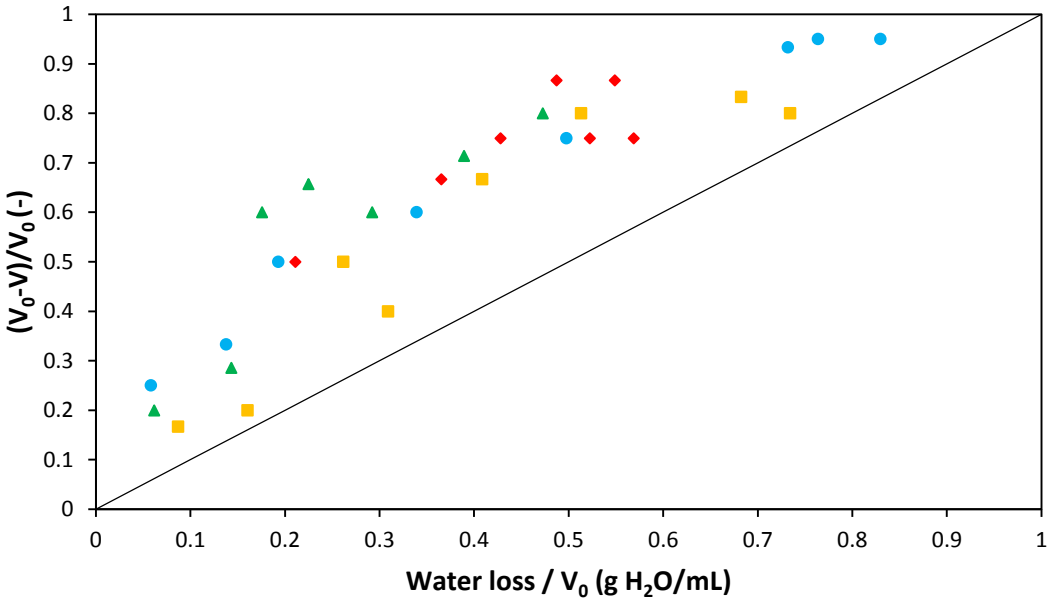

Figure 6-14. Volumetric shrinkage during convective drying of *Fucus vesiculosus* at 35ºC (♦), 50ºC (♦), 60ºC (♦) and 75ºC (♦).

An empirical fit equation is proposed for experimental shrinkage modelling, (Eq. 6-5):

$$V/V_0 = \frac{(a + c \cdot X)}{(1 + b \cdot X)} \qquad \text{(Eq. 6-5)}$$

Where a (-),b (d.b.$^{-1}$) and c (d.b.$^{-1}$) are fitting parameters, Table 6-4. Fitting goodness can be considered as acceptable (R^2>0.95 with the exception of shrinkage model at 50ºC and E_{RMS}<10.52). Figure 6-15 shows experimental data for each temperature and the corresponding model plotting:

Table 6-4. Parameters for the modelling of progression of volume with moisture content at different temperatures.

Parameter	35ºC	50ºC	60ºC	75ºC
a (-)	-0.71	19.54	13.95	17.48
b·10^3 (d.b.$^{-1}$)	1.15	-1.47	-1.69	-1.18
c ·10^3 (d.b.$^{-1}$)	59.9	0.6	4.5	22.3
R^2	0.996	0.846	0.95	0.96
E_{RMS}	3.33	8.03	10.52	5.34

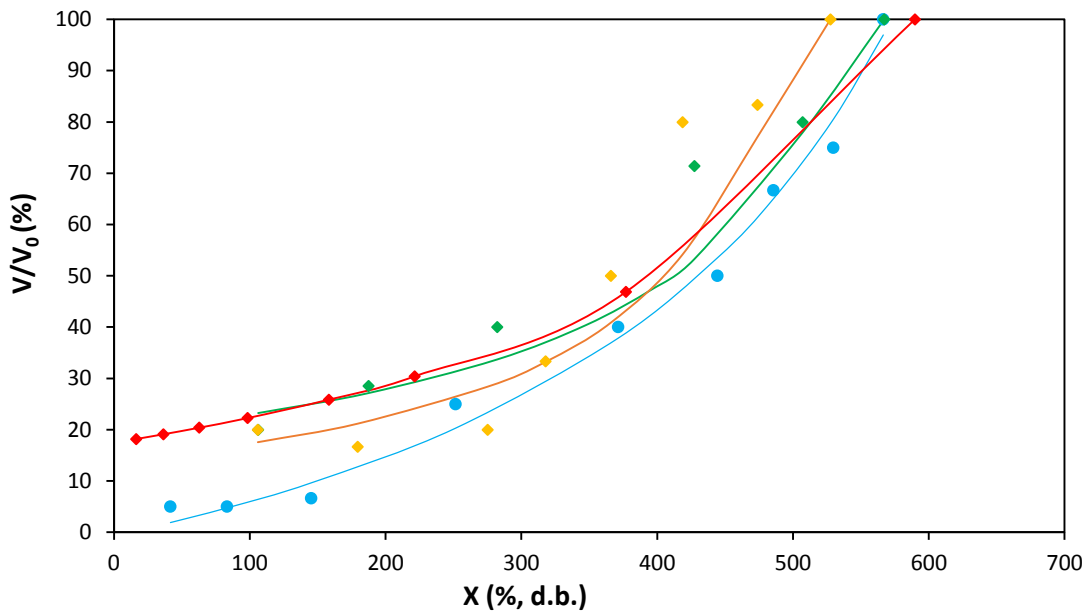

Figure 6-15. Volume shrinkage vs moisture content at different temperatures: 35ºC (♦), 50ºC (♦), 60ºC (♦) and 75ºC (♦).

Shrinkage modelling was introduced into the evaluation of drying rate curves (by means of moisture loss over time). The subsequent representation of the drying rate per unit of surface area curves is shown in Figure 6-16:

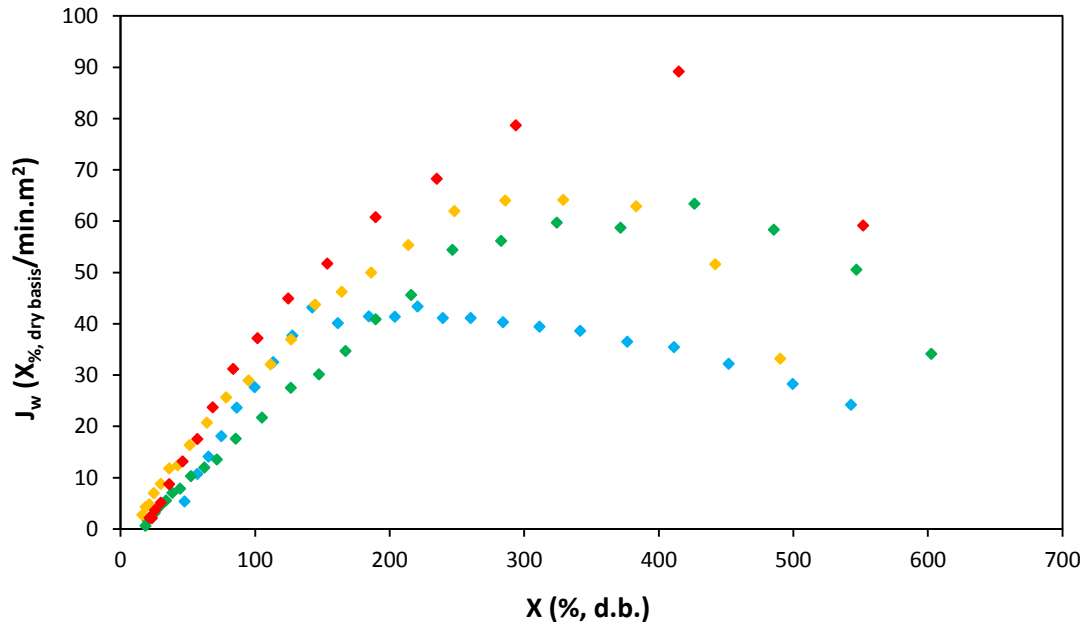

Figure 6-16. Effect of shrinkage on drying rate curves for *Fucus vesiculosus* (thin layer configuration) at different drying temperatures: 35ºC (♦), 50ºC (♦), 60ºC (♦) and 75ºC (♦).

Figure 6-16 shows that there is a constant drying rate and a falling rate period at each drying temperature. The moisture cross-point of both periods corresponds to the critical

moisture content. This moisture content increases with drying temperature increases. In other words, at higher temperatures, the constant drying rate period is shortened. Table 6-5 collects the critical moisture content at each drying temperature for *F. vesiculosus*:

Table 6-5. Critical moisture content (X_c) at different drying temperatures of *F. vesiculosus*.

Drying temperature (ºC)	X_C (%, d.b.)
35	161
50	249
60	293
75	300

These values were used as initial moisture content for the determination of water effective coefficient of diffusion. From that point, it is considered that drying is governed by mass diffusion and, thereby, Fick's second law equations may be applied.

It is important to note that shrinkage of a single sample cannot be introduced into deep-bed configuration kinetics, since the behaviour is altered by moisture gradients throughout the bed.

Below, modelling of the falling drying rate period is depicted.

6.2.2.2. Thin layer configuration modelling

Drying kinetics of *F. vesiculosus* modelling under thin layer configuration and in the post-critical period was performed applying equations (Eq. 4-17) and (Eq. 4-19), and conditions presented in Table 4-3, to drying experimental data beyond critical moisture content for each temperature. The radius considered is the average radius for all systems when volume shrinkage is almost negligible (0.00175 m). Volume is considered constant at this sftage, as it is a requirement for the application of diffusional modelling equations.

Table 6-6 shows the effective diffusional coefficient calculated for each temperature.

Water coefficient of diffusion increases with temperature, doubling its value when temperature is raised from 35ºC to 75ºC.

Table 6-6. Estimation of water effective coefficient of diffusion for *Fucus vesiculosus* at different drying temperatures. †

Temperature (ºC)	$D_{eff}\cdot10^{-12}$ (m^2/s)	R^2	ERMS
35	95.00±0.01[a]	0.995	0.082
50	153.75±0.02[b]	0.993	0.065
60	192.50±0.02[c]	0.993	0.034
75	260.03±0.08[d]	0.992	0.037

†: Data are presented as means of ± standard deviation. Data value of each parameter with different superscript letters in rows are significantly different, $P \leq 0.05$

It is hard to compare effective diffusion coefficient with bibliography, since its value strongly depends on the geometry chosen to model drying kinetics. A similar approach was made by Vega-Gálvez et al. (2008) for *Gracilaria chilensis* ($2.76 – 22.41\cdot10^{-9}$ m^2/s) and *Macrocystis pyrifera* ($5.56 – 10.22\cdot10^{-9}$ m^2/s) within a range of temperatures of 50 to 80ºC. In these cases, drying kinetics were adjusted to an infinite slab geometry. Taking into account that difference, it can be said that *F. vesiculosus* shows a considerable lower effective diffusion coefficient for all drying temperatures.

Effective diffusivity coefficients were correlated making use of linear (Eq. 6-6) and Arrhenius relationships (Eq. 6-7):

$$D_{eff} = a + b \cdot T \qquad \text{(Eq. 6-6)}$$

$$\ln(D_{eff}) = \ln(D_0) - \frac{E_a}{R \cdot T} \qquad \text{(Eq. 6-7)}$$

Where a (-) and b (-) are equation parameters, T (K) is the temperature, E_a is the energy of activation (J/mol) and R (8.314 J/K·mol) is the universal constant of gases.

The linear correlation (Eq. 6-6) is displayed on Figure 6-17. On the other hand, Arrhenius adjustment (Eq. 6-7) is displayed on Figure 6-18. The parameters of both fittings are shown in Table 6-7:

Table 6-7. Linear and Arrhenius fitting parameters of effective diffusivity coefficients at different drying temperatures.

Linear (Eq. 6-6)	a (m^2/s)	b ($m^2/s\cdot K$)	R^2
D_{eff} (m^2/s)	$-1\cdot10^{-9}$	$4\cdot10^{-12}$	0.998
Arrhenius (Eq. 6-7)	**E_a (kJ/mol)**	**$\ln(D_0)$**	**R^2**
D_{eff} (m^2/s)	22.38	-14.3	0.992

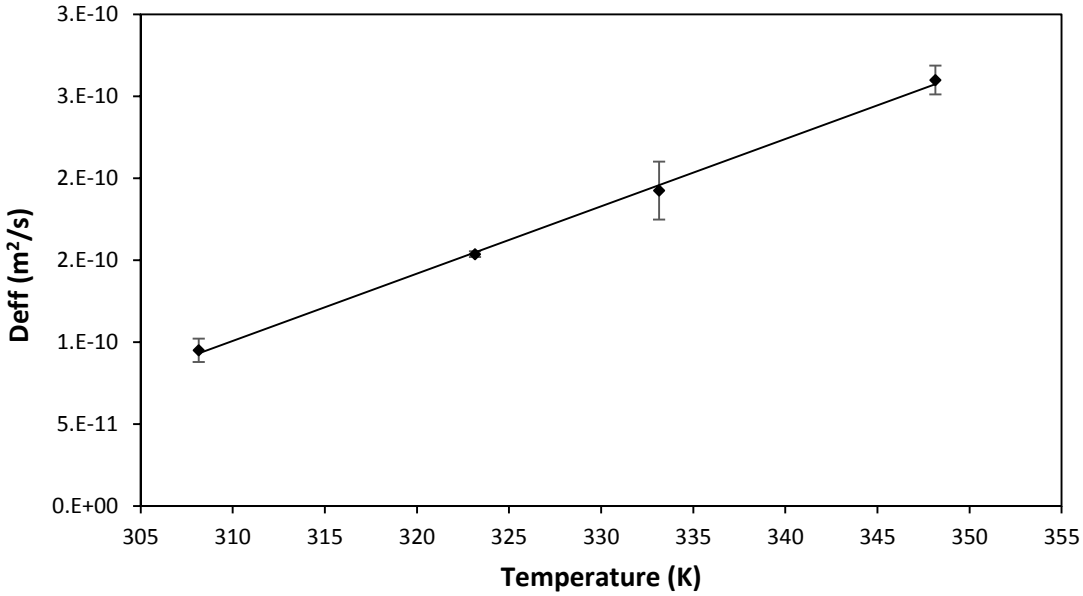

Figure 6-17. Fitting of water coefficient of diffusion with temperature by means of (Eq. 6-6) and parameters shown in Table 6-7.

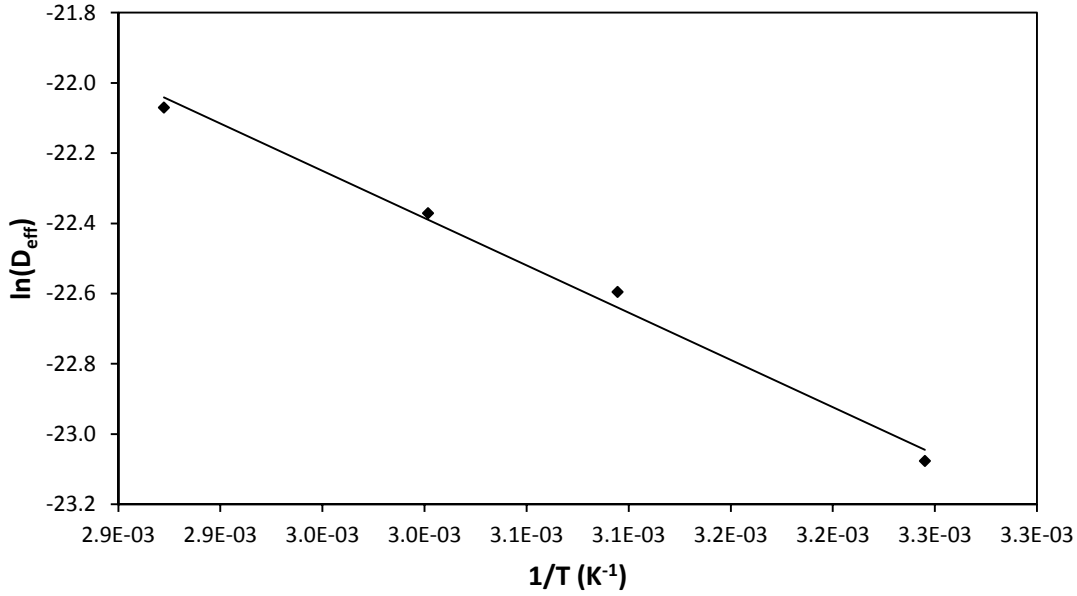

Figure 6-18. Fitting of water coefficient of diffusion with temperature by means of (Eq. 6-7) and parameters shown in Table 6-7.

Energy of activation (E_a) can be obtained from the slope in the Arrhenius correlation (Figure 6-18), and is equal to 22.38 kJ mol^{-1}, which is within the range 12.7 – 110 kJ mol^{-1} exhibited by other food materials (Zogzas et al. 1996) and other seaweeds like *Macrocystis pyrifera*, 19.87 kJ mol^{-1} or *Gracilaria chilensis*, 39.92 kJ mol^{-1} (Vega-Gálvez et al. 2008).

6.2.3. Effect of load density on drying kinetics

The effect of load density was studied at a drying temperature of 75ºC. Four load densities were considered: 14.88, 3.07, 2.48 and 1.25 (kg/m^2). Systems required, respectively, 660, 116, 108 and 40 minutes to achieve a moisture ratio of 0.1. A linear correlation (R^2 = 0.999) between drying time and load density could be established Figure 6-19.

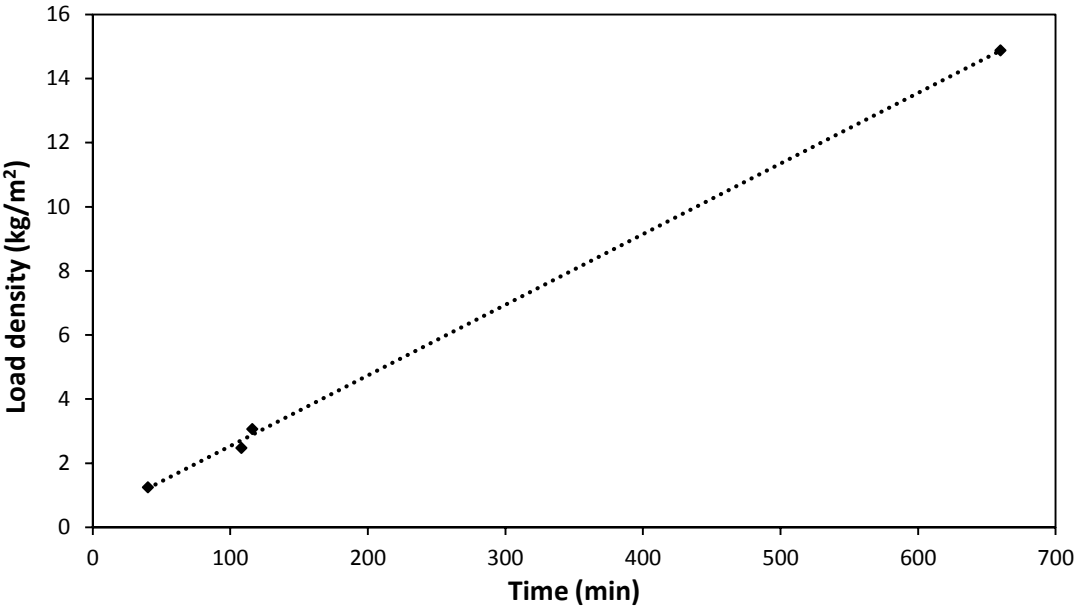

Figure 6-19. Effect of load density on drying time required to achieve a moisture ratio of 0.1.

Page's model was used to adjust experimental data. The parameters determined for said model are displayed in Table 6-8:

Table 6-8. Effect of load density on Page model parameters.

Load density (kg/m^2)	k·10^3(min^{-n})	n (-)	E_{RMS}	R^2
1.25	61.40	0.89	0.024	0.995
2.48	25.89	0.95	0.001	0.999
3.07	14.54	1.07	0.001	0.999
14.88	14.91	0.79	0.013	0.999

In Figure 6-20, the experimental drying kinetic curves are represented along with the profiles obtained with Page's model:

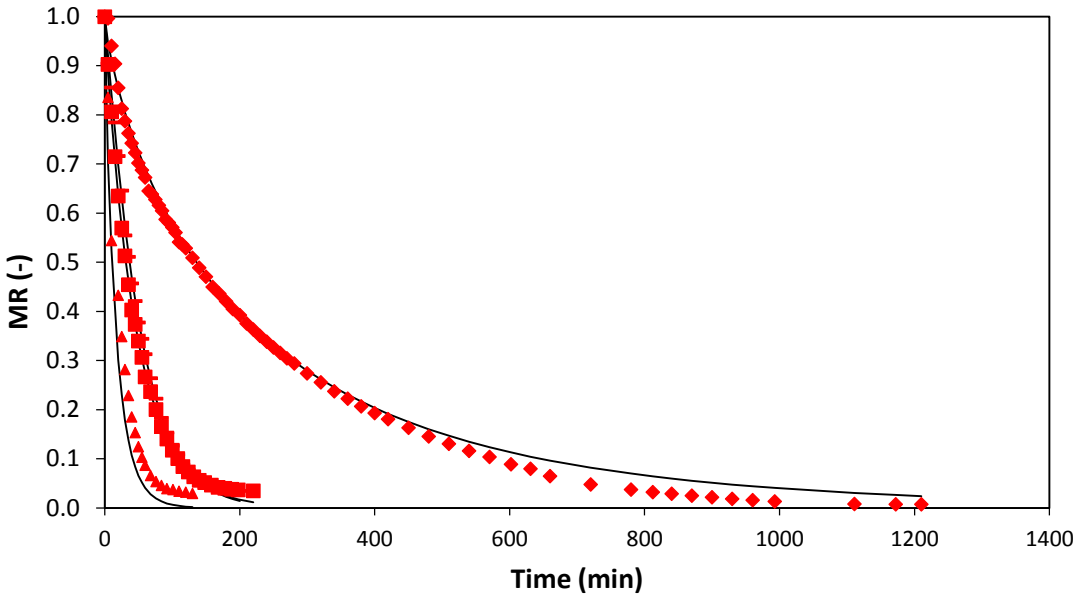

Figure 6-20. Effect of load density on drying curves (14.88 (♦), 3.07 (-), 2.48 (■) and 1.25 (▲) kg/m^2) and fit of Page's model (—).

System dried with a load density of 14.88 kg/m^2 shows a clear induction stage at high moisture content. In the case of the system dried with a load density of 3.07 kg/m^2, a small induction phase is observed. It cannot be distinguishable when adjusted to Page's model. When a water content of around 250 %, d.b. is reached, all systems converge. At that point (critical moisture), diffusion of water through the solid (bed in this case) becomes the limiting factor. This transition was better observed on the thin layer configuration and the subsequent modelling. In this case, the assumptions needed to adjust experimental data to diffusion models are not fulfilled, as moisture profiles are generated through the material depth during drying.

The effect of load density on drying rate can also be appreciated on Figure 6-21. The main difference of drying rate with different load densities was observed at high moisture content, where free water removal is carried out during the initial stages of drying. Page's model provided a good fit of the drying rate curves.

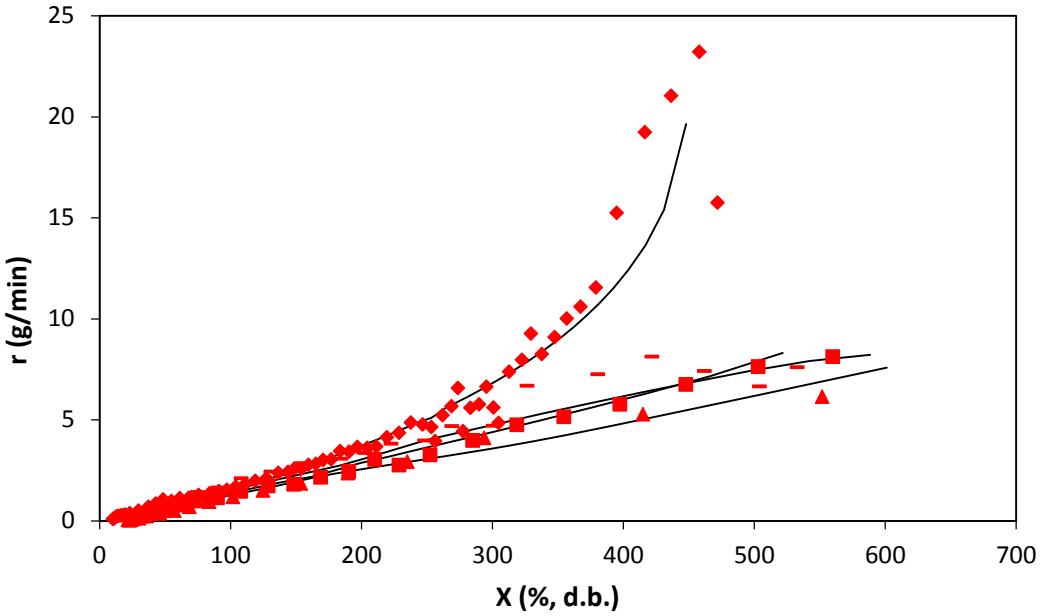

Figure 6-21. Effect of load density on drying rate curves (14.88 (♦), 3.07 (-), 2.48 (■) and 1.25 (▲) kg/m^2) and fit of Page's model (—).

6.2.4. Colorimetric characterization

Table 6-9 shows the fresh and the final colour parameters of *F. vesiculosus* seaweed for all four drying temperatures studied:

No big differences were appreciated between receptacles and lamina initial and final colour parameters.

It can be observed that parameter L* (brightness of the product) increases significantly its value after processing at 75ºC for both, receptacles and lamina. This substantial change may be triggered by compounds expelled at high temperatures due to structural damage. Regarding parameter a* (redness – greenness), its diminution could be linked to alterations in algae pigments. Chromatic parameter b* (blueness – yellowness) increase at 75ºC in comparison to the final value at 35, 50 and 60ºC could be related to the reaction of reducing sugars and amino acids producing non-enzymatic browning reactions (Rahman 2006). Nevertheless, it is difficult to correlate colour parameters behaviour to a single process, since they represent the global properties of the materials, and they measure an average change between the degradation of starting materials and the formation of new coloured species (Landrum 2009).

Table 6-9. Colorimetric parameters of fresh and dried (at different temperatures) *Fucus vesiculosus* seaweed. †

Receptacles				
Temperature (ºC)	**L***	**a***	**b***	**ΔE**
Fresh seaweed	16.26±0.48 [a]	1.48±0.45 [a]	7.38±1.72[a]	-
35	16.42±1.17 [a]	0.88±0.24 [b]	3.49±1.21[b,c]	3.78 ±0.11[a]
50	15.72±0.98 [a]	0.09±0.23 [c]	3.30±0.39[b,c]	4.36±0.44[a,b]
60	18.86±0.77 [b]	0.07±0.11 [c]	2.85±0.66[b]	5.01±0.33[b]
75	28.72±0.1 [c]	0.98±0.11 [b]	4.50±0.05[c]	12.79±0.01[c]
Lamina				
Temperature (ºC)	**L***	**a***	**b***	**ΔE**
Fresh seaweed	18.62±2.11[a]	1.38±0.15[a]	6.77±0.71[a]	-
35	20.04±0.92[a]	0.62±0.14[b]	1.54±0.45[b]	5.52±0.64[a]
50	18.66±1.35[a]	0.42±0.05[c]	1.74±0.97[b,c]	4.14±0.01[b]
60	18.95±0.19[a]	-0.28±0.01[d]	2.67±0.18[c]	3.41±0.01[a,b]
75	26.72±0.37[b]	0.22±0.11[e]	3.84±0.54[d]	7.60±0.01[c]

†: Data are presented as means ± standard deviation. Data value of each parameter with different superscript letters in rows are significantly different, $P \leq 0.05$.

According to the scale displayed in

Table **4-4**, systems processed at 35, 50 and 60ºC reveal an appreciable colour difference (ΔE*) in comparison with fresh samples. Seaweed dried at 75ºC exhibits a large difference in colour change in the lamina, while it develops an obvious difference in its receptacles.

The relationship between colour perception and water content is not clear. In this case, colour parameters may be affected as water is removed, due to pigments concentration, or their degradation. Furthermore, surface colour parameters may not be representative of the whole food material, as its temperature can reach higher values and that could stimulate the presence of Maillard reactions (Chen & Mujumdar 2009).

6.3. Physical characterization of milled seaweed

After drying, algae was aerated during 1 or 2 days prior to milling. Seaweed powder had an average moisture content of 10.47±1.38 (%, d.b.).

In this section, the measured physical properties of the milled seaweed are discussed.

6.3.1. Granulometric characterization

Granulometric characterization, as stated in chapter 4.2.4.1.2, was achieved by screening with mesh sizes varying from 40 to 500 µm. Table 6-10 displays the fractions acquired for each system assayed:

Table 6-10. Size distribution for seaweed powder formerly dried at different temperatures. †

		Mass fractions (%)			
D_p (µm)	**D_{pi} (µm)**	**FV35**	**FV50**	**FV60**	**FV75**
>500	500	1.49±0.12	1.14±0.66	0.97±1.33	1.64±0.25
250 - 500	375	45.82±4.98	40.81±0.53	38.06±15.64	46.73±1.36
200 - 250	225	9.27±1.24	9.06±2.21	14.32±5.46	9.10±0.41
125 - 200	162.5	14.05±0.54	16.07±1.99	19.27±6.76	14.56±2.83
80 - 125	102.5	10.82±0.80	14.32±5.11	10.51±1.99	11.90±3.64
63 - 80	71.5	7.81±0.58	7.82±3.13	4.22±0.73	6.41±0.91
40 - 63	51.5	7.54±1.31	9.52±7.69	8.33±0.92	6.59±4.22
< 40	30	3.19±5.22	1.26±1.51	4.32±1.12	3.07±4.37

†: Data are presented as means ± standard deviation.

Table 6-10 reflects that, for all systems assayed, the highest fractions are present at a particle size of 375 µm (38.06 – 46.73%). The particle size with the second highest fraction was 162.5 µm (14.05 – 19.27%). The particle size that exhibited the lowest fraction for all systems was the corresponding to fines or lower than 40 µm (1.26 – 4.32% - particle size higher than 500 µm is considered residual, lower than 1.64%). Figure 6-22 shows the size particle distribution plotting. All systems exhibit similar distributions and three distinguishable peaks. The highest is observable at particle sizes of 350 to 400 µm for all systems. The other two were e found at smaller particle sizes (around 50 and 150 µm).

Figure 6-23 the cumulative distribution of seaweed powder dried at different temperatures. A linear correlation is found for the cumulative particle size for all systems.

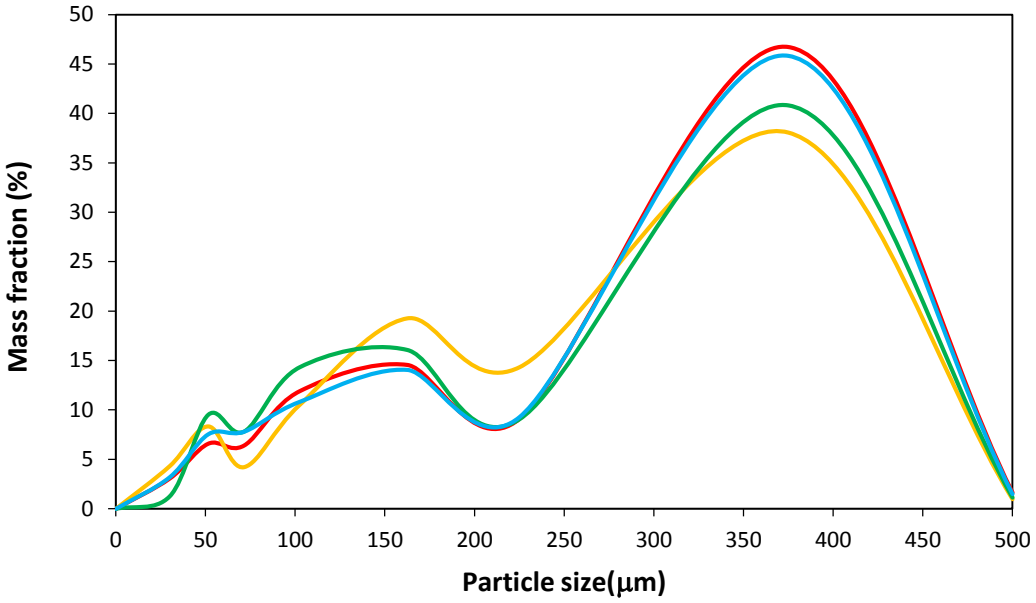

Figure 6-22. Particle size distribution for *F. vesiculosus* powder formerly dried at different temperatures: 35ºC (—), 50ºC (—), and 60 ºC (—) and 75ºC (—).

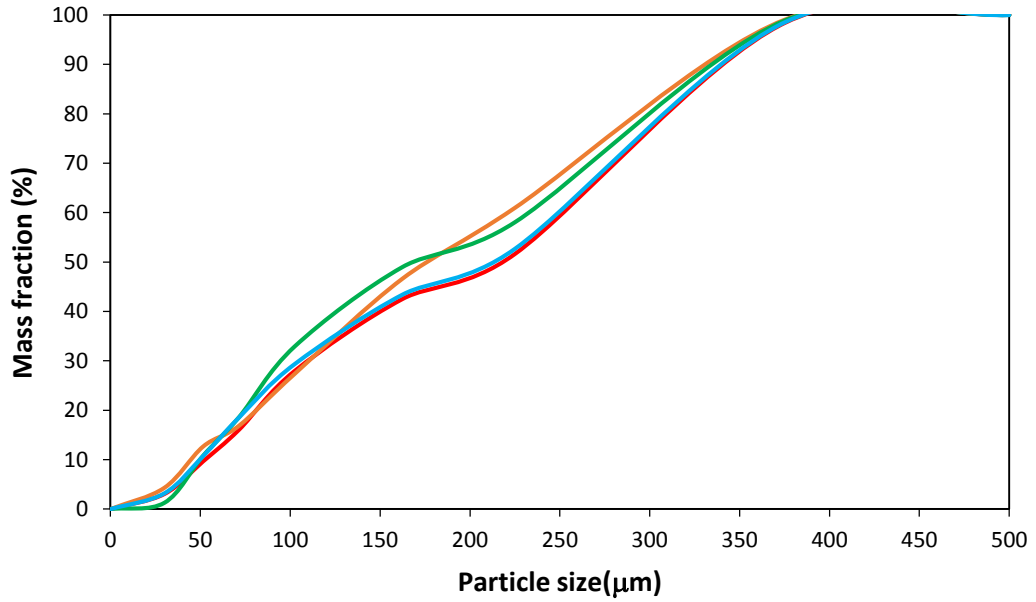

Figure 6-23. Cumulative particle size distribution for *F. vesiculosus* powder formerly dried at different temperatures: 35ºC (—), 50ºC (—), and 60 ºC (—) and 75ºC (—).

Table 6-11 shows the mass mean diameter (D_w), volume mean diameter (D_v) and the surface mean diameter (D_s) calculated employing, respectively, Eqs. (Eq. 4-22), (Eq. 4-23) and (Eq. 4-24) for each system.

Table 6-11. Mean diameters of milled and sieved *F. vesiculosus* previously dried at different temperatures. †

	Temperature (ºC)			
System	**FV35**	**FV50**	**FV60**	**FV75**
D_s (µm)	133±30[a]	139±19[a]	136±19[a]	146±33[a]
D_w (µm)	243±20[a]	231±6[a]	234±38[a]	231±10[a]
D_v (µm)	78±22[a]	91±21[a]	74±5[a]	91±31[a]

†: Data are presented as means ± standard deviation. Data value of each parameter with different superscript letters in rows are significantly different, $P \leq 0.05$.

From Table 6-11 it can be perceived that none of the diameters show significant differences between temperatures employed during drying. No texture differences are observable for all systems when dried at different temperatures. As all systems present similar surface area, it should not have any influence on the extraction yield of *F. vesiculosus* components.

6.3.2. Colorimetric characterization

Colorimetric characterization was carried out measuring the parameters a*, b* and L* over the seaweed powder and the fractions obtained after sieving for each system. Parameter ΔE, that measures difference of colour, was estimated using as reference the colour coordinates of the algae powder prior to sieving. Table 6-12 shows colour parameters of the whole powder and each of its fractions for the seaweed treated at 35ºC and 50ºC. , and 60ºC and 75ºC, respectively.

The first appreciation that can be observed from colorimetric coordinates, is that seaweed powders exhibit a similar qualitative tendency regarding greenness-redness and blueness-yellowness than seaweed after drying. In both cases, greenness (a*) and yellowness (b*) are predominant. On the other hand, when it comes to parameter L*, seaweed right after drying shows more opacity than in powder state. This circumstance could be linked to the structure of the material, that is, porosity and the formation of shades.

At first glance, seaweed in powder form shows similar patterns whether it was dried at 35, 60 or 75ºC, showing the first a slightly more significant yellow tone. Lastly, seaweed powder formerly dried at 50ºC exhibited an emphasized green tinge, as shown in Figure 6-24:

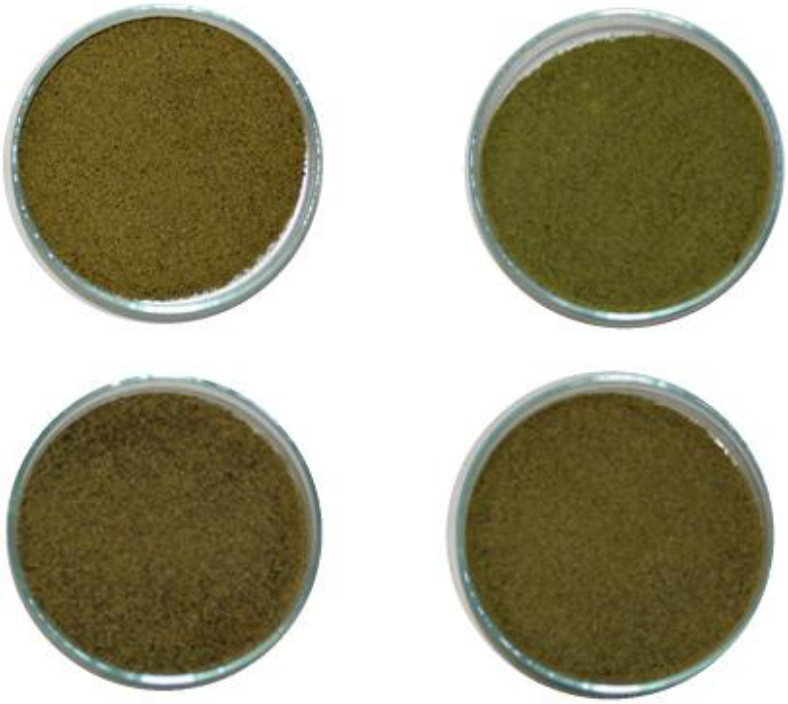

Figure 6-24. Seaweed powder mixture formerly dried at 35ºC (upper-left), 50ºC (upper-right), 60ºC (lower-left) and 75ºC (lower right).

Table 6-12. Colour parameters of seaweed powder formerly dried at 35, 50, 60 and 75ºC and milled with a mesh size of 500 µm and the corresponding size fractions. †

			Fractions (µm)							
System		**Mixture**	**<40**	**40-63**	**63-80**	**80-125**	**125-200**	**200-250**	**250-500**	**>500**
FV35	L*	56.23±1.94	60.56±0.28	61.47±0.61	58.46±1.02	53.74±1.61	55.36±0.62	48.98±0.67	45.22±0.88	39.18±0.95
	a*	-2.95±0.17	-3.04±0.03	-3.18±0.10	-3.18±0.09	-2.85±0.13	-2.90±0.10	-2.41±0.01	-1.92±0.27	-1.35±0.09
	b*	39.19±0.87	44.94±0.29	44.85±0.64	41.30±0.31	37.98±1.15	37.82±0.35	35.01±0.18	30.87±1.51	24.12±0.99
	ΔE		6.53±1.14	7.15±1.16	2.80±1.56	4.29±2.79	2.11±1.37	9.12±0.84	15.30±1.64	23.54±2.59
		Mixture	**<40**	**40-63**	**63-80**	**80-125**	**125-200**	**200-250**	**250-500**	**>500**
FV50	L*	30.68±0.31	70.95±1.59	71.36±1.07	59.34±0.25	53.75±1.17	47.58±0.50	43.10±0.75	47.24±1.89	47.59±0.41
	a*	-5.40±0.03	-10.67±0.11	-11.16±0.06	-9.77±0.05	-8.63±0.17	-7.11±0.02	-6.11±0.20	-6.84±0.47	-6.42±0.48
	b*	24.05±0.16	46.93±0.27	45.96±0.16	38.80±0.26	35.55±0.42	29.61±0.54	25.79±0.81	28.02±0.70	25.23±1.46
	ΔE		46.62±1.76	46.57±0.53	32.53±0.25	25.99±0.91	17.88±0.64	12.57±1.01	17.10±1.84	17.03±0.29
		Mixture	**<40**	**40-63**	**63-80**	**80-125**	**125-200**	**200-250**	**250-500**	**>500**
FV60	L*	34.45±0.56	44.83±0.79	44.30±0.36	30.03±0.49	26.74±0.64	25.06±0.35	26.33±3.05	29.60±0.39	24.79±0.87
	a*	-2.04±0.04	-2.27±0.04	-2.41±0.01	-1.63±0.06	-1.41±0.11	-1.31±0.03	-1.38±0.20	-1.60±0.01	-1.05±0.03
	b*	20.39±0.26	29.88±0.41	27.53±0.27	21.78±0.28	18.01±0.34	14.76±0.14	14.15±1.06	15.04±0.29	10.75±0.39
	ΔE	-	14.07±1.43	12.17±0.17	4.69±0.88	8.09±1.20	10.97±0.92	10.30±3.36	7.24±0.28	13.70±0.23
		Mixture	**<40**	**40-63**	**63-80**	**80-125**	**125-200**	**200-250**	**250-500**	**>500**
FV75	L*	56.60±1.34	64.02±0.38	55.80±0.80	50.65±0.78	48.50±0.65	46.50±0.26	41.91±0.32	39.16±0.13	34.11±0.48
	a*	-1.86±0.06	-2.04±0.07	-1.52±0.03	-1.27±0.08	-1.18±0.08	-1.11±0.04	-0.94±0.09	-0.81±0.10	-0.46±0.15
	b*	31.40±0.47	39.60±0.23	35.23±0.26	31.54±0.21	28.89±0.32	26.45±0.17	22.66±0.15	21.68±0.17	17.95±0.21
	ΔE	-	11.22±1.53	3.99±0.39	6.05±0.85	8.73±1.94	11.14±1.92	17.02±1.67	20.01±1.65	26.31±1.58

†: Data are presented as means ± standard deviation.

The main change in colorimetric parameters is observable for the system formerly dried at 50ºC. The attenuation in yellowness (b*) in FV50 system in comparison with that treated at 35ºC may be associated with reactions experienced by carotenoids or other pigments, which could result in their degradation, or in the formation of alternative coloured substances or volatile compounds (Landrum 2009). This fact is also noticeable in the system FV60, which presents a similar b* value.

Regarding parameter a*, which measures greenness (a*<0) – redness (a*>0), FV50 system revealed a substantial decrease. Under desiccation stress, the most delicate cellular components are membranes. During dehydration, the tonoplast, the plasmalemma and the chloroplast membrane may suffer structural damage and, as a consequence, a solute loss of chlorophyll and carotenoids, among others components (Burritt et al. 2002; Oliver et al. 1998). This damage to cell integrity could be associated with a loss of antioxidant capacity of the food system, as membrane damage could be triggered by an increased ROS production induced by stress conditions (Burritt et al. 2002). As stated in chapter 3.1.6, fucoxanthin is the responsible of brown algae coloration and, in raw seaweed, covers the pigmentation of chlorophyll. However, the leachate of chlorophyll during drying may expose its colour, and consequently, the parameter a* drastically decreases.

During drying at high temperatures (60 – 75ºC), the released chlorophyll undergoes degradation reactions. Chlorophylls are easily degraded in the presence of dilute acids, heat, light and oxygen. Along with degradation produced by external agents, chlorophyll is degraded by chlorophyllase (Erge et al. 2008). Chlorophyllase is an enzyme present in higher plants and algae, bound to the chloroplast membrane and structurally separated from its sustract (chlorophyll). Degradation of the chlorophyll is manifested as yellowing, as it allows the preponderance of carotenoids coloration (Drążkiewicz & Krupa 1991). At ambient temperatures, this enzyme only acts in the presence of high concentrations of organic solvents. However, its optimum activity is found to be within the range of 60 – 82ºC and it loses its activity at temperatures up to 100ºC (Erge et al. 2008).

It is hard to distinguish if chlorophyll breakdown is produced by enzymatic or non-enzymatic reactions but, eventually, they both lead to the formation of non-colorant species (Delgado-Vargas & Paredes-Lopez 2002).

Finally, the additional increase in coordinate b (yellowness) after drying at 75ºC may be induced by Maillard reactions. Moreover, four types of chlorophyll are known to be

present in brown algae: *a*, *b*, *c* and *d*. The first two are the most abundant and they are present in a ratio of 2-4.5 (a-b). Chlorophyll *a* shows a blue-green tone, while chlorophyll *b* presents a yellow-green coloration. The former is thermally less stable than the latter so, higher temperatures might contribute to higher values of b* parameter (Erge et al. 2008).

The release and degradation of chlorophyll, and how carotenoids tinge prevails can also be observed during initial stages of drying at high temperatures. Figure 6-25 shows seaweed during an initial stage of drying (release of chlorophyll), a late stage of drying (degradation of chlorophyll) and when drying is finally over (loss of coloration on the surface of the seaweed).

Figure 6-25. Seaweed during initial (left), late (middle) and final (right) stages of drying at 75ºC.

Regarding fractions colorimetry, system FV35 presents the lowest difference between its fractions and their mixture (average ΔE value of 8), while FV50 showed the hights (average ΔE value of 27). FV 35 biggest fraction (>500 μm) showed the major difference, representing only a 1.49% of the mixture, followed by the 250-500 μm fraction. These two fractions show a clear decrease in L* parameter, linked to brightness-opacity, and a diminished effect of greenness and yellowness. This might be related to the presence of still structurally undamaged parts of the algae present in them and, hence, the similarity with colorimetric parameters of raw algae dried at same temperature. Even so, all fractions are very alike.

In system FV50, the aforementioned scenario completely changes. Smallest fractions show the most substantial differences. This might be due to the chlorophyll extraction explained above. Most of the extracted colorant components are held in the smallest fractions. The presence of traces of these substances are also noticeable on bigger fractions.

Seaweed powder formerly dried at 60ºC exhibits significant brightness, greenness and yellowness loss in all fractions linked to colorants degradation or transformation.

Finally, system FV75 displays the persistent loss in greenness (c*) observed in system FV60, along with the raise in brightness and yellowness related parameters (L*, b*), previously linked to browning reactions.

Drying temperature strongly affected the colorimetric properties of the final product, which are strongly linked to acceptance by consumer (Figure 3-9) and thus, must be carefully selected.

All the discussion described before can be better appreciated in the representation of colorimetric parameters shown in Figure 6-26. Parameters L* and b* show a linear reduction for all systems as diameter is increased. Regarding parameter a*, the main difference is found on FV50 system and more remarkable on the $40 < D_p < 80$ fractions. This fact is also noticeable on the ΔE* parameter, which measures deviation of fractions colour parameters from powder mixture. Tello-Ireland et al. (2011) also reported that drying *Gracilaria chilensis* at 50ºC resulted in the highest ΔE* value, and drying at higher temperatures showed similar colorimetric coordinates to sample dried at a lower temperature (40ºC).

Drying has a substantial effect on appearance of *F. vesiculosus* powder. A yellowish tone predominates for systems dried at 35, 60 ad 75ºC. System FV50 presents a greenish coloration, which is more significant on small fractions.

The selection of drying temperature not only will affect drying kinetics, but will also result in products with different physical characteristics.

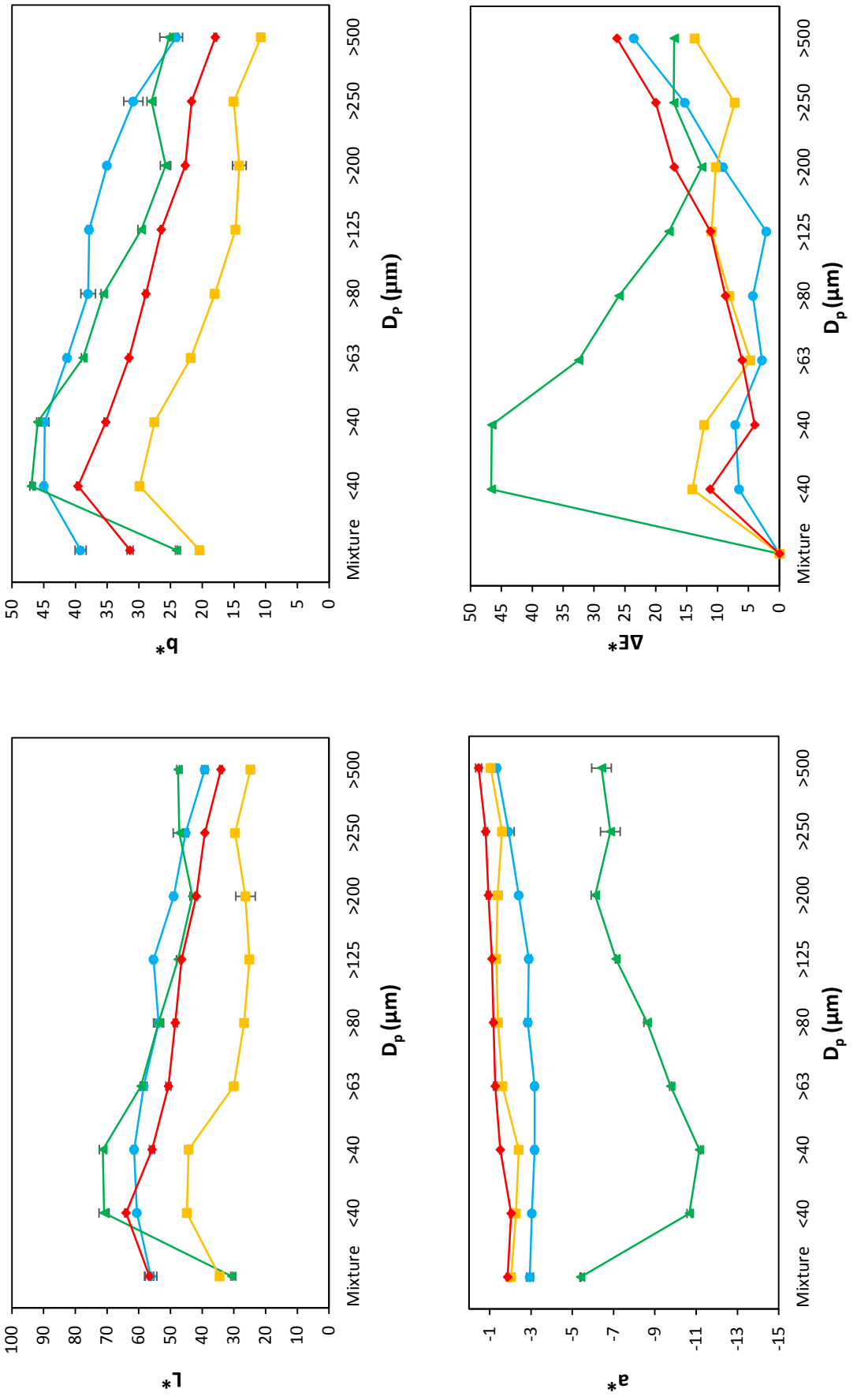

Figure 6-26. Colour parameters for *F. vesiculosus* size fractions previously dried at: *35°C (—), 50°C (—), and 60 °C (—) and 75°C (—).*

6.4. Extracts characterization

6.4.1. Effect of changes in extraction operation conditions

The effect of operation variables were studied on FV35 system.

6.4.1.1. Polyphenols content

Total polyphenolic content (TP) is presented by means of phloroglucinol equivalents referred to sample (mg PHL/100 g dry sample, TP_w) or to total solids content in the extract (mg PHL/100 g dry solids, TP_s).

The first condition studied was the liquid/solid ratio employed for the extraction (L/S) The rest of the conditions remained constant (residence time of 4 minutes and 70 of amplitude level) and the L/S was studied between a 20 and 40 L/S range. Table 6-13 shows the effect of L/S variations on TP:

Table 6-13. Effect of the variation in L/S ratio on TP for FV35 system. †

L/S (g/g)	TP_w	TP_s
20	1007.47±45.61[a]	1433.18±64.88[a]
30	1571.21±75.53[b]	2940.44±141.35[b]
40	1771.52±18.96[c]	2377.29±25.45[c]

†: Data are presented as means ± standard deviation. Data value of each parameter with different superscript letters in rows are significantly different, $P \leq 0.05$.

The highest yield is obtained with the system with a 40 L/S ratio (1771.52±18.9 TP_w). A higher proportion of solids (30 L/S) results in a slightly lower TP content (1571.21±75.53 TP_w). Further increase in L/S ratio reduces TP yield by ~43% (1007.47±45.61 TP_w). This effect is a known problem when applying ultrasound extraction to dispersed phases. In a highly concentrated system, sound wave amplitude may be employed in breaking particle agglomerates (Kadam et al. 2013).

A change in trend is observed when TP is referred to total solids content in the extract. The lowest TP within solids of the extract is again achieved at the lowest L/S ratio (1433.18±64.88 TP_s). The highest is now reached by extraction carried out with a L/S ratio of 30 (2940.44±141.35 m TP_s) System studied with a 40 L/S ratio exhibited a ~30% lower TP (2377.29±25.45 TP_s). Lower L/S ratios may be favourable for an overall extraction of seaweed components. However, a higher L/S ratio appears to be more selective with polyphenols extraction.

The effect of changes in contact time on TP was also studied (Table 6-14):

Table 6-14. Effect of contact time on TP content of extracts obtained with system FV35. †

Contact time (min)	TP_w	TP_s
4	1571.20±75.52[a]	2253.06±108.30[a]
12	1514.25±68.47[a]	2029.01±91.75[a]
20	1334.02±72.00[b]	1758.59±7.16[b]

†: Data are presented as means ± standard deviation. Data value of each parameter with different superscript letters in rows are significantly different, $P \leq 0.05$.

Contact times within the range of 4 to 12 minutes reported little or no influence over TP, achieving 1571.20±75.52 and 1334.02±72.00 TP_w for 4 and 12 minutes respectively. A slight reduction is observed when extraction time is increased to 20 minutes (1334.02±72.00 TP_w). Due to degradation polyphenols fractions may be progressively reduced from 2253.06 to 1758.59 TP_s when contact time is increased from 4 to 20 minutes, respectively. This is due to the higher extraction yields of other substances (i.e. carbohydrates) when applying longer residence times, or the degradation or polyphenols.

Rodrigues et al. (2008) also reported no differences in polyphenols content on extracts of *Ascophyllum nodosum* when varying contact time.

6.4.1.2. Carbohydrates content

Carbohydrates content of extracts, referred to dry sample (mg CHO/100 g_{dw}, CHO_w) or to total solids in the extract (mg CHO/100 g_{ds}, CHO_s)

Table 6-15 shows the effect of varying the L/S ratio of the extraction on carbohydrates content:

Table 6-15. Effect of the variation in L/S ratio on carbohydrate content for FV35 system. †

L/S (g/g)	CHO_w	CHO_s
20	5423.70±344.02[a]	8572.77±543.76[a]
30	5152.44±259.59[a]	8217.62±414.01[a]
40	5204.15±881.63[a]	7759.66±478.89[a]

†: Data are presented as means ± standard deviation. Data value of each parameter with different superscript letters in rows are significantly different, $P \leq 0.05$.

Carbohydrate content showed no significant differences between systems extracted with L/S ratios of 20, 30 or 40 (g/g).

The effect of extraction residence time is displayed on Table 6-16:

Table 6-16. Effect of contact time on carbohydrate content of extracts. †

Contact time (min)	CHO_w	CHO_s
4	5152.44±259.59[a]	8217.61±414.01[a]
12	7438.67±815.22[b]	11300.32±911.74[b]
20	7095.70±168.47[b]	10427.19±247.57[b]

†: Data are presented as means ± standard deviation. Data value of each parameter with different superscript letters in rows are significantly different, $P \leq 0.05$.

The highest extraction yield of carbohydrates is attained for contact times of 12 (7438.67±815.22 CHO_w, 11300.32±911.74 CHO_s) and 20 (7095.70±168.47 CHO_w, 10427.19±247.57 CHO_s). A decline in extraction yield of carbohydrates is observed when contact time is reduced to four minutes (5152.44±259.59 CHO_w, 8217.61±414.01 CHO_s).

6.4.1.3. Alginates

Alginates content is measured by means of glucuronic acid equivalents (mg GLU/100 g_{dw}, GLU_w; mg GLU/100 g_{ds}, GLU_s). The influence of L/S ratio was also studied over alginate content of extracts. Table 6-17 shows the results:

Table 6-17. Effect of L/S ratio on alginate content of an extract obtained with FV35. †

L/S (g/g)	GLU_w	GLU_s
20	1102.36±157.33[a]	1742.40±248.68[a]
30	2069.58±106.82[b]	3300.77±170.36[b]
40	2527.50±435.26[c]	4141.82±649.00[c]

†: Data are presented as means ± standard deviation. Data value of each parameter with different superscript letters in rows are significantly different, $P \leq 0.05$.

The extraction of alginates must be limited if it is carried out with a high concentration of solids. As low L/S ratios diminish the effect of ultrasound waves. Therefore, the highest glucuronic acid content was achieved with a L/S ratio of 40 (2527.50±435.26 GLU_w; 4141.82±649.00 GLU_s), followed by a L/S ratio of 30 (2069.58±106.82 GLU_w; 3300.77±170.36 GLU_s) and, the lowest was obtained for the system extracted with the highest solid content (1102.36±157.33 GLU_w; 1742.40±248.68 GLU_s).

6.4.2. Effect of drying temperature

6.4.2.1. Antioxidant activity

To study the effect of drying temperature of *F. vesiculosus* on the antioxidant activity of the extracts, the extractions were carried out with a liquid/solid ratio (L/S) of 30, a residence time of 4 minutes and a rehydration time prior to extraction of 15 minutes. These conditions would provide the highest content in polyphenols, carbohydrates and alginates in the extracts.

Table 6-18 displays the influence of drying temperature of algae on total polyphenol content of the extracts. TP_{rel} is the relation between TP_w content of the current system and seaweed formerly dried at 35ºC. Experiment was carried out in duplicate, with both systems (A and B) algae gathered and dried separately.

Table 6-18. Total polyphenolic content of *F. vesiculosus* extracts (contact time of 4 minutes and L/S ratios of 30) formerly dried at different temperatures. ǂ

	System A			System B		
T (ºC)	TP_w	TP_s	**TP_{rel}**	TP_w	TP_s	**TP_{rel}**
35	1571.21±75.53^a	2940.44±141.35^a	1.00	1738.46±93.72^a	3514.21±189.46^a	1.00
50	982.69±33.22^b	2006.40±67.83^b	0.63	1258.59±57.97^b	2207.78±101.69^b	0.72
60	943.38±65.76^b	2056.22±143.34^b	0.60	789.07±30.75^c	1695.22±66.07^c	0.45
75	847.50±73.36^b	1670.23±144.57^b	0.54	799.08±11.47^c	1405.42±20.18^c	0.46

ǂ: Data are presented as means ± standard deviation. Data value of each parameter with different superscript letters in rows are significantly different, $P \leq 0.05$.

Both systems showed the same trend. TP decreases when drying temperature is raised, varying within a range of 847.50 - 1571.21 TP_w for system A, and 799.08 - 1738.46 TP_w for system B. The maximum TP was achieved for the extract made with seaweed dried at 35ºC (1571.21±75.53 TP_w, system A; 1738.46±93.72 TP_w, system B). Increasing drying temperature to 50ºC induces a reduction in TP_w of 33±7% and, further increase to 60 or 75ºC, reduces it by 51±7%.

Total polyphenolic content referred to total solids content in the extract shows the same trend and implies that differences in TP is attributed to the effect of drying temperature, and not to a difference in extraction yields.

An extract (system A, FV35) was carried out with an acetone/water mixture (70/30 v/v) to achieve the highest extraction yield, replicating the rest of operation conditions. TP

attained was 11428.29±1123.83 TP_w, which is within the interval of 8–13% of dry matter (reaching maximums close to winter) reported by Ragan & Jensen (1978), close to 10.5% as shown in Figure 3-8 or 16272 TP_w, achieved by Díaz-Rubio et al. (2009), with an extraction with acetone/water and methanol/water mixtures.

The maximum TP obtained employing only water as solvent in the ultrasound extraction accounts for 14.4±1% of TP_w achieved with an acetone/water mixture. Acetone may contribute to a higher degradation of seaweed structure and, therefore, a higher release of these compounds. In addition, polyphenols exhibit a wide difference among their composition and structure and, as a result, in polarity. The use of water as only solvent allows the extraction of water soluble polyphenols, while the addition of acetone promotes the extraction of the non-polar fraction as well (López et al. 2011).

DPPH• radical scavenging activity of both systems is shown in Table 6-19:

Table 6-19. Total DPPH• radical scavenging activity after one hour for *F. vesiculosus* extracts (contact time of 4 minutes and L/S ratios of 30) formerly dried at different temperatures.

	System A	**System B**
T (ºC)	**Scavenging activity (%)**	**Scavenging activity (%)**
35	57.67±3.44[a]	41.68±1.24[a]
50	31.03±1.26[b]	27.51±1.11[b]
60	30.75±3.19[b]	19.49±0.94[b]
75	26.02±1.68[b]	19.40±0.69[b]

†: Data are presented as means ± standard deviation. Data value of each parameter with different superscript letters in rows are significantly different, $P \leq 0.05$.

Extracts obtained system FV35 exhibit the highest radical scavenging activity (57.67±3.44%, for system A; 41.68±1.24, for system B). As in the case of polyphenols, an increase in drying temperature results in a reduced radical scavenging activity. The lowest is that determined for the system FV75 (26.02±1.68%, for system A; 19.40±0.69, for system B). The evolution of radical scavenging activity over time is shown in Figure 6-27.

Linear correlations (R^2>0.98) were found between TP_s and radical scavenging activity (Figure 6-27). The corresponding fittings are: the equation (Eq. 6-8) for system A and the equation (Eq. 6-9) for system B:

$$\%\ \text{Radical scavenging activity} = 0.044 \cdot TP_s - 11.90 \qquad \text{(Eq. 6-8)}$$

$$\%\ \text{Radical scavenging activity} = 0.023 \cdot TP_s + 0.64 \qquad \text{(Eq. 6-9)}$$

The correlation coefficients R^2 for systems A and B were, respectively, 0.998 and 0.98.

Total polyphenolic content and antioxidant activities are reduced when *F. vesiculosus* is dried at higher temperatures. Tello-Ireland et al. (2011) reported the loss of antioxidant activity when drying *Gracilaria chilensis* at high temperatures (70ºC).

Gupta et al. (2011) observed a 30% decrease in TPC of *Himanthalia elongata* when dried at 40ºC for 24 hours in comparison with fresh seaweed. Polyphenols content is reduced as a combination of both, drying temperature and drying time.

The reduction in polyphenols content and antioxidant activity at high drying temperatures may be due to several factors (Gupta et al. 2011; Tello-Ireland et al. 2011; Le Lann et al 2008):

- Release of phenolic compounds bound to cell wall during drying.
- Thermal degradation by oxidative enzymes.
- Phenolic compounds may rapidly degrade at drying temperatures above 40ºC.
- Binding of polyphenols to other substances (proteins) or alterations in their chemical structure which cannot be determined by methods employed.

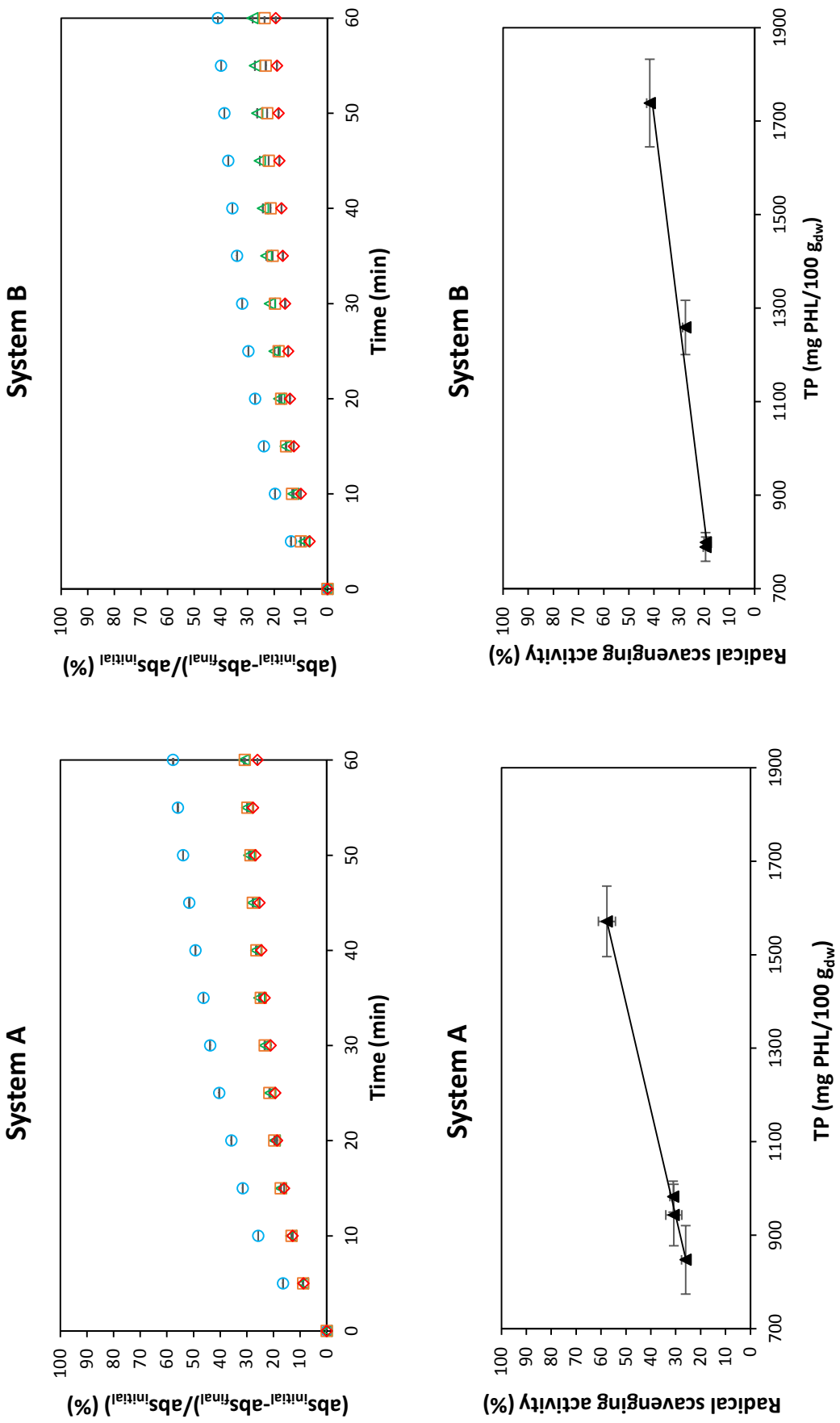

Figure 6-27. Upper figures display radical scavenging activity over time for both systems formerly dried at different temperatures: 35°C (—), 50°C (—), and 60 °C (—) and 75°C (—). Lower figures show the correlation (Eq. 6-8) and (Eq. 6-9) between TP_s and radical scavenging activity.

6.4.2.2. Carbohydrates content

The effect of drying temperature was also evaluated over the carbohydrates content of extracts of *F. vesiculosus* (Table 6-20):

Table 6-20. Effect of drying temperature on carbohydrates content of *F. vesiculosus* extracts (contact time of 4 minutes and L/S ratios of 30). †

T (ºC)	CHO_w	CHO_s
35	5152.44±259.58[a]	8217.61±414.01[a]
50	4591.55±89.88[b]	10282.56±510.86[b]
60	5192.44±523.57[c]	13485.25±1269.26[c]
75	5882.66±357.01[c]	12894.53±782.55[c]

†: Data are presented as means ± standard deviation. Data value of each parameter with different superscript letters in rows are significantly different, $P \leq 0.05$.

Regarding carbohydrate yield referred to raw seaweed powder, carbohydrates content showed no significant differences when *F. vesiculosus* was dried at 35, 50, 60 or 75ºC (average value of 5204.22 CHO_w)

Carbohydrate content referred to total solids content increasingly varies within the range of 8217.61 (35ºC) and 12894.53 (75ºC) CHO_s. Although extraction yields referred to raw seaweed powder are similar, there might be compounds already extracted or degraded during drying at 60 and 75ºC. These substances are not removed at lower drying temperatures and, hence, are extracted during sonication, increasing total solids content of the extract.

An extraction with acetone/water (70/30 v/v) of FV35 was carried out in order to compare the yield of the carbohydrates extraction. The concentration of the carbohydrates in the acetone/water extraction was 11388.15±156.10 CHO_s. System FV75 extract exhibited the highest yield in relation to the acetone/water extract (~52%). As most polysaccharides present in the seaweed are structural substances, a higher drying temperature (75ºC) might have contributed to a better subsequent extraction of carbohydrates.

6.4.2.3. Alginates content

The alginate content of the extracts was determined for two systems: FV35 exhibited a lower content (2069.58±106.82 GLU_w; 3300.77±170.36 GLU_s) than FV 75 (3240.00±266.05 GLU_w; 7101.93±583.17 GLU_s). In contrast with antioxidant activity, alginate content in the extracts appears to be increased when seaweed drying operation is

carried out at high temperatures. Tello-Ireland et al. (2011) observed a similar behaviour with *Gracilaria chilensis*. Higher temperatures reduced the antioxidant activity of the seaweed but also increased the extraction yield of agar (a structural polysaccharide of red seaweeds). A higher drying temperature may allow an easier extraction of structural polysaccharides of algae.

6.4.3. Fractions screening

Extracts of different *F. vesiculosus* size fractions (with the exception of lowest and higher particle diameter fractions) were carried out under the same experimental conditions of temperature screening. For both systems, seaweed powder initially dried at 35ºC was employed. TP values for both systems are displayed in Table 6-21**:**

Table 6-21. Total polyphenolic content of different fractions of *F. vesiculosus* extracts (contact time of 4 minutes and L/S ratios of 30) formerly dried at different 35ºC. †

	System A		System B	
D_p (µm)	**TP_w**	**TP_s**	**TP_w**	**TP_s**
<80	1221.70±55.82^a	2.334±0.107^a	915.92±157.13^a	1390.58±238.57^a
80-125	1672.24±12.54^b	3.258±0.024^b	2272.42±249.76^b	3724.60±409.36^b
125-200	1216.22±75.43^a	2.412±0.150^a	1706.85±162.86^c	3094.63±162.86^b
>200	1041.61±26.29^c	2.265±0.057^a	829.40±81.70 ^{a}	1460.04±81.70^a

†: Data are presented as means ± standard deviation. Data value of each parameter with different superscript letters in rows are significantly different, $P \leq 0.05$.

For both systems, the 80-125 and 125-200 µm fractions exhibited the highest TP (1672.24±12.54 TP_w, for system A; 2272.42±249.76 TP_w, for system B). In system A, <80 µm and >200 µm fractions showed a lower TP (1221.7±55.82 TP_w for 40 – 63 µm fractions; 1216.22±75.43 TP_w for 125 µm fraction). The fractions with lowest TP are those with the highest particle diameter (200 – 250 µm) with a total of 1041.61±26.29 mg PHL/100 g_{dw}.

Concerning system B the 125-200 µm fraction showed the second highest TP (1706.85±162.86 TP_w). The biggest fraction (>200 µm) and the smallest (<80 µm) showed the lowest TP, with 829.40±81.70 and 915.92±157.13 TP_w, respectively, without significant differences.

Both systems presented the highest TP on the 80-125 and 125-200 µm fractions, while the smallest and the biggest fractions exhibited a reduction in TP. This could be attributed to the accumulation of inorganic substances, like salts or metals present in the

seaweed, in the smallest fractions. In the largest fractions, seaweed cells could not be totally degraded and, polyphenols, along with other substances, might not have been released and higher extraction times would be necessary. Hence, most polyphenols are concentrated in the middle fractions.

7. Conclusions

Experimental work performed and subsequent analysis and discussion of the results allowed the formulation of the following conclusions:

1. Water adsorption and desorption isotherms of *Fucus vesiculosus* determined experimentally at 5, 25, 45 and 65ºC are type III at low temperatures (5-25 ºC) and type II at high temperatures (45-65ºC). At low water activities (0.1-0.5), equilibrium moisture content decreases with temperature at the same water activity. Due to a high polysaccharides content of the seaweed, a cross-point between isotherms at different temperatures is observed and at high water activities (0.6-0.9) the aforementioned trend is reversed.
2. Hysteresis cycles are observed for water adsorption and desorption isotherms at the same temperature, at a given water activity, equilibrium moisture content is higher for water desorption isotherms at low temperatures (5-25ºC), it vanishes at 45ºC and is reverted at 65ºC.
3. Halsey's model is the most suitable to fit all water sorption isotherms ($R^2 > 0.97$ and $E_{RMS} < 0.077$) among different bibliographic models tested. Halsey parameters show good linear and Arrhenius correlations. Hence, a model able to estimate the equilibrium data in the range of temperatures and water activities tested is proposed ($R^2 > 0.98$, $E_{RMS} < 0.1$)
4. For deep-bed and thin layer drying configurations of *F. vesiculosus* studied, time required to reach a moisture content close to equilibrium decreased when drying temperature was increased. Thin layer configuration exhibits lower drying times than deep-bed configuration for all temperatures. A linear correlation ($R^2 > 0.999$) exists between drying time and load density (from 1.24 up to 14.88 kg/m^2) drying at 75ºC.
5. Page and modified Page models properly fit deep-bed configuration experimental data ($R^2 > 0.999$ and $E_{RMS} < 0.018$).
6. Experimental shrinkage of *F. vesiculosus* samples during drying is higher than ideal shrinkage (measured by means of water loss estimation). This fact indicates that structural collapse takes place during water removal.
7. Considering the shrinkage of the samples during falling rate period drying and semi-infinite cylindrical geometry, second law Fick's equations is successfully applied ($R^2 > 0.992$ and $E_{RMS} < 0.082$) in thin layer configuration. Values of effective coefficient

of diffusion of water increase with drying temperature (from $95 \cdot 10^{-12}$ up to $260 \cdot 10^{-12}$ m^2/s). An Arrhenius correlation is observed between effective coefficient of diffusion of water and drying temperature.

8. Yellowish coloration is predominant in fresh seaweed. An increase in drying temperature causes an increase in greenish coloration of seaweed and a reduction in yellow-tone.
9. Drying temperature has no effect on granulometric distribution of *F. vesiculosus* after milling ($133 < D_s$ (μm) < 146, $231 < D_w$ (μm) < 243, $74 < D_v$ (μm) < 91). This fact means that no significant textural differences are appreciated between seaweed dried at different temperatures.
10. After drying at different temperatures, seaweed powders exhibit significant differences in colour. Temperatures close to 50ºC causes a greenish coloration of powder. Powders from seaweed previously dried at 35, 60 and 75ºC present a similar yellow tone. Most alterations in colour are present in the smallest fractions (<80 μm).
11. Ultrasound assisted extraction is a feasible method to obtain bioactive compounds from *F. vesiculosus*. Low liquid/solid ratios (20 g/g) decrease the yield of polyphenols and alginates extraction due to weakening of sonic wave's amplitude in highly concentrated systems. Contact times higher than 12 minutes increase the extraction yield of carbohydrates.
12. Drying at low temperatures (35ºC) results in *F. vesiculosus* aqueous extracts with higher phenolic contents and higher DPPH• radical scavenging activities. High drying temperatures (50, 60 and 75ºC) negatively affect the total phenolic content and the antioxidant activity of extracts. There is a linear correlation between the phenolic content of extracts dried at different temperatures and their DPPH• radical scavenging activity. Higher drying temperatures increase alginates yields.
13. Aqueous extracts obtained from 80-200 μm fractions of seaweed powder from *F. vesiculosus* dried at 35ºC result in higher phenolic contents. Employing smaller or larger fractions adversely affect the phenolic content of the extracts.

As a final conclusion, *F. vesiculosus* is a suitable raw material to acquire bioactive compounds, which may have applications in the food, cosmetic and pharmaceutical industries. Dehydration is a key operation for the prevention of spoilage of seaweed. Drying processes conditions must be controlled in order to obtain certain physicochemical properties and extraction yields.

8. Bibliography

Ait-Mohamed, L., Kouhila, M., Lahsasni, S., Jamali, A., Idlimam, A., Rhazi, M., Aghfir, M., Mahrouz, M. 2005. Equilibrium Moisture Content and Heat of Sorption of *Gelidium sesquipedale*. Journal of Stored Products Research. 41 (2): 199–209. doi:http://dx.doi.org/10.1016/j.jspr.2004.03.001

AOAC. 1990. Oficial Method of Analysis, No 934.06. Association of Oficial Analytical Chemists. Washington, USA.

Balboa, E. M., Conde, E., Moure, A., Falqué, E., Domínguez, H. 2013. In Vitro Antioxidant Properties of Crude Extracts and Compounds from Brown Algae. Food Chemistry 138 (2-3): 1764–1785. doi:10.1016/j.foodchem.2012.11.026.

Bell, N. L., Labuza, N. T. 2000. Moisture Sorption: Practical Aspects of Isotherm Measurement and Use. Amer Assn of Cereal Chemists 2nd: St Paul, USA.

Blumenkrantz, N., Asboe-Hansen, G. 1973. New Method for Quantitative Determination of Uronic Acids. Analytical Biochemistry 489: 484–489.

Brand-Williams, W., Cuvelier, M. E., Berset, C. 1995. Use of a Free Radical Method to Evaluate Antioxidant Activity. LWT - Food Science and Technology 28 (1): 25–30. doi:10.1016/S0023-6438(95)80008-5..

Brennan, J. G. 1994. Food Dehydration: A Dictionary and Guide. Woodhead Publishing Limited.: Cambridge, England. doi:10.1533/9781845698294.

Brummer, Y., Cui, S.W. 2005. Food Carbohydrates: Chemistry, Physical Properties and Applications. Chapter 2: Understanding Carbohydrate Analysis. CRC Press: Boca Raton, FL, USA.

Brunauer, S., Deming, L. S., Deming, W. E., Teller, E. 1940. On a Theory of the van Der Waals Adsorption of Gases. Journal of the American Chemical Society 62 (7). American Chemical Society: 1723–1732. doi:10.1021/ja01864a025.

Burritt, D. J., Larkindale, J., Hurd, C. L. 2002. Antioxidant Metabolism in the Intertidal Red Seaweed Stictosiphonia Arbuscula Following Desiccation. Planta 215 (5): 829–838. doi:10.1007/s00425-002-0805-6.

Caurie, M. 1970. A New Model Equation for Predicting Safe Storage Moisture Levels for Optimum Stability of Dehydrated Foods. International Journal of Food Science & Technology 5: 301–307.

Chen, F., Sun, Y., Zhao, G., Liao, X., Hu, X., Wu, J., Wang, Z. 2007. Optimization of Ultrasound-Assisted Extraction of Anthocyanins in Red Raspberries and Identification

of Anthocyanins in Extract Using High-Performance Liquid Chromatography-Mass Spectrometry. Ultrasonics Sonochemistry 14 (6): 767–778. doi:10.1016/j.ultsonch.2006.12.011.

Chen, X. D., Mujumdar, A. S. 2009. Drying Technologies in Food Processing. John Wiley & Sons: Boca Raton, FL, USA. pp. 27-29.

CIELab. 2006. Determination of Chromatic Characteristics according to CIELab. Compendium of international analysis of methods.

Crank, J. 1975. The Mathematics of Diffusion. Oxford Science Publications. Clarendon Press: Oxford, England.

Delgado-Vargas, F., Paredes-Lopez, O. 2002. Natural Colorants for Food and Nutraceutical Uses. Food Science and Technology. CRC Press: Boca Raton, FL, USA.

Díaz-Rubio, M. E., Pérez-Jiménez, J., Saura-Calixto, F. 2009. Dietary Fiber and Antioxidant Capacity in *Fucus vesiculosus* Products. International Journal of Food Sciences and Nutrition 60 (s2): 23–34. doi:10.1080/09637480802189643.

Drążkiewicz, M., Krupa, Z. 1991. The Participation of Chlorophyllase in Chlorophyll Metabolism. Acta Societatis Botanicorum Poloniae. 60 (1-2). doi:http://dx.doi.org/10.5586/asbp.1991.012.

Dubois, M., Gilles, K. A., Hamilton, J. K., Rebers, P. A., Smith, F. 1956. Colorimetric Method for Determination of Sugars and Related Substances. Analytical Chemistry 28 (3): 350–356. doi:10.1021/ac60111a017.

Erge, H. S., Karaden, Z., Koca, N., Soyer, Y. 2008. Effect of heat treatment on chlorophyll degradation and color loss in green peas. Gida 33 (5): 225–33.

Filisetti-Cozzi, T. M., Carpita, N. C. 1991. Measurement of Uronic Acids without Interference from Neutral Sugars. Analytical Biochemistry 197 (1): 157–62. doi:http://dx.doi.org/10.1016/0003-2697(91)90372-Z.

Fito, P. M., Andrés, A. M., Sorolla, A. M. A., Barat, J. M. 2001. Introducción Al Secado de Alimentos Por Aire Caliente. Universitat Politécnica de Valencia. Editorial de la UPV: Valencia, España.

Fudholi, A, Ruslan, M. H., Haw, L.H. 2012a. Mathematical Modeling of Brown Seaweed Drying Curves. Proceedings of the 6th WSEAS international conference on Computer Engineering and Applications.

Fudholi, A, Ruslan, M. H., Othman, M.Y. 2012b. Mathematical Modeling for the Drying Curves of Seaweed *Gracilaria changii* Using a Hot Air Drying. Proceedings of the 6th WSEAS international conference on Computer Engineering and Applications.

Gómez-Ordóñez. 2013. Propiedades Biológicas De Algas Marinas Comestibles . Estudios In Vitro e In Vivo. PhD Thesis. Universidad Complutense de Madrid, Spain.

Guiry, M.D., Guiry, G.M. 2015. AlgaeBase. World-wide electronic publication, National University of Ireland, Galway. http://www.algaebase.org; searched on 05 February 2015.

Gupta, S., Cox, S., Abu-Ghannam, N. 2011. Effect of Different Drying Temperatures on the Moisture and Phytochemical Constituents of Edible Irish Brown Seaweed. LWT - Food Science and Technology 44 (5): 1266–1272. doi:10.1016/j.lwt.2010.12.022.

Hahn, T., Lang, S., Ulber, R., Muffler, K. 2012. Novel Procedures for the Extraction of Fucoidan from Brown Algae. Process Biochemistry 47 (12): 1691–1698. doi:10.1016/j.procbio.2012.06.016.

Halsey, G. 1948. Physical Adsorption on Non-Uniform Surfaces. The Journal of Chemical Physics 16 (10): 931. doi:10.1063/1.1746689.

Hielscher - Ultrasound technology. www.hielscher.com. (Last checked: 05/02/2015).

Hoek, C. 1996. Algae: An Introduction to Phycology. Cambridge University Press: Cambridge, England.

Hui, Y. H. 2008. Food Drying Science and Technology: Microbiology, Chemistry, Applications. DEStech Publications: Lancaster, Pennsylvania, USA.

Jiménez-Escrig, A., Jiménez-Jiménez, I., Pulido, R., Saura-Calixto, F. 2001. Antioxidant Activity of Fresh and Processed Edible Seaweeds. Journal of the Science of Food and Agriculture. 81 (5):530–534. doi: 10.1002/jsfa.842

Kadam, S. U., Tiwari, B. K., O'Donnell, C. P. 2013. Application of Novel Extraction Technologies for Bioactives from Marine Algae. Journal of Agricultural and Food Chemistry 61 (20): 4667–4675. doi:10.1021/jf400819p.

Keyrouz, R., Abasq, M. L., Le Bourvellec, C., Blanc, N., Audibert, L., ArGall, E., Hauchard, D. 2011. Total Phenolic Contents, Radical Scavenging and Cyclic Voltammetry of Seaweeds from Brittany. Food Chemistry 126 (3): 831–836. doi:10.1016/j.foodchem.2010.10.061.

Kyung-tae, K. 2012. Seasonal Variation of Seaweed Componends and Novel Biological Function of Fucoidan Extracted from Brown Algae in Quebec. PhD Thesis. Université Laval. Canada.

Kuda, T., Tsunekawa, M., Goto, H., Araki, Y. 2005a. Antioxidant Properties of Four Edible Algae Harvested in the Noto Peninsula, Japan. Journal of Food Composition and Analysis 18 (7): 625–633.

doi:10.1016/j.jfca.2004.06.015.

Kuda, T., Tsunekawa, M., Hishi, T., Araki, Y. 2005b. Antioxidant Properties of Dried `kayamo-Nori', a Brown Alga Scytosiphon lomentaria (Scytosiphonales, *Phaeophyceae*). Food Chemistry 89 (4): 617–622. doi:10.1016/j.foodchem.2004.03.020.

Landrum, J. T. 2009. Carotenoids: Physical, Chemical, and Biological Functions and Properties. CRC Press: Boca Raton, FL, USA.

Le Lann, K., Jégou, C., Stiger-Pouvreau, V. 2008. Effect of different conditioning treatments on total phenolic content and antioxidant activities in two sargassacean species: comparison of the frondose *Sargassum muticum* (yendo) fensholt and the cylindrical *Bifurcaria bifurcata* R. Ross. Phycological Research 56 (4): 238–45. doi:10.1111/j.1440-1835.2008.00505.x.

Lemus, R., Pérez, M., Andrés, A., Roco, T., Tello-Ireland, C. M., Vega-Gálvez, A. 2008. Kinetic Study of Dehydration and Desorption Isotherms of Red Alga *Gracilaria*. LWT - Food Science and Technology 41 (9): 1592–99. doi:10.1016/j.lwt.2007.10.011.

Lesser, P. M. 2011. Advances in Marine Biology 58. Academic Press: London, England.

Li, L. T. 1998. The Color of Food and Its Optical Properties. Physical Properties of Food, 324.

Li, Y., Wijesekara, I., Li, Y., Kim, S. 2011. Phlorotannins as Bioactive Agents from Brown Algae. Process Biochemistry 46 (12): 2219–2124. doi:10.1016/j.procbio.2011.09.015.

Lianfu, Z., Zelong, L. 2008. Optimization and Comparison of Ultrasound/microwave Assisted Extraction (UMAE) and Ultrasonic Assisted Extraction (UAE) of Lycopene from Tomatoes. Ultrasonics Sonochemistry 15 (5): 731–737. doi:10.1016/j.ultsonch.2007.12.001.

López, A., Rico, M., Rivero, A., Suárez de Tangil, M. 2011. The Effects of Solvents on the Phenolic Contents and Antioxidant Activity of *Stypocaulon scoparium* Algae Extracts. Food Chemistry 125 (3): 1104–1109. doi:10.1016/j.foodchem.2010.09.101.

Ma, Y., Chen, J., Liu, D., Ye, X. 2009. Simultaneous Extraction of Phenolic Compounds of Citrus Peel Extracts: Effect of Ultrasound. Ultrasonics Sonochemistry 16 (1): 57–62. doi:10.1016/j.ultsonch.2008.04.012.

Moreira, R., Chenlo, F., Vázquez, M. J., Camean, P. 2005. Sorption Isotherms of Turnip Top Leaves and Stems in the Temperature Range from 298 to 328 K. Journal of Food Engineering. 71 (2): 193–99.

Mujumdar, A. S. 2006. Handbook of Industrial Drying. CRC Press: Boca Raton, FL, USA.

Ngo, D., Wijesekara, I., Vo, T., Ta, Q. V., Kim, S. 2011. Marine Food-Derived Functional Ingredients as Potential Antioxidants in the Food Industry: An Overview. Food Research International 44 (2): 523–29. doi:10.1016/j.foodres.2010.12.030.

Oliver, M. J., O'Mahony, P., Wood, A. J. 1998. To Dryness and beyond - Preparation for the Dried State and Rehydration in Vegetative Desiccation - Tolerant Plants. Plant Growth Regulation. 1: 193–201.

Oswin, C. R. 1946. The Kinetics of Package Life. III. The Isotherm. Journal of the Society of Chemical Industry 65 (12): 419–21. doi:10.1002/jctb.5000651216.

Picó, Y. 2013. Ultrasound-Assisted Extraction for Food and Environmental Samples. TrAC Trends in Analytical Chemistry 43: 84–99. doi:10.1016/j.trac.2012.12.005.

Polatoğlu, B., Beşe, V., Kaya, M., Aktaş, N. 2011. Moisture Adsorption Isotherms and Thermodynamics Properties of Sucuk (Turkish Dry-Fermented Sausage). Food and Bioproducts Processing. 89 (4): 449–456. doi:10.1016/j.fbp.2010.06.003.

Ragan, M. A., Jensen, A. 1978. Quantitative Studies on Brown Algal Phenols. II. Seasonal Variation in Polyphenol Content of *Ascophyllum nodosum* (L.) Le Jol. and *Fucus vesiculosus* (L.). Journal of Experimental Marine Biology and Ecology 34 (3): 245–58. doi:http://dx.doi.org/10.1016/S0022-0981(78)80006-9.

Rahman, M. S. 2006. Drying of Fish and Seafood. In Handbook of Industrial Drying 3rd Edition. CRC Press: Boca Raton, FL, USA. doi:10.1201/9781420017618.ch22.

Rioux, L. E., Turgeon, S. L., Beaulieu, M. 2007. Characterization of Polysaccharides Extracted from Brown Seaweeds. Carbohydrate Polymers 69 (3): 530–537. doi:10.1016/j.carbpol.2007.01.009.

Rodrigues, S., Pinto, G. S., Fernandes, F. N. 2008. Optimization of Ultrasound Extraction of Phenolic Compounds from Coconut (*Cocos nucifera*) Shell Powder by Response Surface Methodology. Ultrasonics Sonochemistry 15 (1): 95–100. doi:10.1016/j.ultsonch.2007.01.006.

Shao, P., Chen, X., Sun, P. 2013. In Vitro Antioxidant and Antitumor Activities of Different Sulfated Polysaccharides Isolated from Three Algae. International Journal of Biological Macromolecules 62 (11): 155–161. doi:10.1016/j.ijbiomac.2013.08.023.

Singleton, V. L., Rossi, J. A. 1965. Colorimetry of Total Phenolics with Phosphomolybdic-Phosphotungstic Acid Reagents. American Journal of Enology and Viticulture 16 (3): 144–158.

Soria, A. C., Villamiel, M. 2010. Effect of Ultrasound on the Technological Properties and Bioactivity of Food: A Review. Trends in Food Science & Technology 21 (7): 323–331.
doi:10.1016/j.tifs.2010.04.003.

Stephen, M. A., Phillips, G. O., Williams, P. A. 2006. Food Polysaccharides and Their Applications. CRC Press: Boca Raton, FL, USA.

Symons, G. E., Morey, B. 1941. The Effect of Drying Time on the Determination of Solids in Sewage and Sewage Sludges. Sewage Works Journal 13 (5): 936–939.

Tatarenkov, A., Jönsson, R. B., Kautsky, L., Johannesson, K. 2007. Genetic Structure in Populations of *Fucus vesiculosus* (*Phaeophyceae*) Over Spatial Scales From 10 M To 800 Km. Journal of Phycology 43 (4): 675–685.
doi:10.1111/j.1529-8817.2007.00369.x.

Tello-Ireland, C., Lemus, R., Vega-Gálvez, A., López, J., Di Scala, K. 2011. Influence of Hot-Air Temperature on Drying Kinetics, Functional Properties, Colour, Phycobiliproteins, Antioxidant Capacity, Texture and Agar Yield of Alga *Gracilaria chilensis*. LWT - Food Science and Technology 44 (10): 2112–2118.
doi:10.1016/j.lwt.2011.06.008..

Thuy, T. T. T., Ly, T., B. M.,Van, T. T. T., Quang, N. V., Tu, H. C., Zheng, Y., Seguin-Devaux, C., Mi, B., Ai, U. 2015. Anti-HIV Activity of Fucoidans from Three Brown Seaweed Species. Carbohydrate Polymers 115 (1): 122–128.
doi:10.1016/j.carbpol.2014.08.068.

Timmermann, E. O. 2003. Multilayer Sorption Parameters: BET or GAB Values? Colloids and Surfaces A: Physicochemical and Engineering Aspects 220 (1-3): 235–260. doi:10.1016/S0927-7757(03)00059-1.

Truus, K., Vaher, M., Taure, I. 2001. Algal Biomass from *Fucus vesiculosus* (*Phaeophyceae*): Investigation of the Mineral and Alginate Components. 1: 95–103.

Van den Berg, C., Bruin, S. 1981. Water activity and its estimation in food systems: theoretical aspects. A Treatise on the Influence of Bound and Free Water on the Quality and Stability of Foods and Other Natural Products. pp 1-61.
doi:http://dx.doi.org/10.1016/B978-0-12-591350-8.50007-3.

Vega-Gálvez, A., Ayala-Aponte, A., Notte, E., De La Fuente, L., Lemus, R. 2008. Mathematical Modeling of Mass Transfer during Convective Dehydration of Brown Algae *Macrocystis pyrifera*. Drying Technology 26 (12): 1610–16.
doi:10.1080/07373930802467532..

Wang, T., Jónsdóttir, R., Liu, H., Gu, L., Kristinsson, H. G., Raghavan, S., Olafsdóttir, G. 2012. Antioxidant Capacities of Phlorotannins Extracted from the Brown Algae *Fucus vesiculosus*. Journal of Agricultural and Food Chemistry 60 (23): 5874–5883.
doi:10.1021/jf3003653.

Wijesinghe, W., You-Jin J. 2012. Biological Activities and Potential Industrial Applications of Fucose Rich Sulfated Polysaccharides and Fucoidans Isolated from Brown Seaweeds: A Review. Carbohydrate Polymers 88 (1): 13–20. doi:10.1016/j.carbpol.2011.12.029.

Wolf, W., Spiess, W. E. L., Jung, G. 1985. Standardization of Isotherm Measurements (Cost-Project 90 and 90 BIS). Properties of Water in Foods 90: 661-679. doi:10.1007/978-94-009-5103-7_40

Wrolstad, R. E., Decker, E. A., Schwartz, S. J., Sporns, P. 2005. Handbook of Food Analytical Chemistry, Water, Proteins, Enzymes, Lipids, and Carbohydrates. Handbook of Food Analytical Chemistry. John Wiley & Sons, New Jersey, USA.

Zogzas, N. P., Maroulis, Z.B., Marinos-Kouris, D. 1996. Moisture Diffusivity Data Compilation in Foodstuffs. Drying Technology 14 (10): 2225–2253. doi:10.1080/07373939608917205.

9. Annex I: Calibration lines

Calibration lines employed for the chemical characterization of extracts are shown below.

9.1. Total polyphenolic content

The calibration line employed for the determination of total polyphenolic content is presented in (9-1):

$$\left[{}^{\text{mg PHL}}/_{\text{L}}\right] = [\text{Abs}] \cdot 114.94 - 5.03 \quad (9\text{-}1)$$

Where [mg PHL/L] is the TPC expressed as phloroglucinol equivalents and [Abs] is the absorbance (R^2 of 0.992). This calibration line was applied within the range of 20-100 mg PHL/L.

9.2. Total carbohydrates content

Carbohydrate content of the extracts, by means of glucose content, was determined using the following calibration line (9-2):

$$\left[{}^{\text{mg CHO}}/_{\text{L}}\right] = [\text{Abs}] \cdot 74.07 + 0.16 \quad (9\text{-}2)$$

Where [mg CHO/L] is the total carbohydrates content expressed as glucose equivalents and [Abs] is the absorbance (R^2 of 0.992). This calibration line was applied within the range of 10-100 mg PHL/L.

9.3. Uronic acids content

Alginates content is measured by means of glucuronic acids content (9-3):

$$\left[{}^{\text{mg GLU}}/_{\text{L}}\right] = [\text{Abs}] \cdot 208.33 + 4.00 \quad (9\text{-}3)$$

Where [mg GLU/L] is the uronic acids content expressed as glucuronic acid equivalents and [Abs] is the absorbance (R^2 of 0.999). This calibration line was applied within the range of 20-330 mg GLU/L.

10. Annex II: Gantt diagram

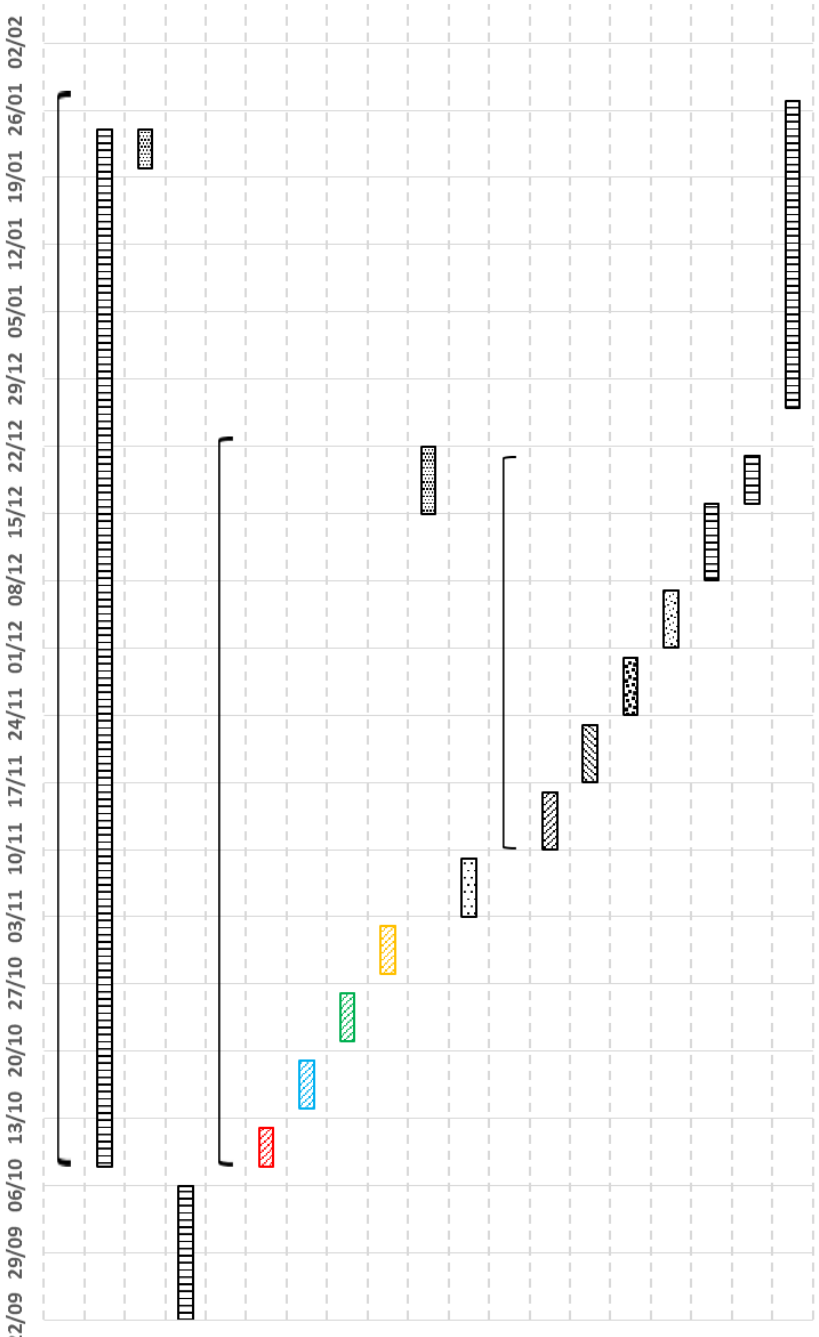

*Each system assayed (FV35, FV50, FV60 and FV75) includes collection and drying with deep-bed and thin layer configurations. Extracts obtention include DPPH● radical scavenging activity and total polyphenols content determination. Powder obtention includes its physical characterization.

11. Annex III: List of figures

12. Annex IV: List of tables